POLYVINYLPYRROLIDONE MODIFIED BIOACTIVE GLASS FIBERS AS TISSUE CONSTRUCTS: SYNTHESIS, CHARACTERIZATION AND RAT MESENCHYMAL STEM CELL RESPONSE

By

BRIAN MATTHEW HATCHER

A THESIS PRESENTED TO THE GRADUATE SCHOOL
OF THE UNIVERSITY OF FLORIDA IN PARTIAL FULFILLMENT
OF THE REQUIREMENTS FOR THE DEGREE OF
MASTER OF SCIENCE

UNIVERSITY OF FLORIDA

2002

This thesis is dedicated to the memory of my mother, Linda M. Hatcher, and also to my father, Tony J. Hatcher. I will always appreciate the love, guidance and support I was so blessed to receive growing up. They have no doubt provided me with every opportunity to succeed, and they have exhibited a level of morals and values I will continually strive to achieve.

ACKNOWLEDGMENTS

First and foremost I would like to thank my advisor and committee chair, Dr. Anthony Brennan, for giving me the opportunity to work on what I have found to be an interesting and challenging project. His guidance, knowledge, and stimulation of critical thinking and independent ideas have contributed to my success and development. I would also like to thank my committee members, Dr. Christopher Batich and Dr. Ronald Baney, for their help and guidance throughout this project.

I would also like to thank the numerous members, past and present, of the research groups of Dr. Brennan, Dr. Goldberg, and Dr. Batich. Collaborations and critical evaluations of ideas and work have no doubt led to an improvement in the quality of my work. The development of the initial procedures for the development of discontinuous bioactive glass fibers by Dr. Rodrigo Orèfice and Dr. Rosana Dominquez has served as the basis for much of the research performed over the past couple of years. Credit goes to Dr. Larry Hench for pioneering this field of research is also due. Additional thanks go out to past members Dr. Jeanne MacDonald, Dr. Jeremy Mehlem, Dr. Charles Seegert, and Wade Wilkerson. I would also like to thank Clay Bohn, Amy Gibson, Adam Feinberg, Thomas Estes, Leslie Wilson, Nikhil Kothurkar, Kiran Karve, Michelle Carman, Paul Martin, Brian Cuevas, and Josh Stopek for all of their insight and assistance in numerous areas of my research. Also I express my deepest gratitude to all of those whom I have failed to mention.

I would also like to thank my fiancée, Robin Shores, for her encouragement, love and support throughout our time together. I consider myself truly blessed to have found someone so incredible and I look forward to the rest of our lives together. I would also like to thank my sisters, Katie, Emily, and Mary Grace, for everything they have done and continue to do. I appreciate and enjoy our memories together.

Financial support through the National Institute of Health, R01 DE 13492-01, is also acknowledged.

TABLE OF CONTENTS

page

LIST OF TABLES

LIST OF FIGURES

Abstract of Thesis Presented to the Graduate School
of the University of Florida in Partial Fulfillment of the
Requirements for the Degree of Master of Science

POLYVINYLPYRROLIDONE MODIFIED BIOACTIVE GLASS FIBERS
AS TISSUE CONSTRUCTS: SYNTHESIS, CHARACTERIZATION
AND RAT MESENCHYMAL STEM CELL RESPONSE

By

Brian Matthew Hatcher

December 2002

Chair: Anthony B. Brennan, Ph.D.
Major Department: Biomedical Engineering

Since their conception at the University of Florida some 30 years ago by Professor Larry Hench, bioactive glasses have received numerous attention for their unique bone forming capabilities. The original bioactive glass was a mixture of sodium, calcium, phosphorous, silica, and oxygen, and had the ability to form a chemical bond with living tissues. The elicitation of this bond was through the precipitation of a hydroxyapatite layer on the glass surface. This mineral is the primary inorganic constituent of bone.

Bioactive glasses have been developed through many processing methods to yield a variety of compositions and forms. Melt and sol gel derived glasses have been examined as particles, fibers, and porous scaffolds for their bone regenerative abilities. Additionally, certain glasses have the ability to bond with soft tissues. The properties of these bioactive materials, including the degree and rate of degradation, and their influence over cellular activity are a function of both composition and form. Therefore,

tailoring of these properties can be used to design implants for specific biological applications.

The development of polyvinylpyrrolidone modified bioactive glass fibers through a sol gel process is described within this work. The addition of this polymer served as a means of modifying the rheological behavior of the sol and facilitating the spraying of discontinuous fibers. Polyvinylpyrrolidone also acted to stabilize the sol, hindering its transformation into a gel. Sprayed fibers were more homogeneous in nature when polyvinylpyrrolidone was incorporated into the sol than when it was not, and furthermore, reproducibility was greatly enhanced.

The bioactive glass fibers were also examined for *in vitro* bioactivity and their ability to influence rat mesenchymal stem cells in culture. Varying the density or spacing between fibers was shown to control the rate and degree of cellular proliferation. This indicated the possibility of using these fibers as tissue engineering substrates in the regeneration of new bone.

CHAPTER 1
INTRODUCTION

Bone is a dynamic organ that serves numerous functions within the body. The skeletal system serves as a means of anchoring muscles, tendons, and ligaments, thereby allowing locomotion. Bones such as the skull and ribs form protective barriers for the internal organs. Additionally, bones serve as a calcium reservoir, maintaining homeostasis. The also are the source of hematopoiesis, thus giving rise to new blood and blood cells.

Bone is composed of dense connective tissue and is a composite material. It is extremely hard and has high tensile and compressive strengths. It is anisotropic in nature, and therefore its properties are directionally oriented, with the greatest strengths being relative to the direction of applied stresses. Bone consists of both inorganic minerals and organic constituents such as cells and collagen. Bone is also viewed as a polymer-ceramic composite in lieu of the collagen and hydroxyapatite (HA) components. The crystalline form of HA and the fibrous nature of collagen further broaden the definition of bone as a composite. These characteristics that describe the physical make up of bone are responsible for its unique properties. Some of the mechanical properties of a human femur are given in Table 1-1[1].

Table 1-1. Some mechanical properties of a human femur.

Property	Value (MPa)
Longitudinal Compressive Strength	205
Transverse Compressive Strength	130
Longitudinal Tensile Strength	135
Transverse Tensile Strength	50

The complex nature and the numerous functions of bone make it a vital tissue that is necessary but difficult to repair following extensive damage. In the US, the total cost for treating all types of fractures was estimated at $14 billion in 1999 [2]. Small fractures in the bone heal remarkably well, assuming the defect is below a critical size and the patient is in relatively good health. Larger fractures or damage to bone caused by disease or trauma are more difficult to reconstruct. This is often seen in elderly patients who may experience osteoporosis or have some type of bone cancer. In western countries, up to 1 in 2 women and 1 in 3 men will sustain an osteoporotic fracture during their lifetime. The proliferation of cells in elderly patients is less vibrant than in those that are younger, and healing of fractures thus occurs at a reduced rate. Therefore, developing methods of treatment that can combat this hurdle may help to improve both the rate and degree of healing, leading to an improvement in the patient's quality of life.

The regeneration of bone within the oral environment for dental implants or the placement of bridges or dentures represents another area of research and development in the reconstitution of new bone. Following the loss or removal of teeth, patients often experience resorption of maxillar or mandibular bone due to an absence of induced stresses upon those bones. Periodontal disease, trauma and infection all lead to the loss

of bone in the oral environment and ultimately play a role in the ability to regenerate new bone.

A number of materials have been examined for their ability to regenerate new bone. Currently, autologous bone remains the preferred material in bone graft and regenerative procedures. This bone, taken from a secondary site within the body is often excised, ground, and reimplanted. It contains both the inorganic mineral hydroxyapatite as well as the cells characteristic of bone. It is therefore a living substitute and can remodel into new and functional bone. Autografts may be combined with supplementary agents such as growth factors or synthetic bone replacement materials [3, 4]. A disadvantage of autologous bone usage is the creation of a secondary trauma sight that must also heal. Therefore its use is limited by availability. Allografts are often used in place of these materials for this reason. These materials are taken from cadavers and are not nearly as constrained by supply; however, they are void of cellular material when implanted. They are often demineralized, leaving behind a collagenous scaffold for the growth of new bone. They also fail to function as proactive materials and do not remodel into living tissue. Also, these materials always carry with them the risk of disease transmission.

To combat the inadequacies of auto and allograft bone, a number of synthetic materials have been examined for their ability to replace or replenish bone. Hydroxyapatite, a mineral composed of calcium phosphate, is naturally present in bone and is one such synthetic material that has been investigated [5, 6]. At first sight, its occurrence in bone makes it a very attractive alternative. When implanted *in vivo*, however, it neither resorbs nor fully integrates with the newly formed bone. It is not a living substitute and new bone is only formed on the surface or internally within the

pores. It merely remains as a static material. This can lead to problems within the host tissue, mainly through micromotion, inflammation, and mechanical fatigue.

Another synthetic material commonly examined and used in regenerating new bone is bioactive glass. These materials have the unique ability to form a chemical bond with the host tissue when implanted. This allows them to retain structural integrity and resist movement within the implantation sight. The chemical bond that occurs through the formation of hydroxyapatite on the glass surface renders it an inanimate part of the host structure. Glass compositions can also be tailored to control resorbability. Resorbed glasses can then be replaced with functional tissue. Studies have also shown beneficial affects on cellular growth by bioactive glasses [7, 8], further substantiating their use. The poor mechanical properties and their inability to function in load bearing situations represent the major downfall of these materials.

The type of material to be used represents only one of the decisions in choosing or designing a tissue engineering substrate. The material form must also be determined. Common uses of the aforementioned synthetic materials are as particles, porous scaffolds, or fibers. Variations in surface areas, diameters, and porosities affect the stability of the scaffold and the ability of cells, blood vessels, nutrients, and metabolic products to infiltrate in or dissipate from the implant sight.

The recent advances in technology through research have opened the door to numerous new methods of treatment, cures, devices and implants in medicine. The incorporation of materials science, cellular biology and engineering together with other fields such as chemistry and biochemistry has contributed to this expansion through a multidisciplinary approach. The integration of the physical and life sciences helps to

address a number of the key issues in fields such as biomaterials and tissue engineering with the goal of bringing functional and practical devices or implants through the physician and to the patient.

Tissue engineering has been described as "applying the principles and methods of engineering, material science, and cellular and molecular biology towards the development of viable substitutes which restore, maintain, or improve the function of human tissues" [9]. This definition highlights the downfall of a number of synthetic bone replacement materials, mainly their inability to integrate with the host tissue and play an active role. The ability of bioactive glasses to precipitate HA, form a chemical bond with the host tissue, and ultimately resorb or become integrated with the bone makes these viable substitutes to restore and improve function.

The assimilation of several disciplines within the field of tissue engineering is accompanied by a lengthy and highly complex process of designing and engineering a material or device. First, a basic chemical and physical understanding of the materials to be used must be obtained. This represents knowledge such as molecular structures, mechanical properties, T_g, and degradation rates and products. Second, these properties must be predicted and confirmed following the coalescence of numerous materials or their construction into an implant or device. The properties of the materials are likely to vary if many fibers are woven together, or a polymer coating is placed over a conductive wire such as in a pacemaker.

The testing of these properties is initially performed in a lab using numerous standardized methods. Upon achievement of the desired chemical and physical properties one must begin to consider and examine those of a biological nature. The most

basic results can be obtained by placing the materials or designs into protein or simulated body fluid (SBF) solutions composed of ionic concentrations similar to those found within the body. More extensive tests should be performed using cell culture lines suited to the material's location and desired performance. If one is constructing an artificial vascular graft it would be beneficial to examine the results of cultured endothelial and smooth muscle cells; likewise if the material is intended to repair bone, cells of mesenchymal origin are preferred. The reactions of the cells can then be used to validate the efficacy of the material and serve as the basis for designing and implementing animal studies.

The implantation of the materials or device into an animal model represents the next step leading up to human clinical trials. Various animal models have been developed and are used for specific applications, however insufficient they may be. Unfortunately, there is no direct correlation between the effectiveness of a material in an animal model and in humans. Along with safety, an attempt must be made to confirm these features prior to human implantation.

In this thesis the first two steps in the design of a material implant have been performed. Discontinuous bioactive glass fibers to be used in the regeneration of new bone have been synthesized and examined *in vitro*. A polymer, polyvinylpyrrolidone, was incorporated into the sol gel synthesis of the bioactive glass fibers to facilitate the process. The polymer served as a rheological modifier and acted to stabilize the sol. An analysis of the procedure and the properties of the fibers were performed. Fibers were able to be arranged into constructs in various packing densities, thereby altering the geometry of the system and the spacing between adjacent fibers. Following their

synthesis the fibers were examined for their *in vitro* bioactivity in both SBF and cell culture. Rat mesenchymal stem cells isolated from the femurs served as the culture model for these experiments. The ability of the constructs to influence their growth was examined.

The achievement of these steps was performed to determine the possibility of using these discontinuous bioactive glass fibers as bone regenerative materials. Analysis of the obtained results can now serve as a means for modifications in the design through the identification of both the positive and negative aspects the BG fibers. These results can also then be used in the design of an animal model in order to begin to determine the bone forming abilities *in vivo*, with the ultimate goal of developing a superior alternative in the regeneration of new bone.

CHAPTER 2
BACKGROUND

The development of bioactive glasses over the past thirty years has led to a unique material with a broad range of attractive properties. The ability of such glasses to form a chemical bond with biological tissues has spurred much interest in the development of various implants and devices for use in biomedical applications. Specifically, the recent explosion in the field of tissue engineering has led to the research and development of these materials for use as scaffolds or substrates for the regeneration of new bone. Variations in the method of synthesis, chemical composition, and final glass form allow for the tailoring of properties to specific applications.

Bioactive Glasses

The development of a single material in the late 1960s by Larry Hench at the University of Florida has since expanded to encompass an entire field of research. The original bioactive glass, BioglassT, was a mixture of sodium, calcium, phosphorous, silica, and oxygen and was intended to repair shattered bones of Vietnam veterans. The metallic and polymeric implants being used at the time were insufficient in fusing the broken bones back together and were met with a high rate a failure often leading to amputation [10]. What Professor Hench developed was a synthetic material that had the ability to interact with living tissues through the deposition of a hydroxyapatite layer on the glass surface.

Bioglass consists of a series of oxides, most commonly SiO_2, CaO, and P_2O_5. Melt derived glasses contain Na_2O, and various other compositions of glasses having small

amounts of MgO, K_2O, and Al_2O_3 have been synthesized [11, 12]. The ratios of the components can be tailored to specific applications, allowing one to control processability or resorption rates *in vivo*. In addition, varying the chemical constituents present in the glass can allow one to synthesize a material capable of forming chemical bonds to both soft and hard tissues.

The development of a mechanically stable interface between the bioactive glass and the host tissue that occurs results in a stabilizing affect within the local environment. The BG can in turn be used alone as a substrate for the formation of new bone or tissue, or it may be used in conjunction with another material or device as a means of holding it in place. This was shown in the coating of hip prostheses [12, 13]. Additionally, Gallardo et al. [14, 15] used a two step sol-gel coating of 316L SS, consisting of an initial silica coating followed by a bioactive coating. The coatings were shown to inhibit corrosion and Fe diffusion and exhibited *in vitro* bioactivity; however no data was presented to indicate whether the implants had a higher degree of fixation *in vivo*. Theoretically, the application of a BG coating on the metallic stem of a hip implant should improve fixation through the substitution of a mechanical fixation with a chemical one. This should help combat micromotion that leads to a local inflammation and decreased performance of the implant. The substitution of a mechanical adhesion formed using bone cements with the chemical fixation through the growth of new bone appears to be a more desirable solution.

The use of such terms as biocompatible, bioinert, or bioactive are widely used in reference to materials implanted within the body and are summarized in Table 2-1.

Table 2-1. Common classifications for biomaterial implants and some of the observed physiological responses by the host tissues.

Material Classification	Observed Biological Response
Toxic	Tissue damage and necrosis
Bioresrbable	Initial immune response followed by eventual breakdown of material. Decomposition products further affect immune reactions.
Biocompatible/Bioacceptable	Fibrous capsul, however the material or implant performs its designed application acceptably
Neutral	Minimal immune reaction resulting in small amount of fibrous tissue
Bioactive	No adverse immune response. Tissue forms chemical bond with implant.

Such classifications are often very subjective, and therefore the context in which they are used must be taken into consideration [12, 16]. A recent article claims poly (l-lactic acid) (PLLA) fibers to be bioactive by the formation of a hydroxyapatite layer on their surface when submerged in a supersaturated simulated body fluid solution [17]. It is the concentration of ions present in the system, rather than the material, that drove this precipitation. Therefore, one can not claim the PLLA fibers to be bioactive; they are more likely to fall within the category of biocompatible.

Similarly, biocompatibility is a term widely used to describe a number of biomaterials. These materials are often deemed those to perform their intended function to a set of acceptable standards. No guidelines or standardized tests are in place for which one can analyze an implant and determine its degree of acceptability. Often the use of biocompatible is subjective, with little quantitative data to describe or characterize the efficiency of the material. In order to rate and compare biomaterials for specific applications, a grading scale in which specific performances are analyzed would be beneficial. Measurable outcomes in regards to the material performance and response, the physiological nature of the tissues, the variability in the immune response, and the

biomechanical behavior are all areas which should be addressed and analyzed. These areas should also be scrutinized in a systematic, temporal sequence representative of the lifespan of expected performance or until complete healing is achieved.

The use of measurable outcomes in characterizing biomaterials and implants will depend on both the type of material and its intended use. A synthetic heart valve may be quantitatively analyzed based upon backflow of blood or anticoagulant dose. Implants used in bone regeneration could be analyzed using bone density measurements, and vascular grafts can be analyzed for compliance and the formation of clots. Further analysis of tissue response can be analyzed histologically to analyze tissue response. The use of standardized grading scales could them be used to describe the type and degree of the response; was their tissue necrosis, ingrowth, or integration? What was the extend to which this occurred, and was this the desired affect or detrimental to the healing process? The biological response to the implant can be further described based upon the immune response as measured by the presence of antibodies or the antibody-antigen complexes in the blood.

The natural periodicity characteristic off the healing process as well as the time dependent properties of most polymers warrants the measurement of such values over time. The healing of tissues takes time, and characteristic events in the process occur in a sequential manner indicating the effectiveness or lack there of for of the implant. The infiltration of mesenchymal stem cells or preosteoblasts into damaged bone followed by angiogenesis, hydroxyapatite deposition and collagen excretion lead to the differentiation of osteoblasts and their entrapment as osteocytes. Osteoclasts are likely to attack the implant and based upon its properties either begin to resorb the material or join together

to form MNGCs around the surface. The initial responses of the tissue and cells to an implant are likely to shape its effectiveness, and ultimately determine the long term success.

Almost all foreign materials implanted into the body will result in an adverse immune reaction and the formation of a fibrous, collagenous capsul around the material. Bioglass (BG), however, is one of the few synthetic materials that can refrain from this response and truly claim to act as a bioactive material. As defined by Hench, a bioactive material is one that "elicits a specific biological response at the interface of the material which results in the formation of a bond between the tissues and the material" [12, 18]. When implanted *in vivo* a layer of calcium phosphate deposits onto the BG surface. This HA layer, with the chemical composition $Ca_{10}(PO_4)_6(OH)_2$, is what in turn forms a bond with the native tissue. It is this feature of Bioglass that makes it particularly attractive for use as an implant material in the regeneration of new bone.

In reality the best biocompatible material is likely to be one that is bioactive. The dynamic nature of the tissues and organs within the body make them difficult if not impossible to replace with a synthetic material. Bone, for instance, not only serves as a structural and connective tissue but also is responsible for the production of numerous cell lines. The mesenchymal and hematopoeitic cells originating within the bone marrow are the precursors for such cells as osteoblasts and chondrocytes as well as red blood cells (RBCs) and leukocytes. It therefore of key importance to restore not only the structural functionality of the tissue, but also its physiological role.

Two categories of bioactivity have been defined by Hench and Wilson and are denoted as Class A and Class B [19]. Bioactive glasses (both melt and sol-gel) are

grouped within Class A while materials such as synthetic HA are Class B. The classes are based upon the rate of tissue response to the implant material, which is highly dependent upon chemical composition, reaction kinetics, and microstructure. Class A biomaterials are both osteoproductive and osteoconductive, whereas Class B are solely osteoconductive. Therefore, Class A materials not only provide a surface suitable for bone migration but also elicit the colonization of osteogenic stem cells in the bone defect environment [12]. Class A materials follow the series of reactions depicted in Table 2-3, discussed later. It is the unique properties of Class A bioactive materials that make them useful in a broad range of biological applications.

Processing

There are two methods available for the synthesis of bioactive glasses; glasses are either melt derived or sol-gel derived. Flow diagrams for the two methods of synthesis are shown in Figure 2-1 [20-22].

The original mechanism of synthesizing bioactive glasses was through traditional melt derived methods. This involves a high temperature synthesis using a highly pure form of silica such as flint glass as the starting material. Melting is then carried out between 1300-1500°C. Highly pure compounds must be used as reagents to ensure a homogeneous final product. The synthesis at high temperatures provides the activation energy for a number of side reactions to occur given the presence of additional compounds or impurities. The high temperatures can also lead to loss of volatile components such as Na_2O or P_2O_5. After obtaining the melt, it is further processed to achieve the usable form of the glass.

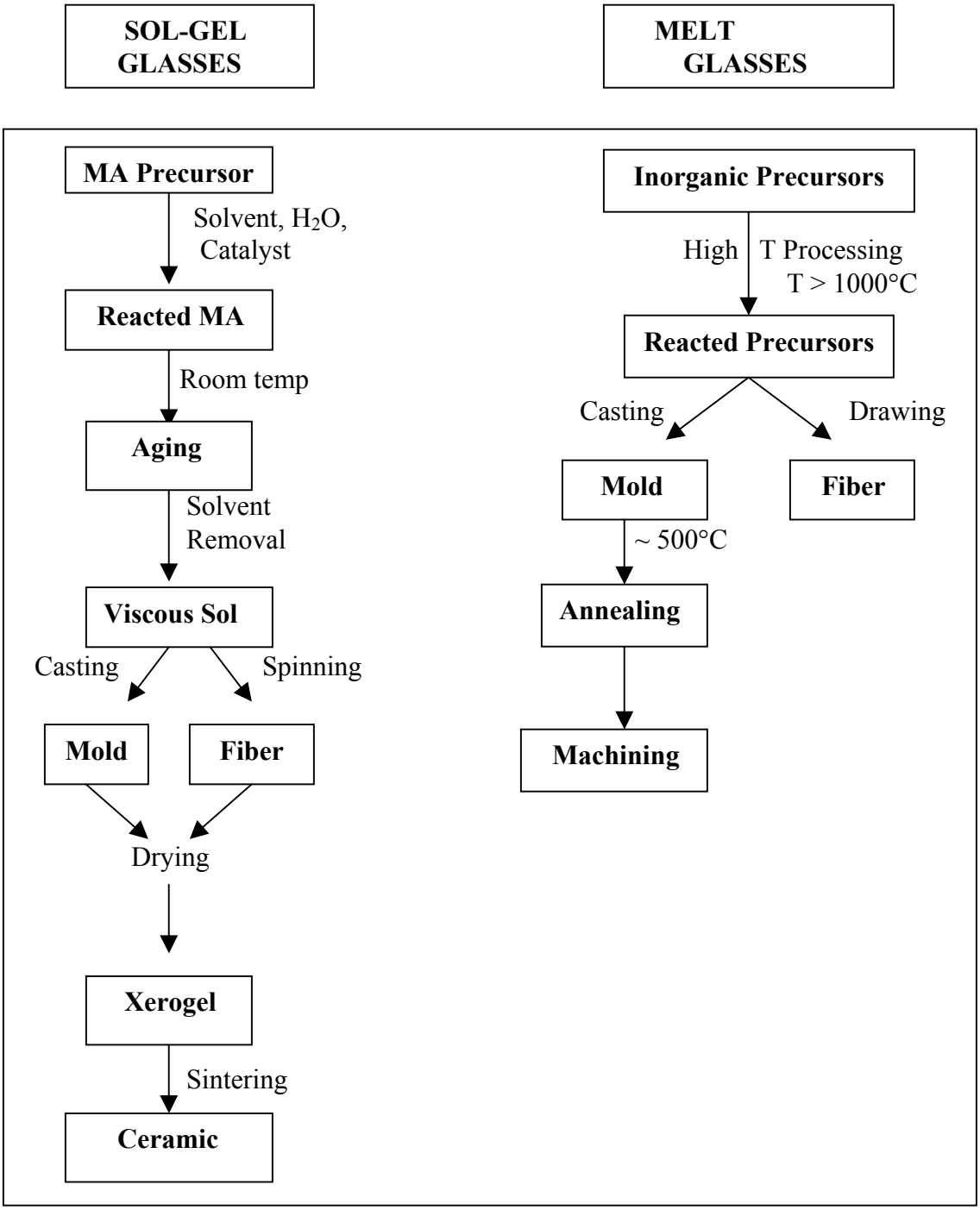

Figure 2-1. Mechanisms of synthesis for melt and sol-gel derived glasses.

Variations in the how the melt is processed affects the microstructure of the final material. This in turn affects the performance of the glass and ultimately it success or failure in various applications. The molten glass can be cast into shapes, sieved into particles, or spun into fibers; however, processing is difficult due to the high temperatures needed to maintain the glass in a workable state.

In addition to the traditional melt derived glasses a second method of synthesis known as sol-gel processing can be used to synthesize inorganic glasses. Sol-gel processing involves the evolution of inorganic networks through the formation of a colloidal suspension, or sol. Continued growth of the networks ultimately results in a continuous phase, at which point the material becomes a gel.

Sol gel derived bioactive glasses are often synthesized using tetraethoxysilane (TEOS) as the silica precursor. A series of hydrolysis and condensation reactions ultimately leads to the formation of a silica network. Addition of reagents such as triethylphosphate (TEP) and calcium chloride (CC) or calcium nitrate yield the oxides of phosphorous and calcium, respectively, and serve as oxide modifiers in the glass. Various heat treatments are used to drive off residual organics and remaining solvent to render the glass bioactive and biocompatible.

Processing of bioactive glasses through sol-gel reactions offers a number of advantages over melt derived glasses. Sol-gel glasses are processed at room temperature, allowing for enhanced control and ease in processability. This allows one to cast or mold the glass into a wider variety of shapes and forms. Glasses have been fabricated into particles [3, 4, 23-26] and fibers [11, 27-30], as well as monoliths such as foams [31] and discs and rods [32-35].

Sol-gel glasses are higher in purity when compared with their melt derived counterparts. This is likely due to a reduction in the number of side reactions that occur when reacting at elevated temperatures. Additionally, sol-gel reactions allow for a broadened compositional range. Melt derived glasses are limited in the amount of silica they can contain while at the same time remaining bioactive, with the maximum amount being around 60%. Glasses containing silica compositions in excess of 60% are accompanied by decreased dissolution rates, leading to prolonged stability *in vivo* [12].

Melt derived glasses are generally denser than their sol gel derived counterparts. The higher density gives these glasses enhanced mechanical properties. Additionally, melt glasses are not completely resorbed, but rather become an integral part of the regenerated tissue. Resorption is dependent upon the percent silica in the glass as well as the size of particles or implanted form. The higher silica content of sol-gel glasses that results in lower densities, higher surface areas, and increased porosities leads to greater overall resorption and a higher bone to graft ratio [24]. This allows one a broader regime to tailor the composition and properties of the glass for specific applications.

Applications

Bioactive glasses have found a number of practical applications, most notably in both the dental and orthopedic fields. Clinical success of the implant depends on both the formation of a stable interface between the tissue and the implant as well as a matching of the mechanical properties of the implant with the host tissue [12]. Examples of biomedical uses for bioactive glasses are given in Table 2-2.

Table 2-2. Some common clinical uses of bioactive glasses.

Clinical Application	Material Form
Dental Implants	Solid shapes, particles
Bone Regeneration	Solid shapes, particles, and fibers
Maxillofacial Reconstruction	Sold shapes. particles
Alveolar Ridge Augmentation	Solid shapes, particles
Ear Prosthesis	Solid shapes
Implant Coatings	Particles

Currently autologous bone grafts remain the gold standard in bone reconstructive procedures. The bone grafts are often derived from the iliac crest or oral bones, depending upon the application, and result in a second injury and additional morbidity. Therefore, they can only be used in limited quantities. Allograft materials as an alternative offer the benefits of an enhanced supply, albeit limited as well, but are accompanied by the risk of disease transmission, immune rejection, and high sterilization and purification costs. These materials are also void of cells, and therefore only serve as substrates for new bone, failing to regenerate into living tissues themselves. The development and use of synthetic materials such as Bioglass for use in dental and orthopaedic applications helps to negate the deficiencies of biological materials through ease in processability, low production, sterilization and shipping costs, elimination of disease transmission, and prolonged shelf lives.

Bioactive glasses such as Perioglass and Biogran are often used in dental applications for the regeneration of new bone. Most commonly these bioactive glasses serve to aid in the formation of a suitable substrate for the fixation or implantation of dentures and

bridges. A study by Cordioli et al. [3] examined the use of Biogran combined with autogenous bone as a grafting material for maxillary sinus augmentation with simultaneous implant placement. Autogenous bone taken from either the mandibular symphysis or the maxillary tuberosity was mixed with Biogran particles (300-350 μm in diameter) in a 1:4 ratio. The composite graft was inserted along with threaded titanium implants for future attachment of a dental bridge into the sinuses. The procedure was carried out in a single step as opposed to traditional two step surgeries. Twelve months post op, 26 out of 27 implants remained stable. Histological evaluation of biopsies taken 9-12 months after implantation contained 30.6% bone. The absence of a control in this study makes it difficult to compare the Biogran composite with autogenous bone alone, however additional studies suggest the enhanced formation of bone that occurs when bioactive glasses are utilized [4, 25, 26].

Similar studies have also examined the use of bioactive glasses in bone regeneration [34] and implant fixation [36] for orthopaedic applications. The low mechanical properties of both melt and sol-gel glasses make them unsuitable for load bearing applications. The integration or formation of new bone with these materials, however, may lead to overall long term success, through the replacement of a static material with a multidimensional, functional tissue.

These applications, as well as numerous others, have focused on the use of bioactive glasses as a means of improving bone ingrowth and fixation of implanted devices. Additionally, these materials could be used alone in the repair of fractured or diseased bones [34]. Similarly, most glasses have been melt derived and examined in particulate form. These particles have low porosities when packed together and high surface areas

that result in faster resorption rates for a given composition. Alternatives such as sol gel derived fibers may prove to be more advantageous due to the ability to control porosities [37] and resorption rates.

Mechanism of Action in Bioactive Glasses

The bioactivity of bioactive glasses has been linked to a series of reactions that occur at the glass surface, leading to the precipitation of a hydroxycarbonate apatite (HCA) layer accompanied by the infiltration and action of osteoprogenitor cells. These reactions are summarized in Table 2-3. The sequence of events is initiated by the exchange of nonbound cations between the glass and the surrounding interstitial fluids. The presence of Na_2O in melt derived leads to an immediate alkalization of the surrounding interstitial fluid. Calcium and sodium ions are exchanged with protons from solution, leading to an increase in interstitial pH. The higher concentration of these ions in melt glasses (51% for 45S5) compared to sol gel glasses (16% for 77S) lead to a much higher increase in pH. This is followed by the cleavage of siloxane bonds to yield silicic acid. As these moieties are released into the surrounding fluid, they condense and repolymerize to form a silica rich gel layer on the glass surface. This gel layer is highly porous and negatively charged due to the negative electrostatic potential from dissociated silanol groups. Calcium and phosphate ions from the glass and surrounding fluids are drawn to the negatively charged surface where they precipitate, forming an amorphous HA layer. This layer ultimately crystallizes following the incorporation of hydroxyl (OH^-) and carbonate (CO_3^{-2}) ions to yield HCA. It is through the HCA layer that the BG is able to form a chemical bond with the native bone. The time scale of these reactions follows a log scale and has been defined to be more rapid for sol gel derived glasses [38].

In addition to the series of chemical reactions that occur leading to the formation of HCA, there are biochemical and cellular responses occurring that give rise to the organic constituents of bone. Giant multinucleated cells infiltrate the site and surround gel glasses, initiating their resorption [24]. Stem cells begin to infiltrate the area, attaching to the glass surface. Initial attachment is followed by a period of differentiation. As the cells begin to differentiate into bone forming cells, they begin to secrete the polypeptide collagen. These fibrous strands further elicit the precipitation of HA within their triple helical structure, resulting in the natural formation of bone. An overlapping of these reactions is also likely to occur. These reactions are less fully understood than those governing the precipitation of HA and variations in experimental results vary within the literature, as discussed in Appendix B. A more detailed understanding of these interactions is necessary in gaining more insight into the mechanisms of bioactivity.

Sol-Gel Chemistry

Sol-gel reactions consist of a series of hydrolysis and condensation reactions of metal alkoxides (MA). First discovered in the late 1800s and extensively studied since the early 1930s, a renewed interest surfaced in the early 1970s when monolithic inorganic gels were formed at low temperatures and converted to glasses without a high temperature melting process [22, 39]. A metal alkoxide has the generic structure M-$(OR)_x$, and is a molecule consisting of a central metallic ion (M) bound to functional organic groups (R) through an oxygen linkage (O). Common metal alkoxide precursors include tetramethoxysilane (TMOS) and tetraethoxysilane (TEOS). Metal alkoxides are common precursors due to their ability to readily react with water.

Table 2-3. Reaction stages of bioactive glasses. For a 77S Bioglass, Steps 1-5 have occurred within 12 hours post submersion in an SBF solution [12, 13, 24, 38].

STAGE	REACTIONS
1	Rapid exchange of Na^+ or Ca^{+2} with H^+ or H_30^+ from solution: $Si\text{-}O\text{-}Na^+ + H^+ + OH^- \rightarrow Si\text{-}OH + Na^+ + OH^-$
2	Loss of soluble silica in the form of $Si(OH)_4$ to the solution resulting from breakage of Si-O-Si bonds and formation of Si-OH at the glass/solution interface: $Si\text{-}O\text{-}Si + H_2O \rightarrow Si\text{-}OH + HO\text{-}Si$
3	Condensation and repolymerization of a SiO_2 –rich gel layer on the surface depleted in alkalis and alkaline-earth cations: $RO_3 – Si – OH + HO – Si – O_3 \rightarrow (Si–O)_3 – Si – O – (Si – O)_3 + H_2O$
4	Migration of Ca^{2+} and PO_4^{3-} groups to the surface through the SiO_2-rich layer forming a $CaO\text{-}P_2O_5$ –rich film on top of the SiO_2 –rich layer, followed by growth of the amorphous $CaO\text{-}P_2O_5$ –rich film by incorporation of soluble calcium and phosphates from solution.
5	Crystallization of the amorphous $CaO\text{-}P_2O_5$ film by incorporation of OH^-, or CO_3^{2-} anions from solution to form a mixed hydroxyl-carbonate apatite layer.
6	Agglomeration and chemical bonding of biological moieties in the HCA layer
7	Action of macrophages
8	Attachment of mesenchymal stem cells
9	Proliferation and differentiation of stem cells
10	Generation of matrix
11	Crystallization of matrix
12	Proliferation of bone

This reaction results in the replacement of alkoxy groups with hydroxyl ones to yield an alcohol. Hydrolysis occurs through a nucleophilic attack on the silicon atom by the oxygen atom in the water molecule. This has been shown using isotopically labeled water that results only in the production of a labeled alcohol, and is the same for both acid and base catalysis [22]. A generic reaction for the hydrolysis of a metal alkoxide is below:

$$Si\text{-}(OR)_4 + H_2O \rightarrow HO\text{-}Si(OR)_3 + R\text{-}OH$$

where –(OR) represents an alkoxy functional group. The ratios of the reagents can be adjusted to control the degree of hydrolysis, ultimately leading to the formation of either clusters or branched polymeric chains.

Following hydrolysis of the metal alkoxide is a series of condensation reactions. These reactions result in the liberation of alcohol and water and contribute to the growth of the reacted metal alkoxide chain. These reactions are illustrated below:

$$(OR)_3Si\text{-}OR + HO\text{-}Si(OR)_3 \rightarrow (OR)_3Si\text{-}O\text{-}Si(OR)_3 + ROH$$

$$HO\text{-}Si(OR)_3 + HO\text{-}Si(OR)_3 \rightarrow (OR)_3Si\text{-}O\text{-}Si(OR)_3 + H_2O$$

As stated, adjustment of the molar ratios of reagents greatly affects the growth mechanisms of the reacting system. Most MAs used in sol-gel reactions are tetrafunctional, allowing for theoretical control over branching through adjustment of the ratio of water:MA (R value). An R value of 2 favors the formation of linear silica chains conducive for fiber spinning. Setting the R value greater than 2 results in nonspinnable sols composed of spherical or disk shaped particles [22].

Sol-gel reactions employ the use of catalysts to efficiently and rapidly promote hydrolysis. Both acidic and basic catalysts are used and include mineral acids or ammonia as well as acetic acid, KOH, amines, and KF. Wilkes and Brennan investigated polymeric catalysts such as polystyrene sulfonic acid, polyacrylic acid, polyvinylpyrrolidone, etc., in sol-gel systems [40]. These catalysts were used in place of traditional acidic or basic catalysts and were accompanied by non detrimental effects on aging behavior. Much like the R value, the type and amount of catalyst used has a significant role in defining the growth of the colloidal structures and the final structure of the gel.

Still another factor in sol-gel reactions is the use of a solvent. The addition of a solvent helps to reduce the miscibility gap between the nonpolar MA and the highly polar water molecules. Common solvents include alcohols such as methanol and ethanol and aprotic solvents such as DMF and THF. In addition to the R value, the amount of solvent present can also affect the hydrolysis and condensation rates. Large amounts of solvent have a diluting affect, reducing the concentration of MA. This in turn will lead to prolonged gelation.

Overall, the large number of variables involved in sol-gel processing make it difficult to perfect. A detailed understanding of the underlying principles and careful control of the numerous components, however, allow one to generate compositions and structures which may be more difficult or impossible to otherwise achieve. Such is the case with the production of bioactive glass fibers. Certain alterations in processing methods can lead to enhanced control over the variables, and this is addressed in the following section.

The Incorporation of Polymeric Modifiers into Sol-Gel Reactions

Various polymers including polyethylene glycol, polypropylene oxide, polyvinylpyrrolidone, hydroxypropyl cellulose, polyurethanes, and polystyrene sulfonic acid have been incorporated into sol gel reactions [40-45]. These polymers have been added to serve as rheological modifiers, dopants, steric stabilizers, phase separating agents, and catalysts. Properties of the polymers such as concentration, molecular weight, and the molecular structure all affect their stability within the sol gel material. Variations in these properties can be used to control the interactions that occur between the inorganic and organic phases, allowing for the design of a material with specific properties.

The addition of a polymer into a sol gel reaction will generally result in one of two phenomena; either the polymer will remain in solution with the sol or a phase separation will occur. For the polymer to remain in solution, the thermodynamic nature of the system must favor the existence of a single, continuous phase. Therefore, the concentration and molar mass of the polymer must be within an appropriate range. The concentration lies within a critical region, being bound by both an upper and lower limit. Small amounts of polymer can result in the coating of the inorganic clusters within the sol, leading to phase segregation [41]. Phase separation can also occur through an entrapment of these clusters within the loops and tails of the polymer chain. This can lead to a precipitation of the clusters through a bridging flocculation mechanism [46-48]. This is indirectly proportional to the molecular weight of the polymer species. Higher MW polymers are composed of longer chains, and thus have greater interactions with the inorganic constituents. Therefore, lower amounts of high molecular weight polymers can result in a phase separation. Additionally, an overabundance of polymer can exceed the

upper limits of solubility, resulting in precipitation. Because large variations in the oxidative properties exist between ceramics and polymers, the organic component can be burned out. Thus, the separation of phases is a common means of creating porous structures.

Adjustment of the polymer concentration to within the realms of solubility can lead to profound benefits and control in sol gel reactions. These include enhanced control over the rheological properties of the sol and stabilization leading to prolonged gelation [41, 44]. The viscous nature of the polymer, as governed by concentration and MW, allow for control over the viscous properties of the sol. The interactions that occur between the molecular species of the polymer and sol further contribute to the viscosity as well as lead to a stabilization of the sol through impedance of gelation. Factors that occur between the organic/inorganic components such as interspecies bonding (H or otherwise) and van der Waals forces can slow the rate at which the network grows, delaying the expansion to a single, continuous phase (gel). This is through interactions between the polymer and sol gel network that hinder gelation by retarding the rate of condensation. Prolonging the length of existence of the sol allows for a broader region over which the material can be further processed into a desired form. This is especially useful when the removal of solvent is necessary for further processing. The removal of solvent increases the concentration of the reacting network and thus results in a greater degree of interactions. This enhances the rate of condensation which ultimately drives the sol into gelation.

Bone

Bone is a composite material consisting of both organic and inorganic constituents. It is a composite in several different senses, being a porous material, a polymer-ceramic

mixture, a lamellar material, and a fiber-matrix material [49]. The organic component of bone, Type I collagen, accounts for approximately 30% of the dry weight, with the remaining 70% derived from the inorganic component, HA. The dynamic nature of bone is found both in the hierarchical levels of structure as well as in its numerous functions. Bone serves as a connective tissue, allowing locomotion and mobility. It also serves to protect the internal organs, act as a calcium reservoir, and give rise to numerous cell lines that span the growth of new connective tissues and blood. A diagram of a long bone is shown in Figure 2-2.

Collagen is a fibrous protein and is composed of a repeated sequence of three amino acids. Every third amino acid is glycine, and many of the remaining positions in the chain are filled by proline and hydroxyproline. Collagen fibrils wind together to form collagen fibers, taking the form of a triple helix. These fibers are directionally oriented, contributing to the anisotropic nature of bone and providing it with its high tensile strength. Deposition of HA occurs within the collagen fibers. Crystals approximately 40 nm long, 10 nm wide and 1-3 nm thick are deposited within these fibers and give bone its tremendous compressive strength [50]. A portion of the HA (20-30%) remains in the amorphous phase for the rapid release of ions to the blood when needed, while the remainder crystallizes into HCA [51]. This serves to maintain homeostasis and intra and extra cellular ion concentrations.

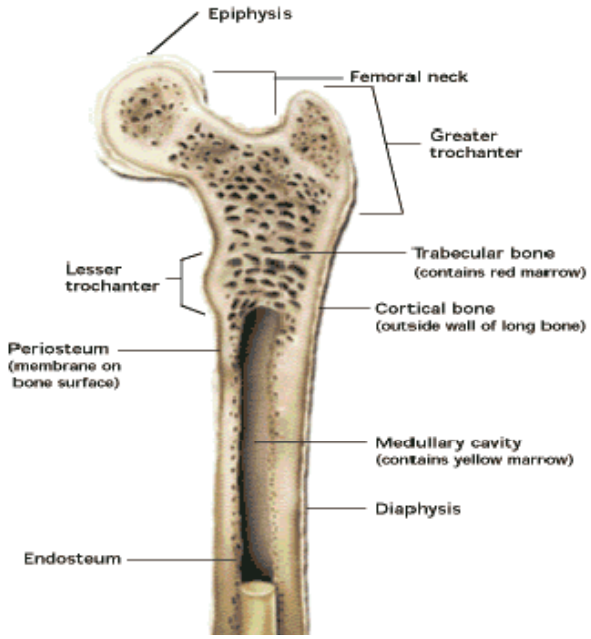

Figure 2-2. Diagram of a femur illustrating the major structural components.

Lamellar bone is the primary form of bone contained in the vertebrae of mammals. It exists in two forms, circumferential lamellar bone (CLB) and osteonal bone(OB). CLB is a parallel arrangement of lamellae, while the more mature OB is an intricate array of lamellae folded into irregularly shaped cylinders [52]. Lamellar bone is composed of sublayers of alternating arrays of collagen fibrils. The collagen fibrils within each lamellae are aligned parallel with one another, with those in adjacent layers rotating 30º. HA crystals are deposited within these fibrils. This structure was first identified in 1906 by Gebhartd and has been referred to as the rotating plywood motif [53]. Inadequacies in mechanical testing have limited the ability to test the individual layers of lamellar bone, however, it is widely believed that this structural organization is responsible for the exceptional strength of bone.

In addition to the HA and collagen components of bone, various cells contribute to its structure and function. Of particular importance, especially in regards to tissue engineering, is the role of these cells in the healing or regeneration of new bone. The primary precursor to the osteogenic cells that form bone is the mesenchymal stem cell (MSC), one of the subpopulations of cells found within the stromal elements of bone marrow. The marrow stroma consists of a network of endothelial, hematopoietic, mesenchymal, fibroblast, adipocytes, and osteogenic cells, among others, contained within a matrix that serves as a physical scaffold and suitable environment for hematopoiesis within the medullary cavity [54]. The osteoprogenitor cells (MSCs) derived within the bone marrow ultimately differentiate into fibroblastic, adipogenic, chondrogenic or osteogenic cells, depending upon oxygen availability and chemical cues such as GFs. Sequential expression of alkaline phosphatase, bone sialoprotein (BSP), and osteocalcin indicate the commitment of MSCs to the osteoblast lineage [55].

Growth factors such as transforming growth factor β (TGF-β) and bone morphogenetic proteins (BMPs) are critical in the early stages of proliferation and differentiation of MSCs [56]. Recent studies by Turgeman et al. showed enhanced proliferation and differentiation of human MSCs transfected with BMP-2 *in vitro* [57]. The genetically engineered cells also formed bone when implanted *in vivo*. Additionally, Andrades et al. showed an upregulation of rat MSCs *in vitro* in the presence of another BMP, osteogenic protein 1 (OP1) [58]. Despite uncertainties in the exact mechanisms, it is abundantly clear that growth factors (GFs) are needed in the regeneration of bone. However, isolating and purifying them for *in vitro* culture with cells and later implantation or therapeutic use is a costly process. The development of implants that can

harvest the maximum potential of GFs *in situ*, without having to include them as a component of the implant material, may prove to be a superior alternative.

Tissue Engineering

Tissue formation within the body is a complex sequence of events in which cell populations proliferate and self-assemble into functional units. Continued organization of functional tissues can result in the formation of fully functional organs. Mimicking these pathways *in vitro* to create functional tissues or organs suitable for reimplantation is the primary goal of tissue engineering; however it is this hierarchical organization that makes this such a difficult task. The implantation of biomaterial scaffolds further complicates matters through the instigation of an immune response. Properties of the material such as surface energy, surface chemistry, mechanical properties and degradability must be tailored for specific applications and tissues.

Tissue engineering has been defined as "applying the principles and methods of engineering, material science, and cellular and molecular biology towards the development of viable substitutes which restore, maintain, or improve the function of human tissues" [9]. A cell based approach to tissue engineering, in which autologous cells are excised from the tissue and culture expanded before reimplantation, is depicted in Figure 2-3.

Current approaches to tissue engineering focus on the need to provide signals to cell populations to promote cell proliferation and differentiation [59]. Current focuses in tissue engineering have included, among others, skin, nerves, vasculature, tendons, ligaments, muscles, and bone [60].

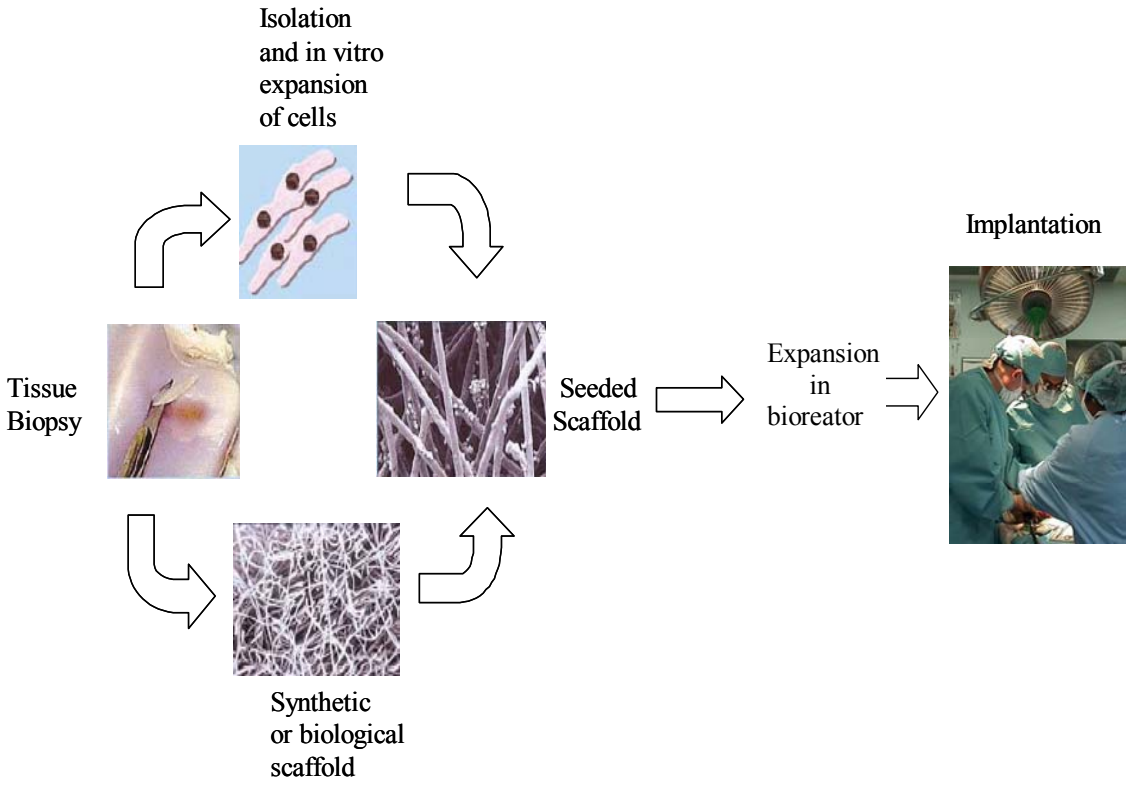

Figure 2-3. A cell based approach to tissue engineering [61].

Damage to the skin can take the form of chemical, electrical or heat burns or may be the result of diabetic ulcers or other superficial wounds. These damages to the epidermal and dermal layers present immediate risks through the increased risk of dehydration and infection. The National Institutes of Medical Sciences estimates that 1.25 million burn related injuries require medical assistance in the US annually. Approximately 50,000 of these patients will require hospitalization, with infection ultimately claiming 10,000 lives [60]. Scaffolds used for the regeneration of new skin must provide a suitable framework for the influx and growth of new cells, sufficient porosity for gas and nutrient exchange, and prevent dehydration and bacterial infection. Common materials for the regeneration of new skin include polyurethane (PU) and keratinocyte seeded PU [60, 62, 63], autografts or allografts [60, 64, 65], nylon mesh [66, 67], silicone elastomer (PDMS)

[65], and gelatin sponge [64]. The use of bioactive glasses in the regeneration of skin or other soft tissues has received relatively little attention, however the ability of certain compositions to bond with soft tissues seems to make them an attractive alternative. Additionally, their use in the fibrous form can serve as a means of allowing oxygen permeability, moisture control, degradation, and wound pH. The expansion of treatments for such injuries to include BG may result in a broadened spectrum of uses.

Most of the research on and applications of bioactive glasses has focused on the regeneration of new bone. The regeneration of this tissue presents a number of challenges due its dynamic nature and complex properties, as described previously. A number of materials have been investigated for use as scaffold materials in the regeneration of bone, including synthetic polymers such as poly(α-hydroxy esters) [6, 68-70]; natural polymers including collagen [71], starch based scaffolds [72], and peptide amphiphiles [73]. Inorganic materials such as hydroxyapatite [5, 6, 18, 68, 74], and Bioglass [8, 11, 27, 28, 75-78] have also been studied extensively. These materials have been examined in a number of forms, including particles, fibers, and porous scaffolds. Regardless of the material chosen or the implantable form, there are numerous deficiencies that arise. Bioactive glasses are weak and non load bearing, nonbioactive materials are bound only by mechanical adhesion and experience micromotion, and natural materials are limited by donor availability and encompass a risk of disease transmission. Forms such as particles are also structurally insufficient and have limited porosities and diffusivities. Therefore the development of new materials in various forms is worthy of further investigation.

The use of bioactive glass fibers in the regeneration of bone offers a number of advantages over the above systems. The ability of the material to form a chemical bond with the surrounding tissue should result in decreased motion of the implant and less local inflammation. Degradation rates can also be adjusted based upon the chemical composition and size of the fibers. Adjusting the spacing between the fibers can be used to control the exchanges of nutrients and metabolic products, as well as allow for the infiltration of cells and vasculature. Weaving or compositing the fibers with a polymer can help compensate for the poor mechanical properties of bioactive glasses, resulting in enhanced strengths more comparable to bone. Critical in their development and success as tissue engineering substrates is an understanding of the interactions that occur between these materials and cells.

Interactions Between Bioactive Glasses and Cells

The series of reactions leading up to the precipitation of an HA layer on the surface of bioactive glasses has long been understood and is well documented [18, 38, 79]. The interactions that occur between these materials and cells, and perhaps the roles of these cells in the deposition of HA, are less established. The implantation of a foreign material into the body initially triggers the onset of an immune response. The wound healing cascade is spawned and is characterized by the infiltration of numerous proteins, GFs and cells leading to the formation and remodeling of a clot. The implantation of bioactive materials has been shown to instigate an immune response far less severe than with other polymers or materials. Various histological examinations have shown mixed results relative to macrophage activity on implanted bioactive glasses, varying from an absent or reduced response to the typical infiltration of macrophages expected for a foreign body reaction [24, 80, 81].

The responses of cells to bioactive materials will vary depending upon if the material is examined *in vitro* or *in vivo*. Implantation is accompanied by a drastic complication of the system due to an increase in the number of proteins, cell types, GFs and cytokines as well as the inclusion of blood flow and antibodies present within the environment. Various *in* vitro studies have been performed in an effort to control the variables present to try and determine their individual effects [11, 56, 82, 83]. However, these factors act synergistically *in vivo*, making it difficult to draw any definitive conclusions. Both *in vitro* and *in vivo* response are discussed below.

The adsorption of proteins onto the glass surface is the first step in governing the interactions likely to occur between a bioactive material and cells. These reactions begin within a short timefollowing implantation or the introduction of fibronectin or serums *in vitro*. Kaufmann et al. have showed the delayed formation of HA on the glass surface in the presence of serum proteins [84]. The nucleation of HA crystal was found to preferentially form on areas of high surface energy such as irregularities on the glass surface. Proteins however, were seen to uniformly adsorb onto the surface, forming a protective coating and hindering the formation of HA.

The adsorption of fibronectin *in vitro* has also been shown to affect the rate at which HA deposits of the surface of bioactive glass [83]. Fibronectin (Fn) has an isoelectric point of 5.5-6.0 and is thus negatively charged at physiologic pH. This cell adhesion protein is therefore prone to bond cations, such as the divalent Ca^{+2}. When compared with nontreated BG particles, Fn coated BG led to a much slower rate of HA deposition and crystallization. The competitive binding of calcium ions by the Fn led to a decrease

in available calcium for the deposition of HA. Therefore, the advantage of preferential cellular attachment is countered by a decrease in the rate of bioactivity.

Lobel et al. have shown the dependence of protein adsorption on the composition of the glass [20, 21]. Increasing the silica content present in the glass led to a decrease in the reaction kinetics of protein adsorption, thereby reducing the gap in bioactivity seen between melt derived and sol gel glasses. This affect is likely to influence cellular activity as well. Similarly, 45S5®, 58S and 77S bioactive glasses have all been compared and shown to exhibit differences on cellular metabolism, intracellular ion concentration, and viability [85].

Xynos et al. investigated the effects of the ionic products of 45S5 Bioglass ® on the gene expression profile of human osteoblasts derived from the femoral head of THA patients [7]. A 1% w/v solution of particulate Bioglass was incubated in Dulbeco's MEM for 24 hours and resulted in an 86,000% increase in Si, 10% increase in Ca, and 10% decrease in P within the medium. Subsequent culture of osteoblasts in the dissolution medium followed by cDNA microarray analysis showed an upregulation in excess of 1.5x for 76 mRNA species. Of particular interest were the following increases: fivefold for RCL (growth promoting agent), twofold for nuclear factor I (osteoblast proliferation), fourfold for cyclin D1 (cell cycle), and sevenfold for CD44 (osteocytic differentiation). These results indicated the direct effect of the ionic dissolution products on the gene expression in osteoblast cells.

The influence over bio and cellular activity by various proteins and dissolution products represents only one mechanism of action that can be harnessed from bioactive scaffolds in tissue regeneration, mainly that of a chemical influence. Further control over

cellular responses leading to the formation of new tissue can also be elicited through topological and structural cues. Variations in topography are known to affect the proliferation and morphology of cells [86]. The use of fibers to control these responses is particularly advantageous. The ability to adjust fiber diameters and compositions to tailor porosity, modulus and degradability allow for the engineering and design of constructs with well defined properties. Fibers can be used to direct cellular growth and extracellular matrix deposition through the contact guidance of cells, leading to the formation of mechanically iso or anisotropic tissues.

Various fibers such as silk, spider web, fibrin strands, glass and nylon [87-90] have been investigated for their abilities to mediate cellular growth and behavior. While the chemical nature of the fibers does have an affect on cellular response, the physical nature of the fiber can play an even more pronounced role in the organization of cells. Fiber diameters of less than ~100 μm have been shown to have the most profound affect on the orientation of cells with respect to the long axis of the fiber, with an inverse relationship between diameter and elongation. As diameters increase above this critical value, the control over the growth of cells diminishes, and cells grow in a spiraling manner around the circumference of the fiber. In addition to fiber diameter, spacing between adjacent fibers has a controlling affect on the growth of cells. Cells have been seen to span across voids between fibers, creating a sail or bridge like structure. This new surface creates supplementary pathways for the growth and expansion of cells. These cells can also generate tensions needed for cellular differentiation and tissue formation.

Coupling the bioactive properties of bioactive glasses with the ability of fibers to influence cellular proliferation and differentiation is what makes these materials so

attractive as tissue engineering substrates for the regeneration of new bone. The ability to control porosity and degradation rates of sol gel glasses further extends the benefits. The broad range of attractive properties encompassed by these materials is responsible for the topic of this thesis.

Concluding Remarks

The preceding chapter has focused on the chemical, physical, and biological properties of bioactive glasses. The use of sol gel processing to synthesize discontinuous bioactive glass fibers results in a material with a number of advantageous properties. A fundamental understanding of such properties is the first step in designing and engineering materials for implantation into the human body. Observations and conclusions can then serve as a means of predicting *in vivo* and *in* vitro behaviors. While such an understanding may allow one to predict behavior *in vivo* it in no way has a direct correlation with *in vitro* observations. Differences are also common place between species. Results from a rat model may in fact have no connection with a human study. These experiments must be carried out, however, in order to develop rational and well thought out predictions. Variations in actual behaviors can then be analyzed in a systematic manner. Similar designs of experiments by researchers can further serve as a means of analysis through direct comparisons and analysis of the literature.

While much work has focused on the use of bioactive glasses in the particulate form, there is a much smaller database on these materials in the fibrous form. Additionally, most glasses that have developed through the research stage and onto clinical use are melt derived. Described within this work is the development of sol gel derived bioactive glass fibers through the incorporation of the polymer polyvinylpyrrolidone. The addition of this polymer was found to have benefits on the processing and stability of the synthesized

glass sol. The chemical and physical properties of these materials have been examined *in vitro*, as has their biological activity and influence over rat mesenchymal stem cell behavior. The observations and results obtained from such experiments intends to serve as a basis for the further development of these materials for use as tissue engineering substrates in the regeneration of new bone.

CHAPTER 3
SYNTHESIS AND CHARACTERIZATION OF POLYVINYLPYRROLOIDONE MODIFIED BIOACTIVE GLASS FIBERS

Introduction

Since their conception some 30 plus years ago by Larry Hench at the University of Florida, bioactive glasses have undergone extensive study and development. The nature of these materials that leads to the formation of a chemical bond with the host tissue has made them particularly attractive as substrates for bone regeneration. The advent of sol-gel chemistry as a method of synthesis has led to an increase in compositional ranges, facilitation in glass processing, and controllable rates of degradation. This has broadened the range of applications for bioactive materials, allowing them to be used as particles, fibers, films, and coatings [4, 11, 14, 15, 23, 25-29, 31, 78, 91, 92]. Various compositions of some common bioactive glasses are shown in Table 3-1.

Table 3-1. The oxides compositions of a various bioactive glasses. The oxides are given in mol percent.

Glass	**Processing**	**SiO_2**	**CaO**	**P_2O_5**	**Na_2O**
45S5	Melt	46	27	2.6	24.4
58S	Sol	60	36	4	0
77S	Sol	80	16	4	0
86S	Sol	90	6	4	0
100S	Sol	100	0	0	0

The production of sol-gel derived silica and bioactive glass fibers has been described by a number of authors [11, 27-29, 91, 93, 94]. All systems were based upon the hydrolysis of tetraethoxysilane using an acid catalyst (HCl or HNO_3), followed by the removal of solvent (ethanol) to yield a viscous sol. The sol was then drawn or extruded through a spinneret and wound onto a rotating drum (dry spinning) to yield fibers. The sizes and shapes of the fibers can thus be controlled through adjustments in sol viscosity, the spinneret diameter, aspect ratio, and shape as well as the drum speed, circumference, and distance from the spinneret.

Key to the success of spinning sol gel derived silica fibers is the size and structure of the silica chains. Following hydrolysis, condensation of silanol groups leads to the formation of water and siloxane bonds. Adjusting reagent ratios to favor the formation of linear silica chains is advantageous to spinning fibers. Such is the case when the ratio of water: TEOS is fixed at 2:1, although a statistical distribution of the number of hydrolyzed ethoxy groups will occur. Setting this ratio at 2:1, however, is more likely to result in a higher distribution of TEOS molecules in which 2 of the 4 ethoxy bonds are hydrolyzed. Additional water will lead to a greater degree of hydrolysis, with a greater percentage of the TEOS molecules having 3 or 4 hydrated ethoxy bonds. This increased degree of hydration will then lead to the formation of groups and clusters through an increase in the functionality of the reacted TEOS.

Kursawe et al. showed that the initiation of silica chain growth during condensation was highly dependent upon the amount of remaining solvent in the sol [93]. As the amount of ethanol was reduced, the size of the chains or particles was found to increase exponentially, as shown by SAXS. Sols were spinnable only when the particle radii were

between 2.0 and 2.5 nm. When the particle sizes exceeded these limits it resulted in their aggregation to form a gel.

The rapid sol to gel transformation seen by Kursawe is a common and difficult problem faced during the processing of sol-gel derived materials. Elevated temperatures and solvent extraction result in a rapid growth of the colloidal network and an increase in sample viscosity. Continued growth of the network leads to the formation of a single continuous phase, known as a gel. In order to address such issues the use of polymeric modifiers in sol gel reactions has been examined [40-45]. The use of such agents can serve as catalysts, stabilizers, and rheological modifiers. This allows for enhanced control during processing. The addition of a viscous polymer component to the system facilitates control over the viscosity during solvent evaporation. This leads to a shift in the derivation of the rheological properties from the sol towards the polymer, reducing the profound increase in viscosity seen near the rapid sol to gel transformation.

The research described within this thesis was initiated by the works of Orèfice and Dominques, who developed a method for the fabrication of discontinuous bioactive glass fibers [27, 28]. The process utilized a spraying technique, in which a bioactive glass sol was synthesized, concentrated, and sprayed through an air gun. The use of an acid catalyst, a water:alkoxide ratio of 2:1, and suitable viscosities (~1.7 Pa sec) presumably led to the formation of a linear silica chain suitable for drawing into fibers. The numerous variables associated with the process, however, made it difficult to reproduce with any regularity. Slight variations in the amount of catalyst, solvent purity and method of evaporation, aging of the gel, sol viscosity, and spraying methods all affected the ability of the sprayed material to yield fibers. Likewise, the rapid transition of the sol

to a gel near the viscosities needed for the production of fibers made it difficult to isolate a suitable material. This chapter describes improvements in the method of synthesis, mainly through the incorporation of a polymeric modifier (polyvinylpyrrolidone) into the synthesis of the glass sol. The addition of PVP was shown to enhance control over the rheological properties of the sol, particularly near those viscosities needed for spraying fibers. This led to a more reproducible and consistent mechanism of spraying and enhanced control over fiber morphologies.

Materials and Methods

Sol-Gel Synthesis

A 77S bioactive glass sol was synthesized from tetraethoxysilane (TEOS), triethylphosphate (TEP), and calcium chloride dihydrate. All reagents were used as received from Aldrich. Initially, DI H_2O was adjusted to a pH of 1.6 using 12N HCl. Varying volumes of a 5% weight solution of polyvinylpyrrolidone (PVP), $M_n = 1 \times 10^6$ g/mol, were further diluted in absolute ethanol (EtOH). For the purpose of fiber spraying approximately 1% of the total volume of the sol was comprised of the 5% PVP solution. The weight and mole fractions of PVP to the Bioglass sol were 3×10^{-4} and 4×10^{-8}, respectively. Both the H_2O/HCl and PVP/EtOH solutions were stirred for 10 minutes each, after which point they were combined and stirred for an additional 5 minutes. TEOS was then slowly added to the mixture and subsequently hydrolyzed for 60 minutes. The ratio of TEOS:H_2O:EtOH was fixed at 1:2:4. TEP and $CaCl_2$*$2H_2O$ (CC) were then added sequentially, with each reagent requiring a 60 minute reaction period. Temperature and pH variations throughout the course of the reaction were monitored using an EA 920 Expandable Ion Analyzer from Orion Research. The structures of the components used in the synthesis are shown in Table 3-2.

Table 3-2. Molecular structures of materials used in the synthesis of the Bioglass sol.

Reagent	Structure
Tetraethoxy Silane	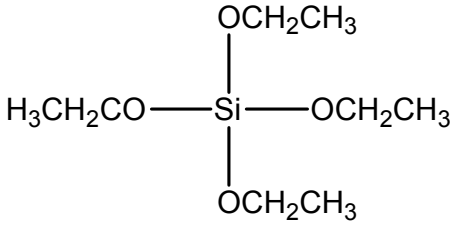
Triethyl Phosphate	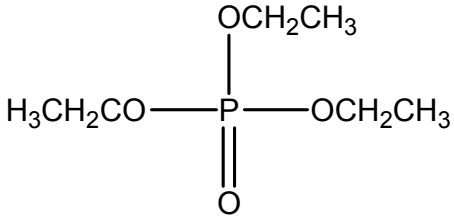
Calcium Chloride Dihydrate	$CaCl_2 \times 2H_2O$
Polyvinylpyrrolidone	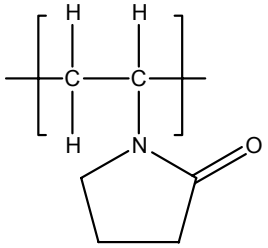

Fiber Synthesis and Characterization

Bioglass fibers (BGFs) were produced using an air spray technique, as illustrated in Figure 3-1. Prior to spraying the viscosity of the filtered sol was adjusted through the removal of EtOH, initially at 80 °C and then under partial vacuum. Viscosities were monitored using a Brookfield DV11 Digital Viscometer. When the sol viscosity reached approximately 2 Pa sec it was examined for its ability to yield fibers when sprayed. If the sprayed material was still particulate in nature further solvent was removed until a fibrous spray was observed. Upper viscosity limits for a spinnable sol approached 3 Pa sec. Fiber spraying was performed using a Badger Air Brush gun with N_2 at a pressure of 50 psi. A double action air gun was used which allowed for the simultaneous control over

the flow rate of the gas and the intake volume of the sol. Fibers were sprayed onto a polypropylene surface with surrounding airflow from approximately 1.5 meters.

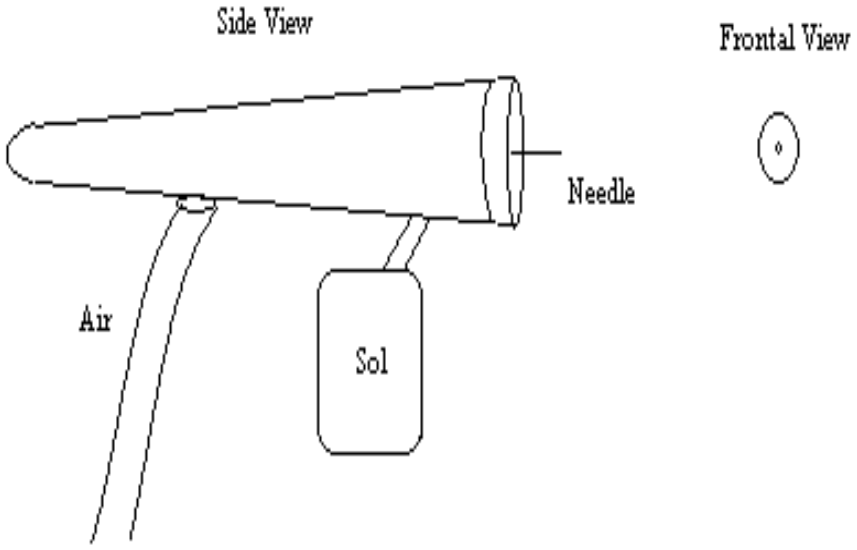

Figure 3-1. Schematic diagram illustrating the gun used to spray discontinuous Bioglass fibers. A double action gun was use to control the flow rate and sol volume passing through the gun.

After spraying the fibers were air dried overnight, stored in a dessicator, and sintered at 900°C for 3 hours (ramp rate of 2°C/min). Morphological examination of the fibers was performed using both optical and scanning electron (JEOL 6400) microscopies. Thermal analysis using a Seiko TG/DTA 220C was performed on both sintered and gelled fibers in order to monitor the transitions and mass losses that occurred during sintering. Ground fibers (~10 mg) were ramped to 1100°C at a rate of 20°C/min under an air environment.

Results and Discussion

Sol-Gel Synthesis

A 77S Bioglass sol was synthesized as described and the balanced chemical reactions are shown in Table 3-3. The adjustment of the TEOS:H_2O ratio at 1:2 favored the hydrolysis of 2 of the 4 functional ethoxy groups attached to the silicon atom. Hydrolysis of 2 of these groups increases the conducivity of the sol to yield fibers through the theoretical formation of a linear silica chain. Further addition of water to the system results in subsequent hydrolysis of the remaining ethoxy groups, leading to the formation of branched groups and clusters.

Similarly, acid catalysts in sol gel reactions favor the formation of weakly branched extended structures more suitable for spinning than sols synthesized with a basic catalyst, which results in the formation of particles and clusters. An acid catalyst also results in a slow condensation rate, allowing one to greatly enhance the viscosity through solvent removal without premature transformation of the sol into a gel [22].

Following the hydrolysis of the TEOS molecule to yield silanols is a series of condensation reactions. The remaining ethoxy groups along with the newly formed silanols condense as ethanol and water, as shown in Steps 3 and 4, respectively. This results in the formation of a linear chain containing siloxane bonds along the backbone. It is this inorganic polymer that represents the precursor of the silica backbone of the Bioglass fibers. Addition of TEP and calcium chloride dihydrate complete the network through the formation of P_2O_5 and CaO.

Table 3-3. Balanced chemical reactions for the synthesis of a 77S Bioglass sol. Continued condensation of silanol groups leads to the formation of an extended silica chain.

Step	Reaction Type	Balanced Reaction
1	Hydrolysis of TEOS	$Si\text{-}(OCH_2CH_3)_4 + 2H_2O \Leftrightarrow Si\text{-}(OH)_2(OCH_2CH_3)_2 + 2CH_2CH_3OH$
2	Alcohol Condensation	$(OCH_2CH_3)_2\ Si\text{-}(OCH_2CH_3)_2 + (OCH_2CH_3)_2\ Si\text{-}(OH)_2 \Leftrightarrow (OCH_2CH_3)_2Si\text{-}O\text{-}Si(OCH_2CH_3)_2 + 2CH_2CH_3OH$
3	Water Condensation	$(OCH_2CH_3)_2Si\text{-}(OH)_2 + (OH)_2\text{-}Si(OCH_2CH_3)_2 \Leftrightarrow (OCH_2CH_3)_2Si\text{-}O\text{-}Si(OCH_2CH_3)_2 + 2H_2O$

The thermodynamic variations in temperature and pH through the course of the reaction are illustrated in Figure 3-2. The temperature and pH variations of the sprayable 77S BG sols synthesized with PVP closely matched that of the synthesis of a 77S BG sol without the addition of PVP, indicating a minimal affect on reaction kinetics with the addition of PVP [27]. The exothermic hydrolysis of TEOS led to a near two fold increase of the reaction temperature from 20.5°C to 36.0°C. Additionally, this hydrolysis resulted in an increase in the pH of the system from a value of 1.6 to a peak value of 4.0. This may be attributable to the reactivity or complexation of the acid catalyst resulting in the formation of silanol groups on the original TEOS molecule and the liberation of ethanol moieties. The decrease in pH to near the initial value of 1.5 following the hydrolysis of TEOS indicates the liberation of the complexed catalyst to its original form, and a rapid hydrolysis of the TEOS molecule.

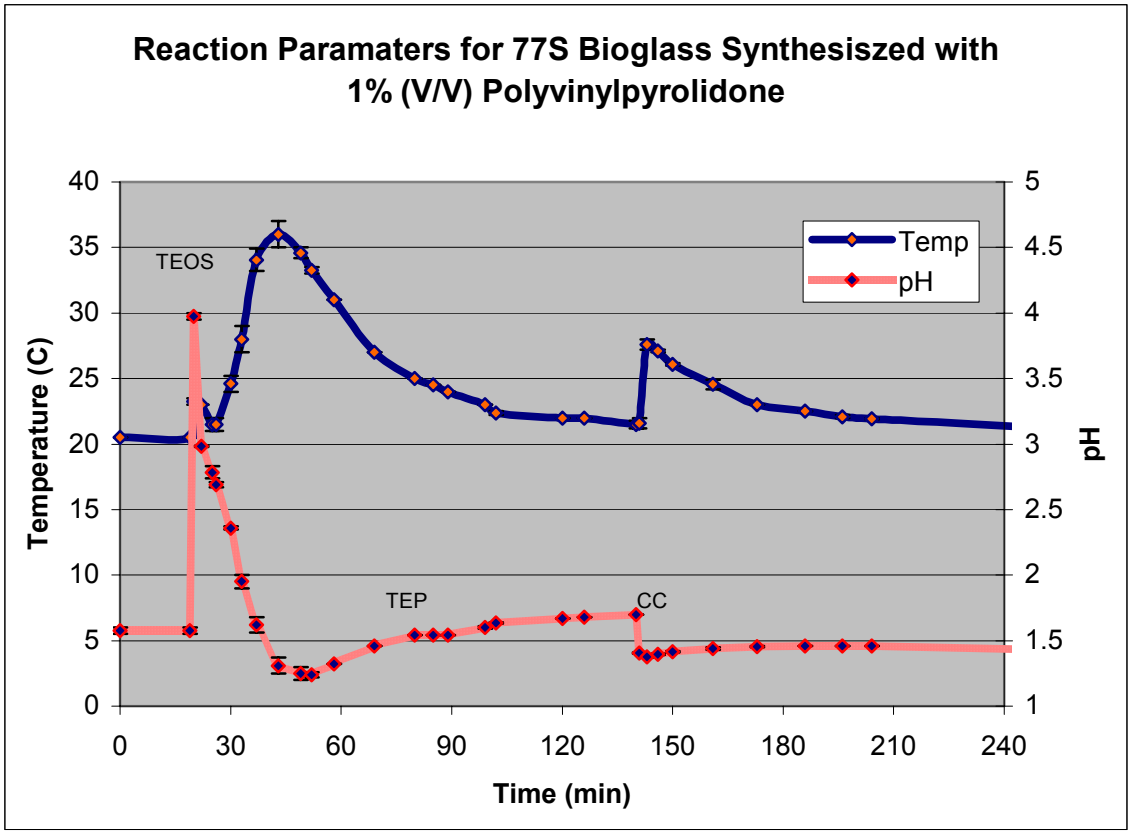

Figure 3-2. Reaction conditions during the synthesis of a 77S Bioglass sol containing polyvinylpyrrolidone.

Incorporation of Polyvinylpyrrolidone In a Sol-Gel Reaction

Polyvinylpyrrolidone was successfully incorporated into the synthesis of the Bioglass sol. The addition of the polymer was initially done to enhance control over the rheological properties but was found to have additional benefits, mainly through the stabilization of the sol resulting in prolonged gelation.

Addition of PVP to the BG sol during synthesis resulted in a two phase phenomena. The addition of small amounts of PVP would result in a phase separation, clouding the solution. This was followed by an aggregation of the majority of the precipitate. Continued stirring of the sol did not result in resolubilization. This was

observed when the added volume of PVP was less than 1% of the total sol volume. DSC confirmed the precipitate as being PVP through a comparison of the T_g with unreacted PVP. The 2 T_g's were within 5°C of each other. As the amount of PVP added to the sol was increased a different mechanism was observed. Initially the sol would become cloudy; however, continued stirring resulted in an aggregation of the precipitate followed by dissolution back into solution. Varying the amounts of the PVP solution from ~1-45% of the entire sol volume were seen to follow this phenomena.

Polyvinylpyrrolidone dissolved in EtOH was observed to remain soluble when individually added to TEOS and water. During the hydrolysis of TEOS, however, a phase separation led to the formation of a precipitate, indicating insolubility of PVP in the intermediate structure containing silanol and ethoxy groups. For the low concentration PVP solutions (C<1%) the precipitate failed to redissolve. The polymer acted as a flocculation agent, resulting in the aggregation of the TEOS intermediates and their subsequent precipitation [41, 46]. The amount of the polymer was insufficient to completely coat the forming silica chains and in turn led to the entrapment of the TEOS intermediate within the loops and tails of the polymer chain and subsequent precipitation [48]. The use of polymers in this manner is a common means of precipitating small molecules, thus acting as a filtration system. Common practices are seen in such areas as sewage treatment.

As the amount of PVP added was increased the resulting precipitate was short lived. Continued stirring led to the return of the aggregate to solution after approximately 10 minutes. In these sols the amount of PVP was increased above the lower limit of solubility. The increased amounts of PVP may have acted to completely coat the silica

chains, thus resulting in a solubility between the inorganic and organic phases. These samples were found to have advantageous properties. Interchain bonding led to favorable interactions and a remaining of PVP in solution.

Because of the phase separation that was seen upon the addition of PVP, an adjustment to the procedure was developed. The EtOH solution containing PVP was added to TEOS and stirred for ~10 minutes. This was accompanied by a retention of PVP in solution. Following this was the addition of DI water. The small amount of water relative to TEOS allowed for a more rapid introduction to solution and was without precipitation. The more rapid introduction of the water to TEOS most likely also led to a more homogeneous hydrolysis. This would have advantages in fiber spraying.

Those sols without precipitate were observed to remain in the solution state much longer than BG sols synthesized without PVP (Figure 3-3). Gelation was prolonged for 4 months in quiescent samples stored under ambient conditions (~23°C and 70% humidity), whereas those synthesized without PVP would often gel within three to four weeks. Varying the amount of PVP solution added to encompass the entire volume of required EtOH also had a similar affect, prolonging gelation in excess of 3 months. Addition of PVP led to steric stabilization of the sol and enhanced the shelf life [44, 45].

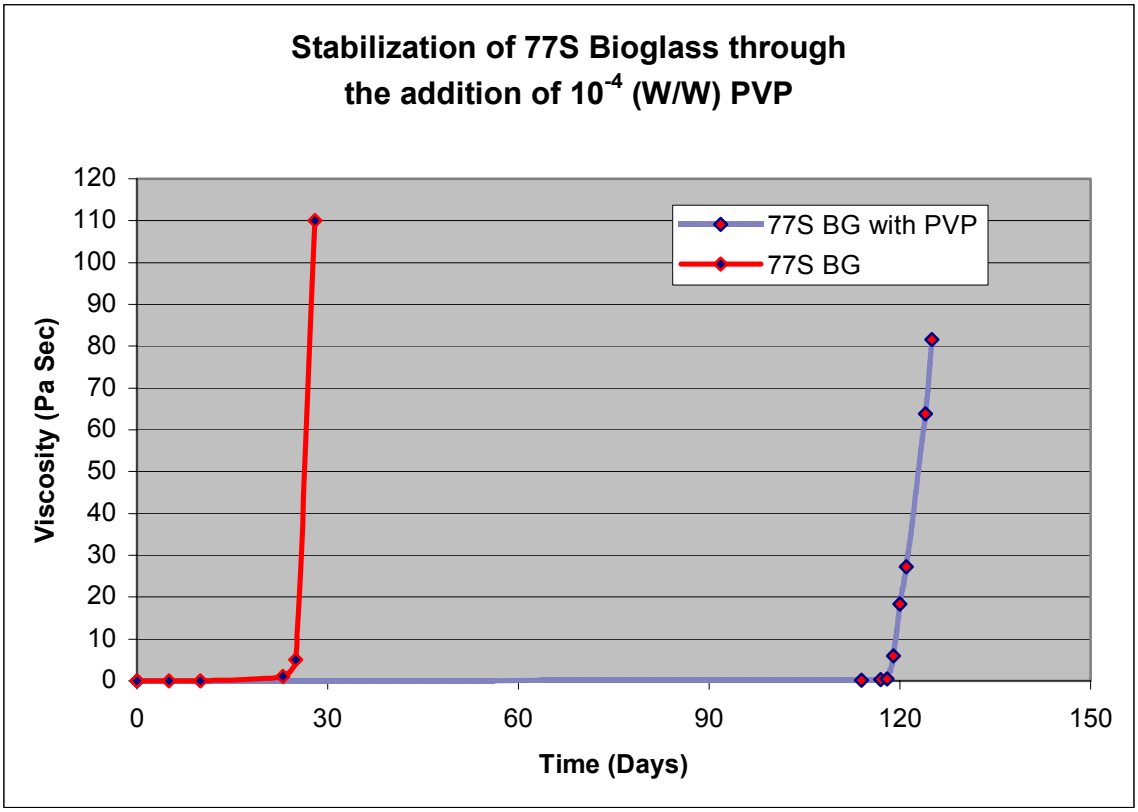

Figure 3-3. The stabilization affects of polyvinylpyrrolidone added during the synthesis of a Bioglass sol. Sols containing PVP remained in the solution state much longer than those sols without PVP.

The interactions that occurred between the silica chains and the PVP incorporated into the sol contributed to the stabilization. These interactions may have hindered the further collisions of silica chains, impeding the growth of the network to a single, continuous phase. Hydrogen bonding between the nitrogen and oxygen present of the PVP molecule with the silanol groups on the hydrated TEOS may have served to stabilize the intermediate structure, slowing condensation and the growth of the silica network. This decreased rate of condensation would lead to a slower rate of polymerization and prolonged gelation of the sol. Hydrogen bonding between water and PVP may have also acted to reduce the rate and degree of hydration. Additionally, the high molecular weight of PVP likely acted to further stabilize TEOS by sterically hindering it from further

reactions. The ability of the large polymer chain to coat or surround the partially reacted TEOS hindered the ability of water to attack the central silicon atom by a nucleophilic mechanism. This steric hindrance resulted in a further reduction in hydrolysis.

Fiber Spraying

Discontinuous, short BGFs were produced as described and can be seen in Figure 3-4. The fibers formed an intertwined, randomly oriented mesh that took on the appearance of a glass wool like material. Fibers were relatively soft prior to sintering, but following heat treatment they were much more brittle in nature.

The addition of PVP to the BG sol led to a profound affect on the facilitation of the spraying process. The spraying of the BG sol into fibers is greatly affected by a number of variables. Mediation of each and every one is critical in the success of the process. These variables, discussed below in detail, are initiated with the synthesis of the sol and proceed through the spraying of the material.

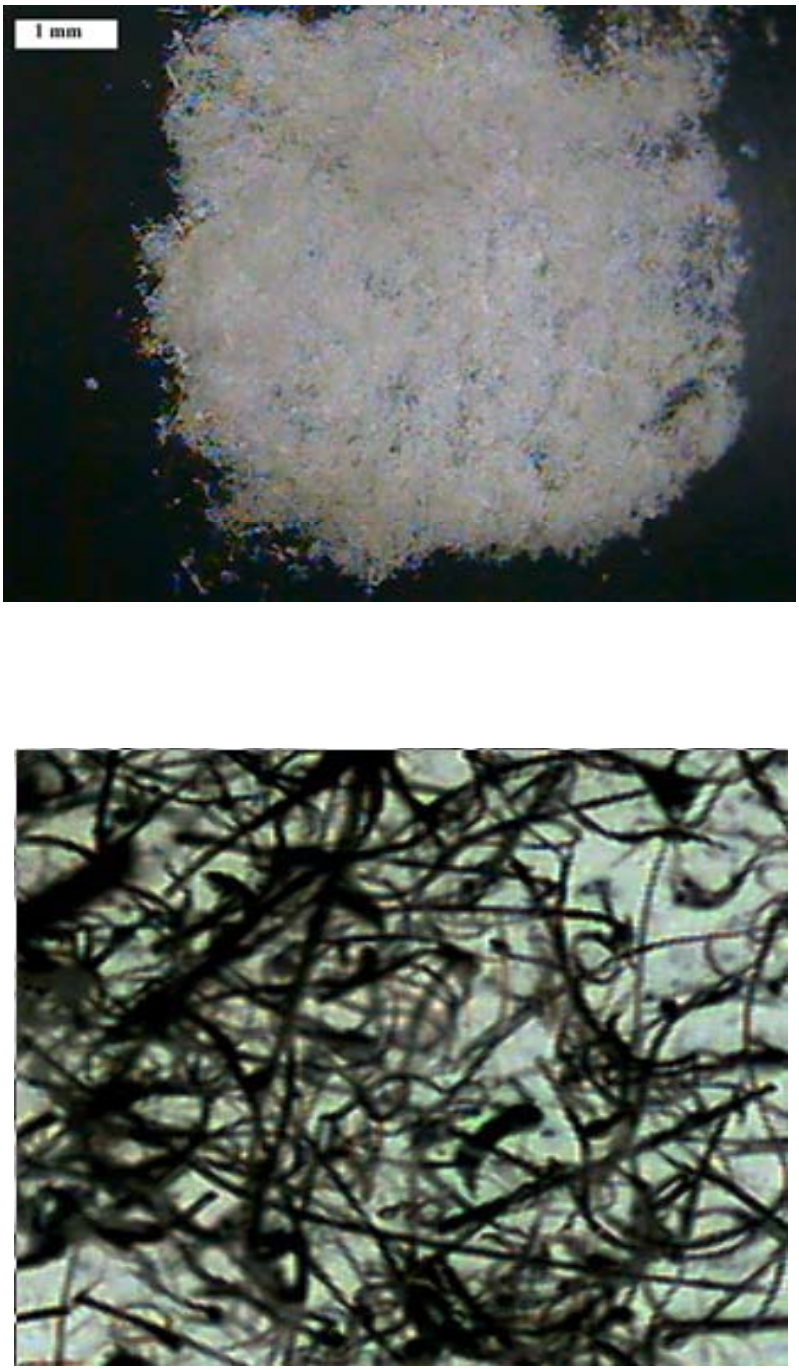

Figure 3-4. Images of 77S Bioglass fibers synthesized with polyvinylpyrrolidine and sintered at 900°C. Figure (a) illustrates the glass wool like nature of the fibers (SB = 1 mm). Figure (b) is a 60x optical micrograph of the fibers.

Polyvinylpyrrolidone as a Rheological Modifier

The addition of PVP to the BG sol greatly facilitated the spraying process. Previous synthesis of a BG sol without the incorporation of PVP led to a material which was often difficult to spray into fibers due to the rapid sol to gel transition. The range of acceptable spraying viscosities was closely mirrored by the transition of the sol to a gel, and as the material approached viscosities near those suitable for spraying the sol would often gel. Isolation of a sol suitable for spraying was therefore difficult to achieve due to the rapid transition in the viscosity range of interest. Addition of PVP allowed for enhanced control over the rheological properties, negating the need to precisely isolate the sol just prior to its transformation into a gel. Modulation of the sol viscosity in this manner thus broadened the region over which the material could be sprayed into fibers. A generic illustration of the prolonged gelation during the removal of solvent is shown in Figure 3-5.

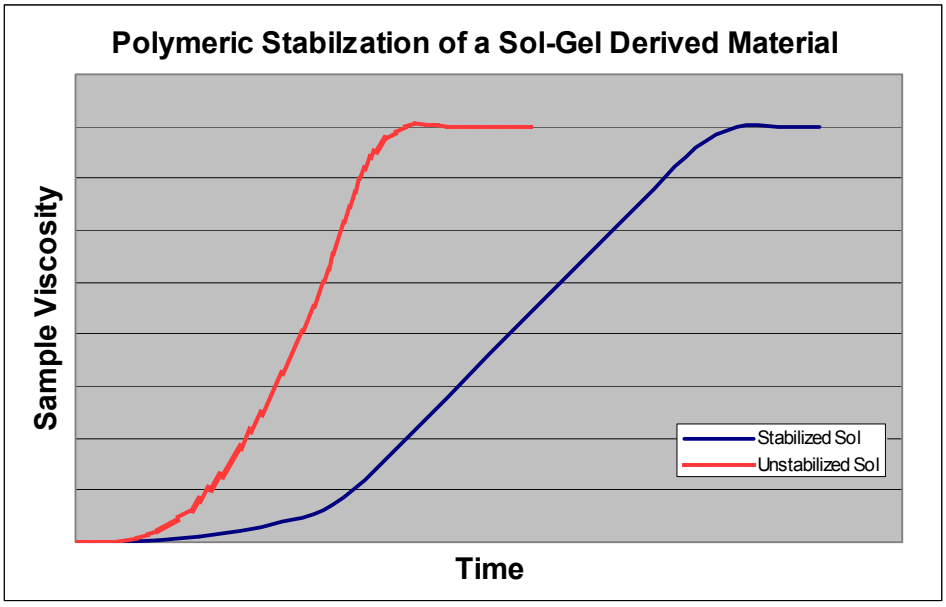

Figure 3-5. Generic diagram illustrating the stabilizing effect of polyvinylpyrrolidone on a Bioglass sol through the delay of gelation during solvent removal. Both the point at which gelation began to occur as well as the rate at which it proceeded were shifted through the addition of PVP.

The incorporation of polymers to into sol gel derived materials can serve as both stabilizing agents and rheological modifiers [40-43]. The regulation of sol viscosity is of key importance when the synthesized material is to be further processed into fibers. The synthesis of an organic-inorganic hybrid material composed of silica chains and a high molar mass PVP addressed this issue and allowed for an enhancement in fiber production. The lengthy PVP chains were able to interact with the silica chains, increasing the sol viscosity most likely through hydrogen bonding and van der Waals interactions.

Variables of the Spraying Process

The ability of a sol-gel derived material to produce fibers is dependent on a number of variables. The ratios of the reagents and the pH of the system are two important parameters that have previously been discussed. Additionally one must consider the method and degree of solvent removal, the final viscosity of the sol, and the addition of viscosity modifying agents.

The manner in which ethanol was removed from the system was found to have a profound affect on the facility with which fibers could be sprayed. Removal of solvent was carried out in two steps, initially at 80°C and then under partial vacuum. Concentration of the sol in this manner allowed for improved control over the rheological properties, hindering the rapid onset of gelation. When solvent was removed in a slow and mediated manner from the BG sol, the resulting material was most often a Newtonian like fluid. Those sols without PVP or when solvent removal was carried out in a more rapid manner often yielded a psuedoplastic fluid. The Newtonian fluid was sprayed into fibers much more easily than the shear thinning fluid, most likely due to its ability to

maintain the integrity of the silica network when subjected to the high shearing forces of the spraying process. The Newtonian like sol containing PVP resulted in a highly homogeneous distribution of fibers, with less particulate material than was observed in a shear thinning or BG sols alone. Thus, mediation of the viscosity through PVP addition yielded a sprayable material that led to an increase in the efficiency of fiber production. Viscosity profiles of both a sprayable and nonfiber producing sol are shown in Figure 3-6. Despite having a viscosity within the defined limits for fiber production (2-3 Pa sec), the shear thinning nature of the nonfiber producing sol led to a much more particulate material.

Fiber Characterization

Fibers were characterized through microscopic observation and thermal analysis, as discussed below.

Microscopic Evaluation

Fibers were examined and characterized through microscopic observation. SEM images of representative fibers are shown in Figure 3-7. SEM analysis of fibers gave a mean diameter of 9.37 ± 5.34 μm ($n = 53$), with an upper and lower limit of 22.0 and 2.55 μm, respectively. The percentage of fibers having diameters between 5 and 15 μm was 66%. The fibers had a wide distribution of lengths ranging from 0.5-2 mm, with an estimated average length of 1mm.

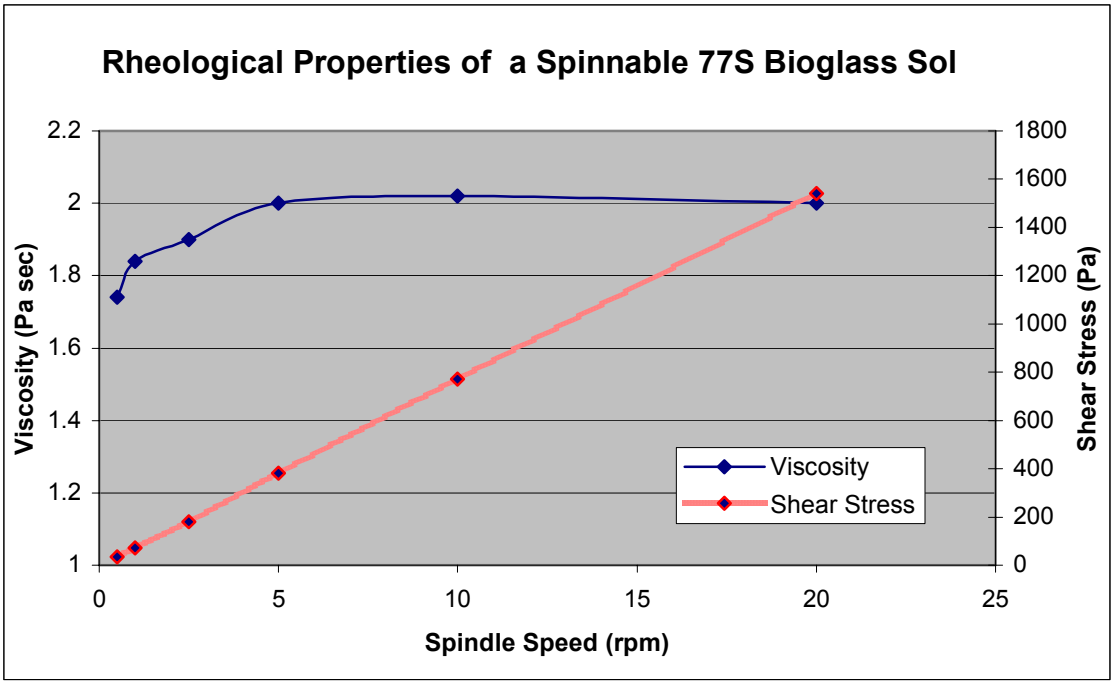

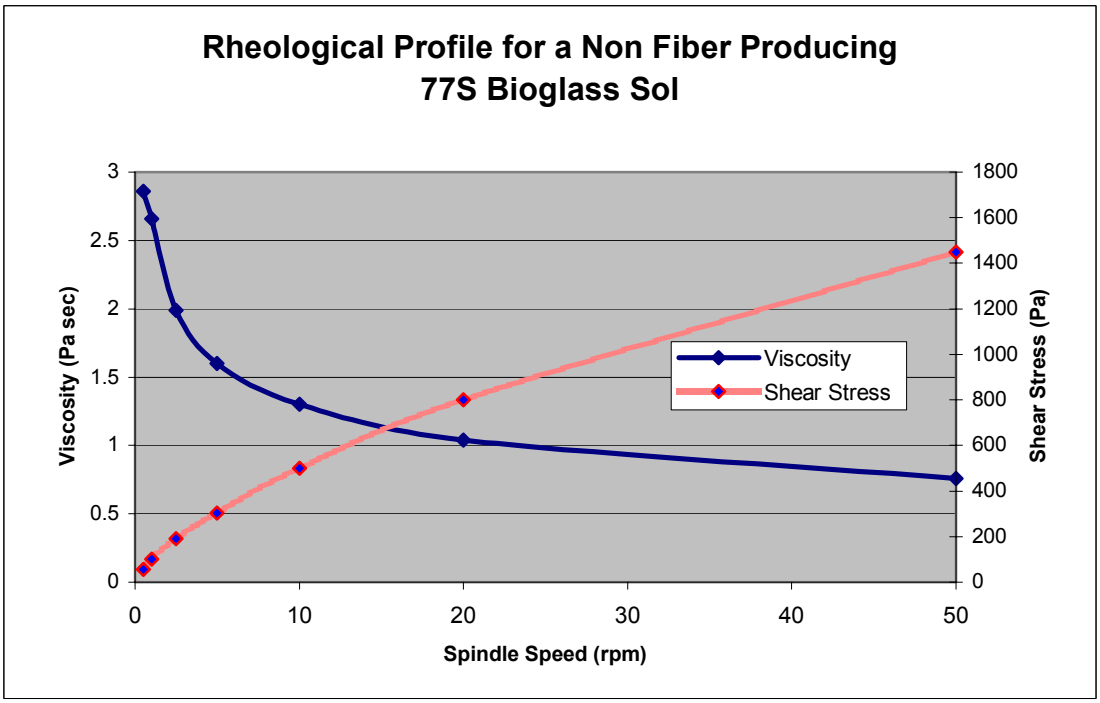

Figure 3-6. Viscosity profiles of both spinnable and nonspinnable 77S Bioglass sols. Those sols that were synthesized with PVP led to a Newtonian like fluid (a) which was more easily sprayed into fibers. Those sols without PVP were often shear thinning in nature, and those that were highly shear thinning like the sol depicted in (b) were unable to yield fibers.

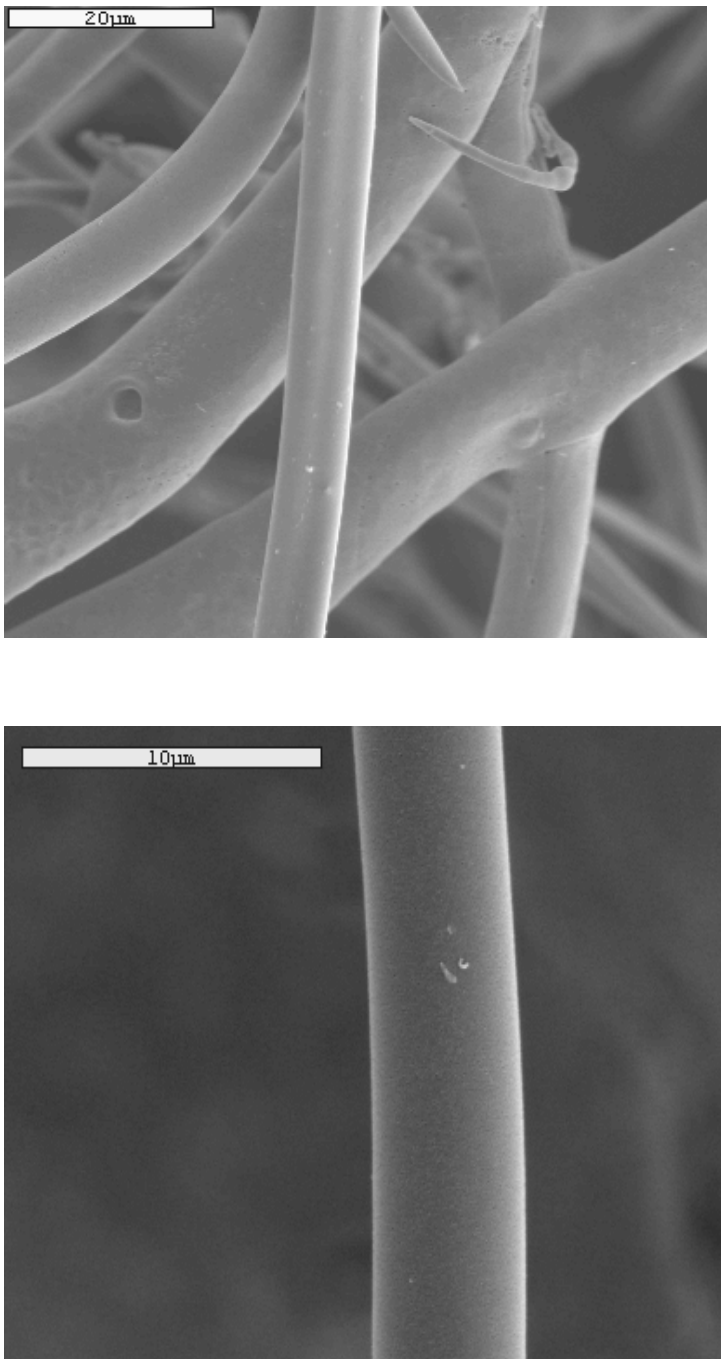

Figure 3-7. SEM images of sintered 77S Bioglass fibers. Figure (a) is a grouping of fibers (1300x, SB = 20 μm) and (b) shows a single isolated fiber (4500x, SB = 10 μm).

Bioglass fibers were sintered at 900°C as a means of collapsing the pore structure, densifying the fibers, and pyrolizing the remaining ethoxy moieties attached to the backbone. An unsintered Bioglass fiber can be seen in Figure 3-8 and can be compared with a sintered fiber in Figure 3-7b. The gelled fiber has a highly porous surface, with an increased number of voids and sites of weakness when compared with sintered fibers. It is therefore likely that the nonheat treated fibers would result in an increased resorption rate and decreased performance in mechanically stressed environments.

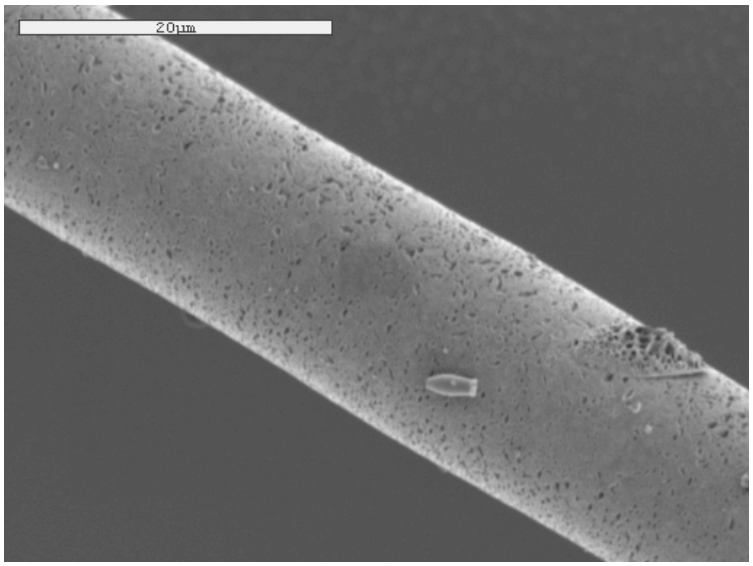

Figure 3-8. Gelled 77S Bioglass fiber. The absence of heat treatment leaves a rough, porous surface which presents enhanced opportunities for mechanical weakness and an increased surface area leading to faster resorption.

Sintered fibers examined under SEM were generally observed to have one of two morphologies. Most fibers were seen to have smooth, nonporous surfaces post sintering, as seen in Figure 3-7b. This smooth, nonporous surface is likely to lead to an enhancement in the strength and mechanical properties of these fibers due to the absence of large or numerous voids. In addition, these fibers are more prone to remain

structurally intact *in vitro* or *in vivo* due to a lower surface area when compared to a porous structure. In conjunction to the smooth and nonporous morphology seen in most fibers, certain batches of fibers exhibited rough and porous surfaces, somewhat similar to those seen in gelled fibers, Figure 3-8. The increased porosity in these samples was most notably seen when solvent evaporation was carried out in a rapid manner, often utilizing a single step evaporation procedure at 80°C. The porosity present in these samples is a result of a phase segregation between the various oxide components of the 77S Bioglass. As the rate and degree of polymerization is increased, changes in the interactions between the chemical components are altered and can lead to a separation of the phases. This was shown by Yu [95] and Kaji, Nakanishi and Soga [96-98]. The faster polymerization rates that were shown to initiate phase separation earlier in their systems were also seen in the single step evaporation of solvent in the present work. Fibers derived in this manner were most often the ones that exhibited higher degrees of porosity.

The compatibility of multiple components resulting in a single phase network was described by Flory and is based on the free energy of the system [98]. The Flory-Huggins theory for the free energy change upon mixing for polymer solutions is given as:

$$\Delta G = (N_T/\beta)\ \{\varphi_1 \ln\varphi_1 + (\varphi_2/P) \ln\varphi_2 + \chi\, \varphi_1\varphi_2\}$$

where φ_1 and φ_2 represent the volume fractions of the solvent and polymer, respectively, P represent the degree of polymerization, $\beta = 1/kB_T$ is the inverse temperature, N_T is the total number of lattice cells, and χ is the interaction parameter. Increasing the degree of polymerization will shift the value of ΔG towards more positive values, until eventually $\Delta G > 0$. When the second derivative of delta G with respect to φ is zero,

$d^2(\Delta G/N) / d\varphi = 0$, spinodal separation occurs [99]. Additionally, removal of solvent will further affect the solubility parameters of the system through changes in the volume fractions. This introduces a complication to the theory however, due to its assumption of constant volume during mixing. Continued growth of the silica chain accompanied by the non highly regulated removal of ethanol resulted in the formation of a porous structure characteristic of a phase separation mechanism.

Thermal Analysis

The thermogram for unsintered fibers is shown in Figure 3-9. Gelled 77S BG fibers exhibited a 42.5% mass loss from 0-1100 °C, with the thermal transitions being distributed into three regions [22]. The initial transition region, denoted by the endothermic peak on the DTA curve, represents the evaporation of residual solvent and physically adsorbed water. In this region between 25˚C and 150˚C, the BG fibers experienced a 21.9% loss in mass. The large amount of solvent and water lost during this phase are attributable to the absence of drying and a relative humidity in excess of 70% during processing. The second transition confined to 150˚C to 500˚C accounted for a 14.6% loss in mass, primarily due to the loss of organic compounds associated with condensation of the residual metal alkoxides. The R value was fixed at 2:1 in these sols, thus leaving two of the four ethoxy bonds unreacted. Both an endothermic and exothermic DTA peak within this temperature range are likely attributable to carbonization and oxidation, respectively [22]. The final transition region from 500˚C to 1000˚C has a total mass loss of 3.1%. In this region 2 endothermic peaks on the DTA curve were observed at ~770˚C and 975˚C, which may be ascribed to a small amount of residual $CaCl_2$ or the glass transition of the material. The PVP was also pyrolyzed during

the sintering of the fibers, although its small contribution to the overall weight of the material made it difficult to discern any transitions. As expected the TG/DTA run of fibers sintered at 900˚C showed no transitions or mass loss in the temperature range analyzed.

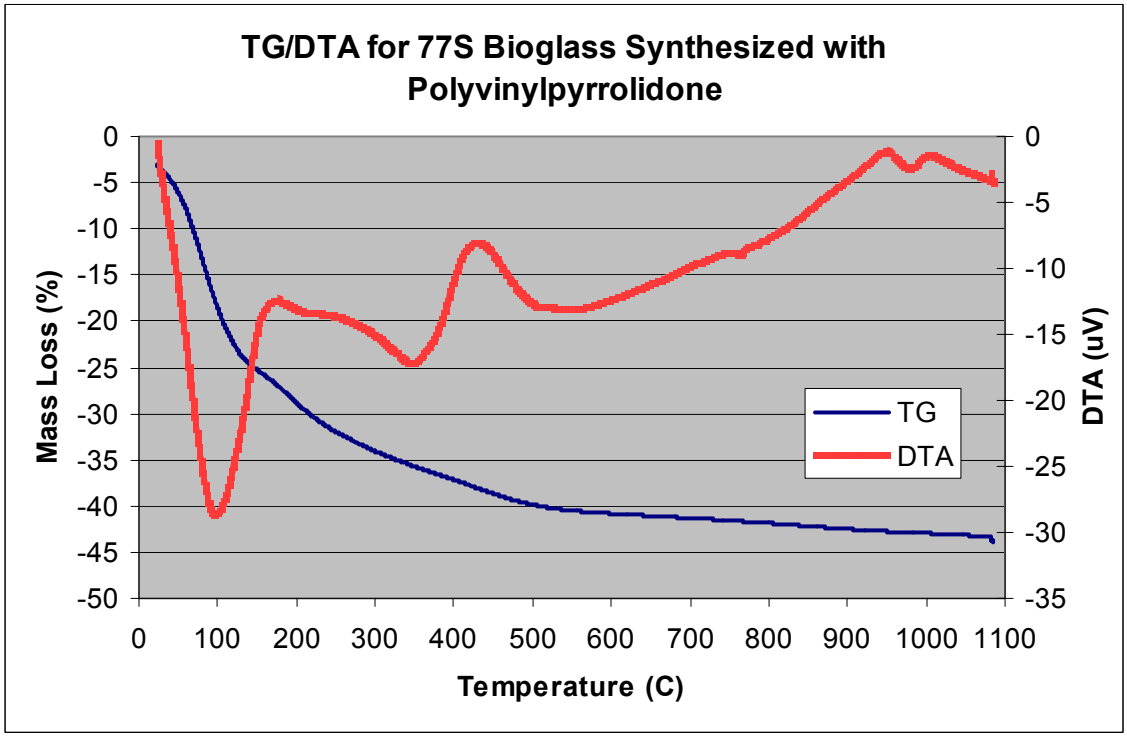

Figure 3-9. Thermogram for gelled 77S Bioglass fibers synthesized with 1% polyvinylpyrrolidone.

Conclusions

Bioactive glass fibers were successfully synthesized with the incorporation of PVP. This led to a profound improvement over the rheological properties of the sol, markedly facilitating the spraying process. Combining inorganic and organic materials to create novel materials such as these fibers allows one to tailor the properties necessary to fabricate the final, usable structures. The spraying of discontinuous fibers from a sol gel derived material is a difficult task to reproduce with any consistency, due to the feeble nature of the sol gel reaction and the necessity to isolate a viscous sol just prior to its

transformation into a gel. The incorporation of polymers, and in particular PVP, is a suitable and beneficial manner of enhancing control over such a system. The PVP was also shown to have a stabilizing effect on the synthesized sol, delaying gelation for periods far exceeding unmodified sols. Such results allow one to synthesize larger volumes of sol and to keep them stored until needed, and may lead to the commercial synthesis and distribution of pre-synthesized sols.

Various concentrations of PVP were found to be compatible with the BG sol, remaining in solution as a single phase. Although the polymer was removed from the ceramic fibers through pyrolysis, modifications in the methods of heat treatment could be used to synthesize composite fibers of Bioglass and PVP. Varying the concentrations of PVP could be used to fabricate composite structures of differing degrees. These new fibers may have additional uses and biological applications, with potentially tailorable bioactivities and degradation rates. The incorporation of PVP also opens the door for the integration of other polymers, most notably those that are water soluble. Likewise, these may be used to create composite fibers for which properties such as degradation and mechanical strength can be tailored.

The synthesis of these fibers represents the first in a number of steps of development, moving through *in vitro* analysis, animal testing, and ultimately implantation in humans as a means of regenerating new bone. The facilitation of spraying and the ability to reproduce their fabrication with consistency gives way to the second stage of analysis, the *in vitro* bioactivity of the fibers and their ability to generate and guide cellular responses. These two subjects are addressed in the following chapter.

CHAPTER 4
IN VITRO BIOACTIVITY AND RAT MESENCHYMAL STEM CELL RESPONSE TO DISCONTINUOUS BIOACTIVE GLASS FIBERS

Introduction

The *in vitro* bioactivity of bioactive glasses leading to the formation of a hydroxyapatite layer on the glass surface has been well documented [12, 13, 24, 38]. As discussed in Chapter 2, however, the interactions that occur with cells is less understood. Numerous studies have published conflicting results on the interactions of cells with bioactive glasses, the presence of macrophages, the mechanisms of bone formation and the dissolution of glasses [24, 25, 34, 80, 81, 85, 100, 101]. A detailed comparison can be found in Appendix B. Because of the simultaneous occurrence of cellular and bio activity within the body, it is important to develop an understanding of their synergistic actions.

Cells derived from the marrow stroma of bones are the precursors to a number of cell lines including the osteoblast lineage. Under the right conditions these MSCs will differentiate into bone. This is dependent upon oxygen availability, GF induction, and in the case of implanted materials is affected by the nature of the scaffold. The ionic products and formation of HA on bioactive materials can affect the genetic expressions of MSCs and mediate phenotype [7]. It is also known that the presence of proteins affects the deposition of HA onto the surface of bioactive glasses [83]. Their adsorption onto BG surfaces begins immediately following implantation or exposure to serums. These

molecules play a prominent role in the actions of cells, and are often necessary in their adhesion, growth, proliferation, and differentiation.

The ability of bioactive glasses to generate the inorganic component of bone coupled with the formation of the organic ECM and mature bone cells derived from MSCs make the use of these materials an attractive option in tissue engineering new bone. Small amounts of autogenous MSCs can be isolated from a patient and expanded in culture in the presence of the implant scaffold. This can further be mediated with the addition of GFs. Following development of these materials *in vitro* they can be implanted into a tissue defect or abnormality as a means of regenerative therapy. The influential ability of discontinuous bioactive glass fibers on rat MSCs is investigated in this chapter.

Material and Methods

In vitro Bioactivity

In vitro bioactivity of the fibers was performed in a simulated body fluid (SBF). The SBF was prepared by dissolving NaCl, $NaHCO_3$, KCl, K_2HPO_4, $MgCl_2*2H_2O$, $CaCl_2*2H_2O$, and Na_2SO_4 in ultrapure water, and contains ionic concentrations representative of interstitial fluids [102]. The concentrations of the ions in the SBF are listed in Table 4-1.

Approximately 50 mg of fibers were submerged in 2.5 mL of SBF and incubated at 37°C. Fibers were maintained under quiescent conditions for 1, 5, 10, 20 and 30 days. The SBF was changed every other day for the first 10 days and then every fifth day thereafter. After submersion, fibers were washed in EtOH (3x) and dried at 37°C overnight prior to mounting for SEM.

Table 4-1. Ionic concentrations present in the simulated body fluid solution.

Ion	Concentration (mM)
Na^{+}	1.42E+02
K^{+}	5.00E+00
Mg^{+2}	2.01E+00
Ca^{+2}	2.50E+00
Cl^{-}	1.49E+02
HCO_3^{-}	4.17E+00
HPO_4^{-2}	9.98E-01
SO_4^{-2}	5.00E-01

Fibers were examined under SEM (JEOL 6400) and the presence of hydroxyapatite was confirmed using Energy Dispersive X-Ray Spectroscopy (EDX) and X-ray analysis (XRD). A Phillips APD 3720 X-ray powder diffractometer was used to analyze samples with CuKα radiation (40kV and 20 mA). XRD spectra were obtained over a 2θ range of 10-60˚ with a step size of 0.02˚ and scan rate of 0.02˚/sec.

Rat Mesenchymal Stem Cell Culture

Rat mesenchymal stem cells (RMSCs) were obtained from both femora of grown (~ 250 g) Wistar rats, courtesy of Dr. Colin Sumner's lab, following the procedure initially describe by Maniatopoulos et al. [103] and later by Lennon and Dennis et al. [54, 104]. The procedure was as follows:

The femurs were harvested by blunt dissection, cleaned of remaining muscle and tissue, and soaked in medium highly supplemented with antibiotics. Both epiphyses were removed to slightly expose the proximal and distal ends of the marrow cavity. The marrow plug was flushed from the cavity using an 18G needle and 25 mL of α minimum essential medium (α MEM) into a PS petri dish. Repeated aspirations through a clean

needle were performed in order to break apart the tissue. Cells were then seeded into a 75 mm^2 culture flask and allowed to grow for 7 days. The method of extraction is illustrated in Figure 4-1.

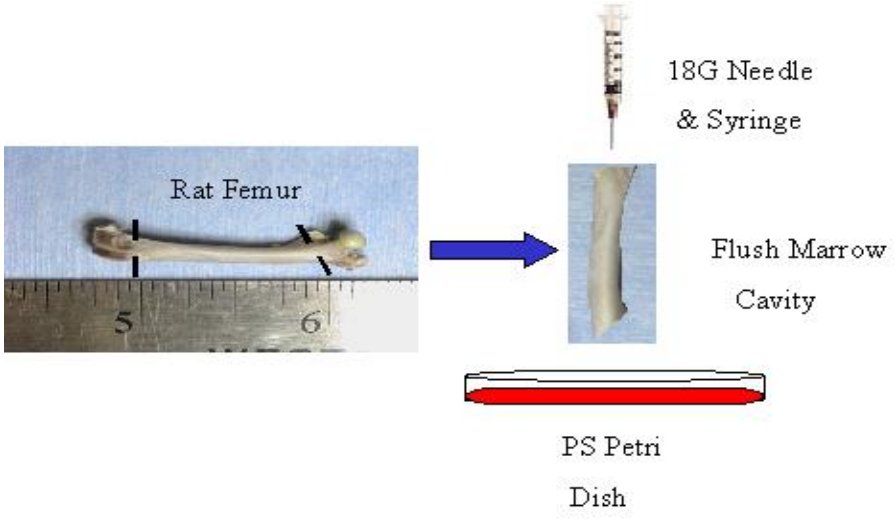

Figure 4-1. The procedure for the extraction and culture of cells present within the bone marrow of rats.

First passage was performed at this point, following the removal of noncontact dependent cells through a discarding of the medium and repeated washings with Hank's balanced salt solution (BSS). Cells remaining adherent to the flask floor were trypsinized and resuspended in a fully supplemented medium (FSM) containing ascorbic acid (50 μg/mL), glutamine, 10 mM β Glycerophosphate, gentimycin, penicillin, and fetal bovine serum (15%). Passaged cells were resuspended using a dilution factor of 3. Additional passages were carried out when cells had begun to approach confluence on the flask floor, varying from 3-7 days. After 1-2 passages cells were seeded onto Bioglass fibers contained within a polypropylene (PP) disk and mica ring, Figure 4-2.

Figure 4-2. PP/Mica construct loaded with 60 mg of 77S Bioglass fibers.

For the purpose of examining the effects of fiber density or spacing on cellular proliferation, various masses of the BG fibers were seeded into the constructs ($d = 9.17 \pm 0.05$ mm, $h = 1.85 \pm 0.09$ mm; $V = 122.0 \pm 7.6$ mm^3). Masses of 0, 10, 20, 40, and 60 mg of fibers were packed into the constructs. In order to compare the volume of the fibers with that of the constructs and hence determine the porosity, the densities of the fibers were obtained based upon Archimedes Principle. A density apparatus (Mettler Toledo) was used to determine the density of the fibers from the following equation:

$$\delta = m_1 / (m_2 - m_3) \times 0.801$$

where m_1 was the mass of the fibers on the balance pan, m_2 was the mass of the fibers hanging from the apparatus, and m_3 was the mass of the fibers when submerged in ethanol. The difference of $m_2 - m_3$ thus represented the mass of the displaced fluid, which upon correction for the density of EtOH was used to calculate the volume. The known density was then used to determine the volumes of the various masses of fibers from the simple relationship $V = m/\delta$.

Fibers and constructs were steam sterilized, wetted with ethanol, and soaked in fibronectin (25μg/mL) for 1 hour. A stainless steel screen was placed over the top of the construct to maintain the fibers within the construct. Upon passaging, trypsinized cells were quenched with medium and 1 mL was added to each well of a 24 well plate. Cells were then cultured for various time periods, with repeated changes of the medium every 3rd day.

For the purpose of determining cell numbers, a Beckman Coulter Multisizer III was used. Cells were counted on days 3, 7, 10, 14, and 21. After trypsinization, the cells were pipetted 5x to further agitate and cleave the peptide bonds adhering them to the fibers and construct surface. The suspension was then diluted in an Isoton salt solution (100 mL) and a 500 μL sample volume was passed through the counter at a flow rate of ~38μL/sec.

Results and Discussion

In vitro Bioactivity

SEM analysis of 77S Bioglass fibers in Figure 4-3 reveals crystal formation 24 hours following submersion in SBF. Both the number and size of the crystals on the fiber surface increased following extended periods in SBF. Small crystals present after 1 day in SBF (b) preceded larger crystals seen on fibers submerged for 5 days (c). At 10 (d), 20 (e), and 30 (f) days the formation of larger crystal structures can be seen. The morphology of the crystals ranged from cuboidal (b and c) to needle like (d) to larger aggregations of many smaller crystallites (e and f).

EDX spot analysis (Figure 4-4) of was performed to analyze the elemental constituents present within the crystals (b-f) and BG fibers (a). The spectrum revealed peaks at 1.5, 1.75, 1.8, and 3.75 keV representing the presence of oxygen, silicon,

phosphorous, and calcium, respectively. A peak at 0.1 keV was also present from the carbon coating; however, this peak did not interfere with any of the presumed species present within the glass. The composition of the crystals was shown to exhibit elevated amounts of calcium, phosphorous and oxygen (the primary constituents of HA) when compared to unreacted Bioglass fibers. Additional peaks, characteristic of sodium and chlorine, were observed when analyzing certain crystals. It is therefore likely that additional salts such as NaCl or $CaCl_2$ had precipitated on to the fiber surface.

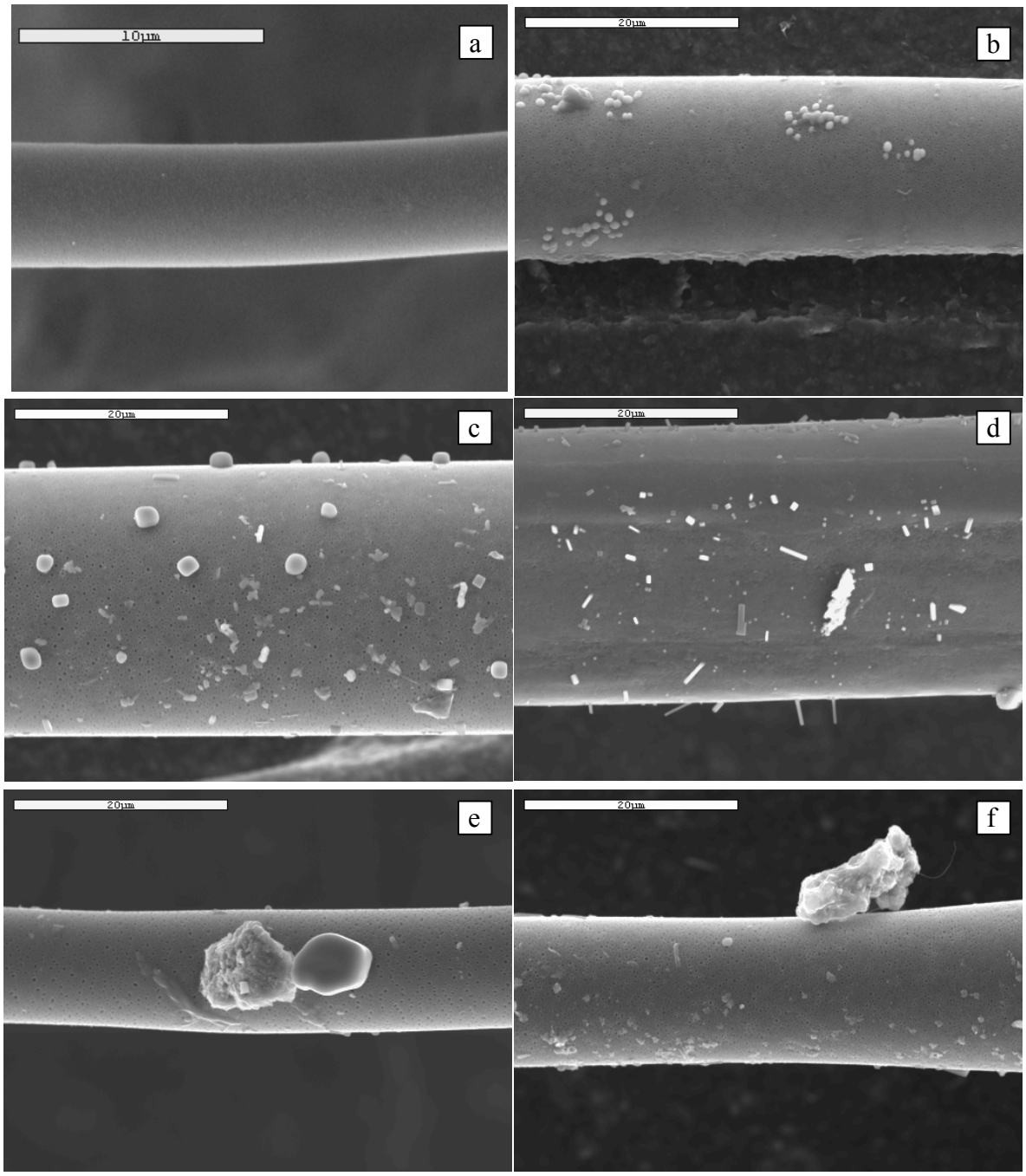

Figure 4-3. SEM images of 77S Bioglass Fibers submerged in SBF for (a) 0, (b) 1, (c) 5, d) 10, (e) 20, and (f) 30 days. SB = 10 microns (a) and 20 microns (b-f).

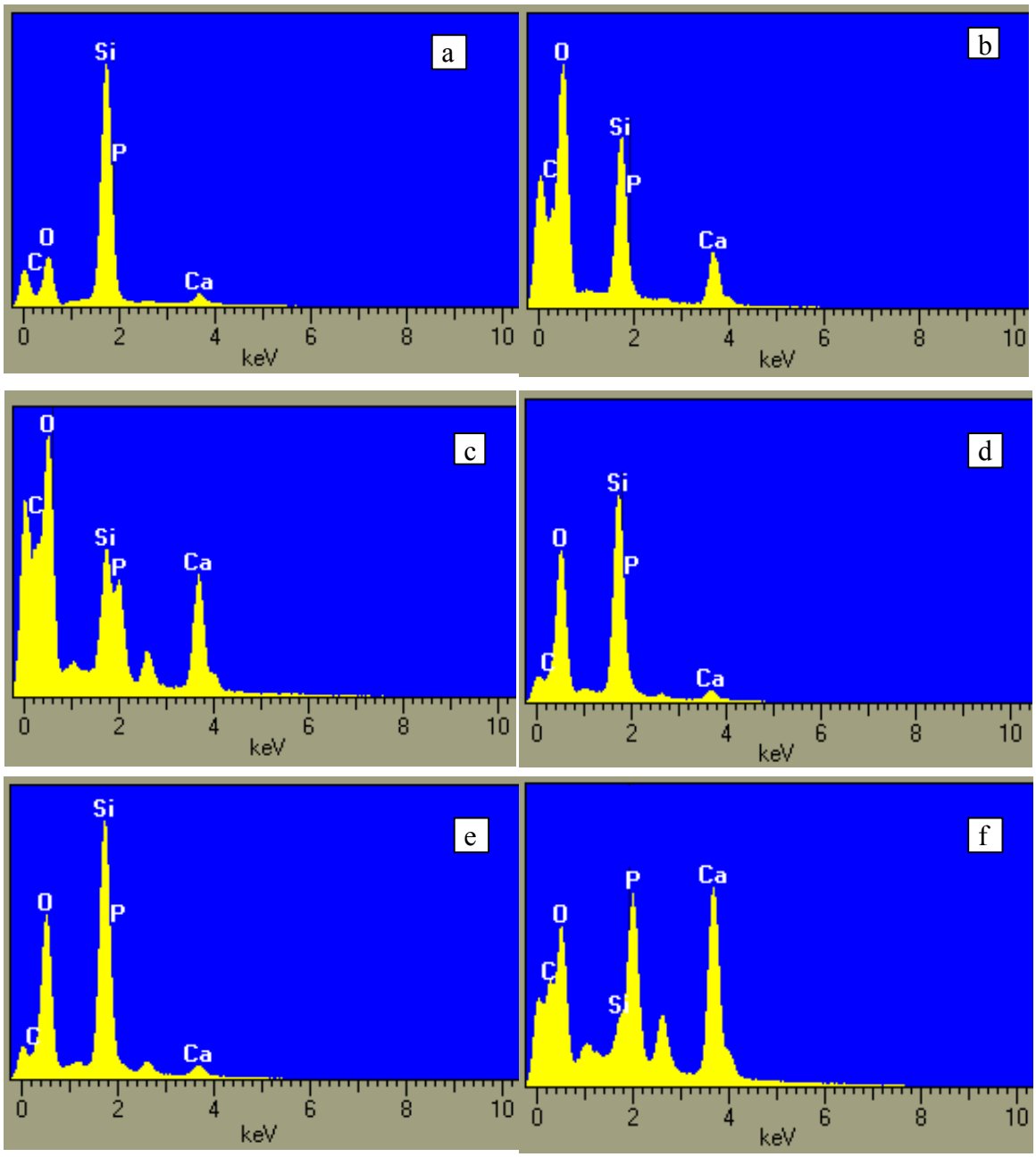

Figure 4-4. EDX spot analysis of fiber (a) and crystals (b-f) seen in Figure 4-3.

The verification of the elemental components characteristic of HA by EDX is insufficient in analyzing the molecular species present. X-ray diffraction data was also obtained on the fibers following submersion in SBF to further confirm the presence of HA. This technique is based upon the diffraction patterns and energies characteristic of specific crystal structures. The x-ray spectra obtained for the samples in the above SEMs are shown in Figure 4-5.

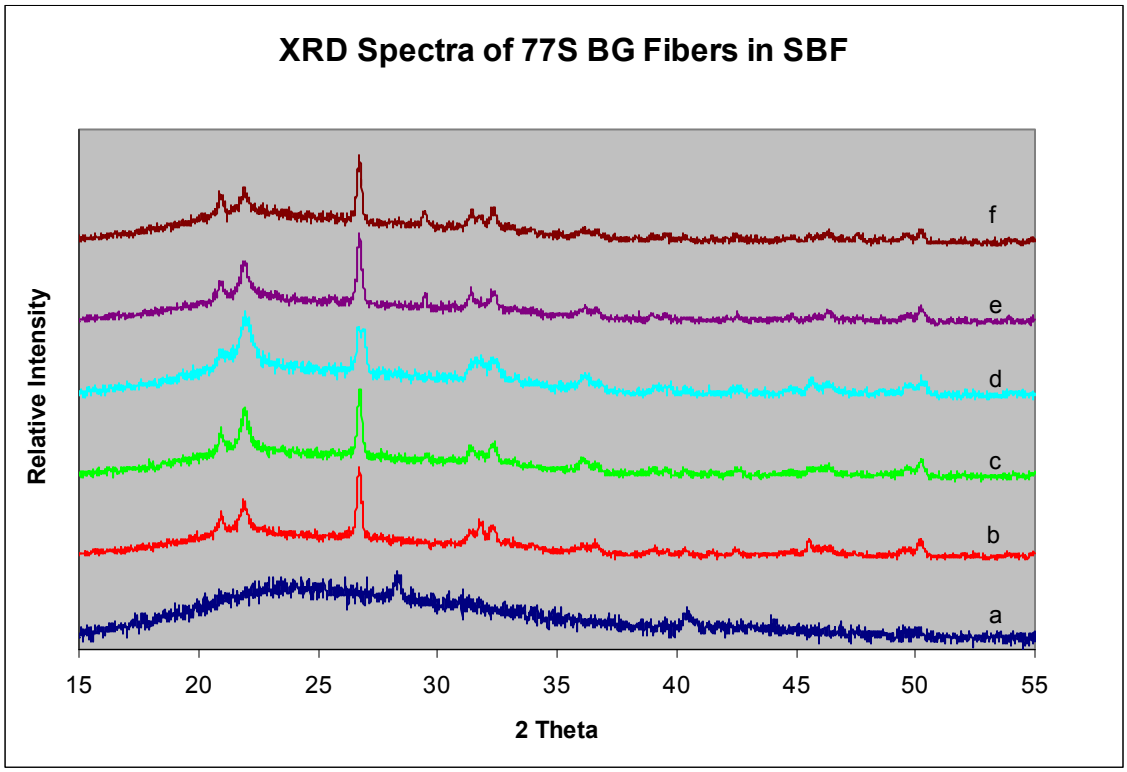

Figure 4-5. Xray Diffraction data obtained for 77S Bioglass fibers submerged in SBF for a) 0, b) 1, c) 5, d) 10, e) 20, and f) 30 days.

The spectrum of the BG fibers not submerged in an SBF solution (a) contained only 2 small peaks (~28.5º and 40.5º), and were otherwise indicative of a noncrystalline or amorphous material. The remaining spectrum contained peaks at 2 theta values of 26˚, 31-32˚, and 50˚, with the most prominent peak appearing at 26˚. These peaks are characteristic of those expected for HA [34, 105]. All samples submerged in SBF also

show a small peak at 37˚, corresponding to the presence of CaO. Two additional peaks at ~21˚ were also seen in these samples.

Of an interesting note was the formation of crystal structures of BG fibers that had no exposure to an SBF solution. Post sintering these fibers were stored in a closed container and left on a lab bench where the average humidity was ~70% for approximately 2 months. The amount of water vapor present in the atmosphere was apparently sufficient to generate a surface rich layer of silica gel. Subsequent migration of calcium and phosphate ions from within the glass structure led to the precipitation of crystals on the glass surface. SEM and EDX analysis of these fibers and crystal are shown in Figures 4-6 and 4-7, respectively. Some of the observed crystals had a similar size and structure to the crystals observed on samples submerged in SBF, and EDX confirmed the elemental composition to be consistent with HA. The peak from the presence of a gold coating on these fibers coincides with that of phosphorous, thereby making it impossible to distinguish between the two.

The 77S Bioglass fibers synthesized with PVP were shown to exhibit crystal deposition within 24 hours post submersion in a simulated body fluid solution. This is representative of the rapid rate of bioactivity seen in sol gel glasses due to their high surface areas and mesoporous structures. Additionally, crystal formation was observed on fibers with no exposure to an SBF solution, indicating the highly bioactive nature of these fibers.

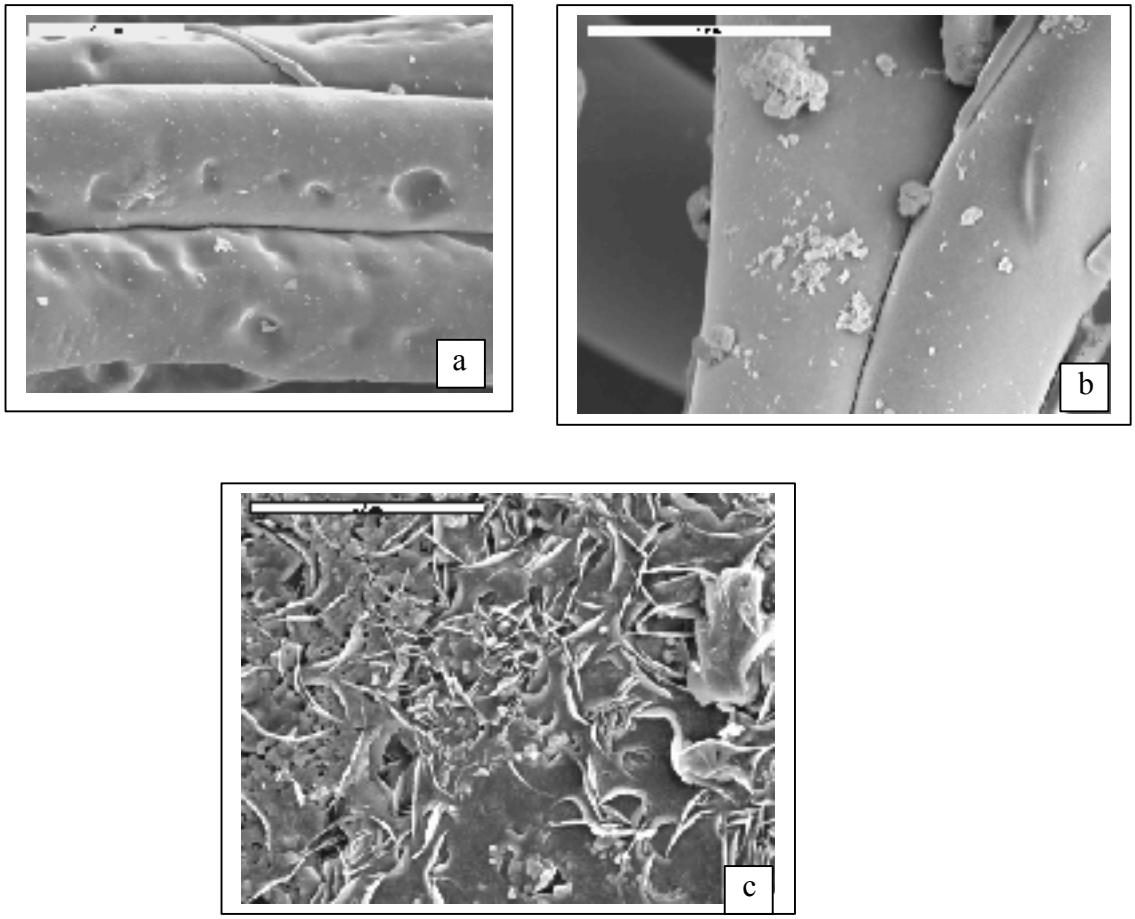

Figure 4-6. SEM images of 77S Bioglass fibers with crystal formation following storage at near atmospheric conditions. These fibers had no exposure to an SBF solution. SB = 20μm (a and b) and 10μm (c).

Isolation and Culture of Rat Mesenchymal Stem Cells

Both the femurs and the cells isolated from the femurs of Wistar rats were analyzed by SEM observation prior to the culturing of the cells on BG fibers. These results are summarized below.

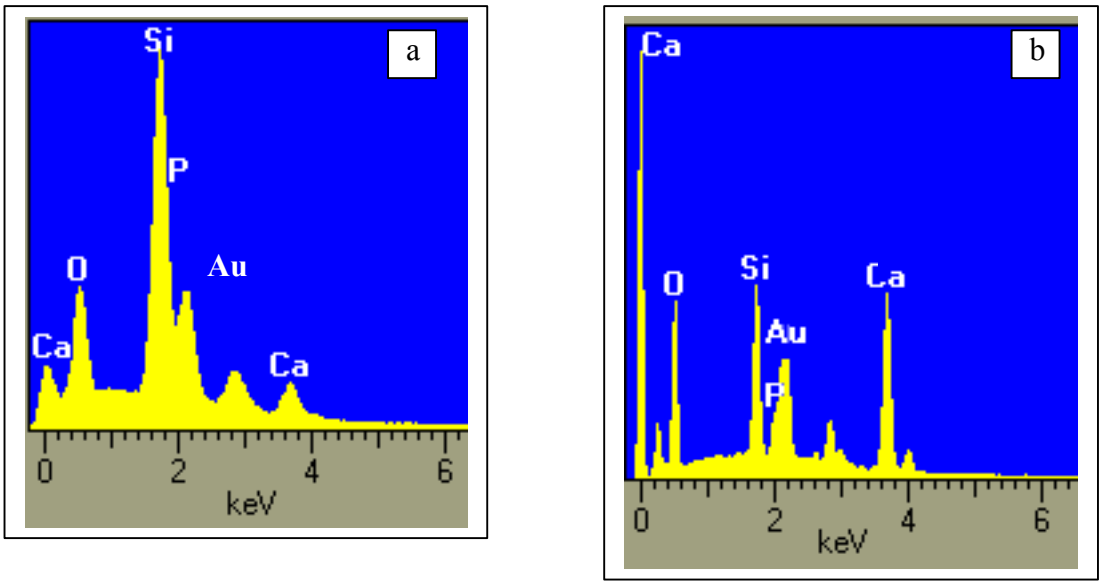

Figure 4-7. EDX spectra of 77S Bioglass fibers (Figure 4-6 a and c). Note the increase in oxygen (a and b) and calcium (b) indicative of the formation of HA on the glass surface.

SEM Evaluation of Femur Microstructure and Bone Marrow

Prior to the culturing of cells, the bone and the cells obtained from the bone marrow were analyzed. Femurs harvested from the rats were fixed in 4% formalin and dehydrated in a graded alcohol series. Both longitudinal and transverse cross sections of the diaphysis were obtained using a diamond saw. No enzymatic or acidic treatments were performed to clean cellular and mineral components, respectively, although this may be useful for obtaining more detailed information about the microstructure.

SEM analysis of the bone revealed various organizational levels of structure depending upon the degree of magnification (Figure 4-8). The morphology seen in Figure 4-8a is characteristic with fracture surfaces of long bones obtained by Weiner, Traub, and Wagner [106]. Their SEMs revealed numerous lamellar layers. Each lamellae was composed of 5 sublayers, each containing collagen fibrils arranged at 30º

angles relative to adjacent layers. Deposition of HA crystals within the collagen fibrils of each sublayer is also directionalized, with their arrangement occurring in parallel layers that traverse the fibril. This mechanism of orientation has been described as the twisted plywood motif [106, 107]. A 10,000x image shows the fibrous nature of the bone (Figure 4-8b).

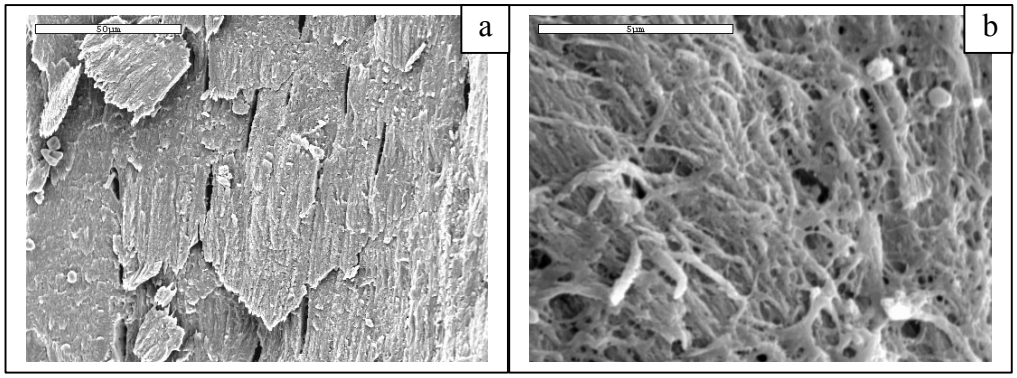

Figure 4-8. SEM images taken from a longitudinal cross section of a rat femur. A) 750x image depicting the shale like layers of the bone, indicative of the plywood motif of lamellar bone (SB=50μm). B) 10,000x image illustrating numerous collagen fibers present within the bone (SB=5μm).

The broad nature of the cells present within the bone marrow can be seen in Figure 4-9. The marrow contained predominately RBCs (green arrows), but larger leukocytes (red arrow) were also present in a high concentration. Analysis of the marrow did not reveal any identifiable mesenchymal stem cells. This is not unexpected, however, due to their low concentrations relative to the entire population of cells in marrow. Pittenger et al. have estimated the number of MSCs present in human marrow to be around $1{:}10^4$, a concentration two orders of magnitude less than the frequency of hematopoietic cells [108]. Additionally, one can see the presence of vasculature (yellow arrow) and the extracellular support matrix composed of fibrin and collagen fibers (blue arrow).

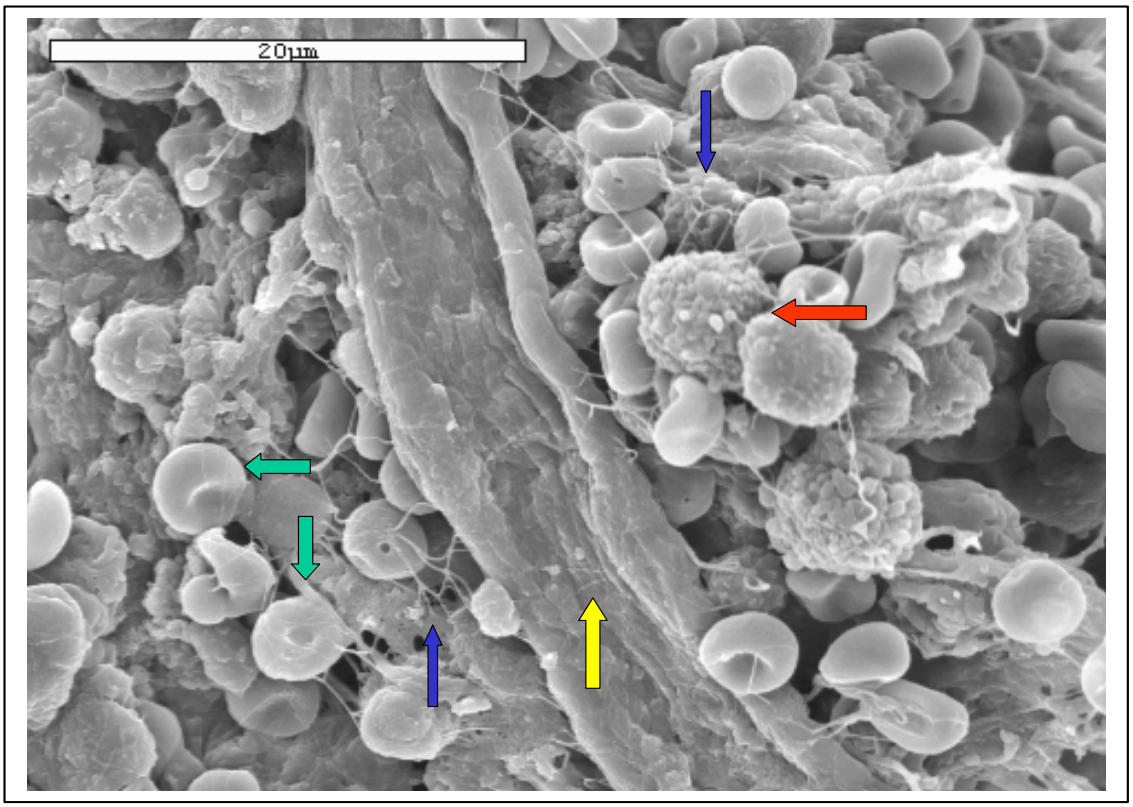

Figure 4-9. 2500xSEM image of cells obtained from the marrow contained within the femurs of rats. The cells were fixed in 4% formalin and dehydrated in a graded EtOH series before examination in the SEM. Notice the large number of red (green arrow) and white (red arrow) blood cells as well as the vessel (yellow arrow) and collagen and fibrin strands (blue arrow). SB = 20µm.

Proliferation of MSCs on Bioglass Fibers

The calculated density of the sintered fibers was found to be 1.70 ± 0.03 g/cc. The volumes of the various masses of fibers along with the corresponding porosities of the constructs are listed in Table 4-2. Porosity was defined as the fiber volume divided by the construct volume. The constructs exhibited porosity values ranging from 70-100%, with the 100% porous sample representing the control containing no BG fibers.

Table 4-2. The volumes and corresponding porosities of the 77S Bioglass fiber constructs used to determine the effects of fiber spacing on MSC proliferation.

Fiber Mass	Fiber Volume	Porosity
mg	cc	%
0	0.00E+00	Control
10	5.88E-03	95.2
20	1.18E-02	90.4
40	2.35E-02	80.7
60	3.53E-02	71.1

The growth curves of the rat MSCs as a function of both fiber density and culture period are shown in Figures 4-10 and 4-11. The rate of proliferation and the total number of cells was found to depend on both the porosity of the scaffold and the time in culture. The concentration of cells was shown to increase as the spacing between the fibers decreased. The difference in proliferation between the samples of 5% (10 mg) and 10% (20 mg) porosity was the least substantial, as is particularly evidenced in the 10 day sample, Figure 4-10. This is likely attributable to an actual similarity in the densities of the two samples, as the 10 mg sample did not completely fill the construct. Addition of another 10 mg was added to the top of the 10 mg sample, and additional packing of the fibers to fill the construct was less severe than in the remaining samples. Therefore, the spacing between the fibers was similar, with the primary discrepancy being the difference in the surface area available for the colonization and expansion of cells.

Influence of cellular proliferation was the greatest between the control and a 5% density as well as from ~80% to 70% porosity. The introduction of fibers to the control resulted in an average increase in proliferation of 19.4% (0-95% porosity, not including the 3 day sample). Therefore, samples with only a slight amount of fibers had a profound affect on the proliferation of rat MSCs. Likewise, the decrease in porosity from 81% to 71% led to an increase in proliferation of 17.8%, further illustrating the ability of preferentially spaced Bioglass fibers to influence proliferation in the rat MSC system.

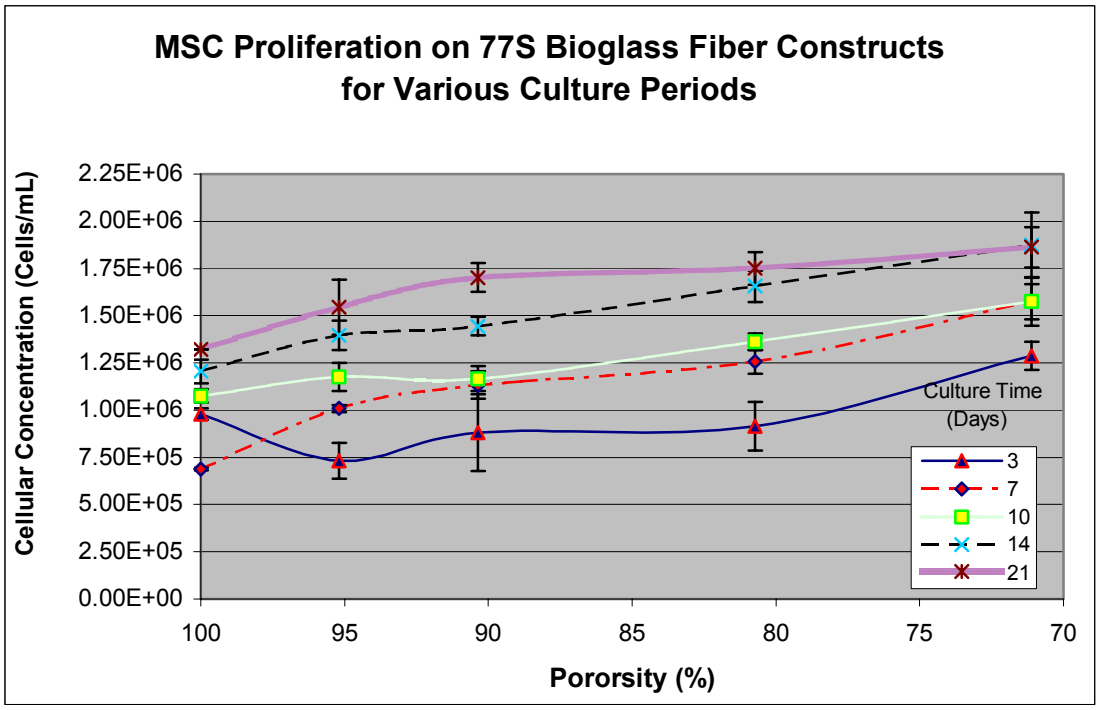

Figure 4-10. The proliferation of rat MSCs on 77S Bioglass fiber constructs as a function of construct porosity. The spacing between the fibers was shown to influence the rate and degree of proliferation.

The growth patterns of the rat MSCs in Figure 4-11 indicates 2 regions of proliferation bridged by a region of relatively little increase in cell number. Cells had a relatively high proliferation rate following seeding until approximately day 7, at which point the rate slowed drastically or reached an equilibrium state. From day 3 to day 7 the concentration

of cells increased by 18.7% at a rate of 4.46 x 10^4 cells/mL per day (excluding the sample with no fibers). Between day 10 and 14 the concentration increased an additional 19.2%, with the concentration growing 6.10 x 10^4 cells/mL per day. Between days 14 and 21 the rate slowed to 8.0% with the concentration increasing by 1.74 x 10^4 cells/mL per day. During this time period the sample corresponding to a porosity of 71% had a decrease in the concentration by 0.6%, indicating an equilibrium between the rate of proliferation and death of the cells. The cessation of a high proliferation rate in this sample indicates progression of these MSCs into a differentiated state.

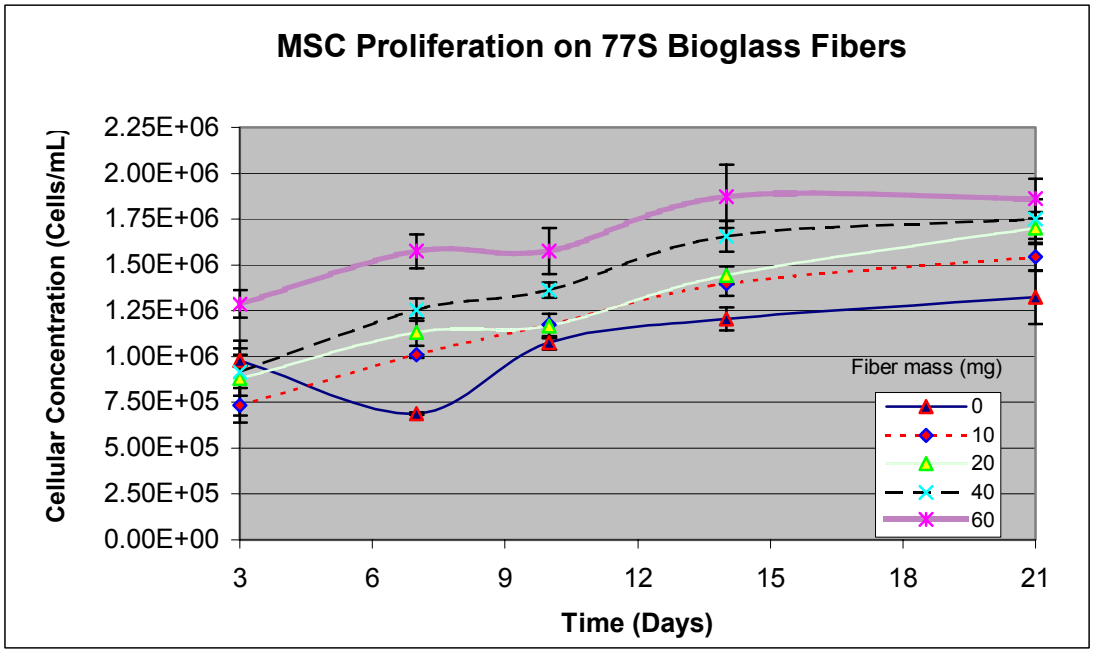

Figure 4-11. The proliferation of rat MSCs on 77S Bioglass fiber constructs as a function of culture period.

The discrepancy seen in the sample containing no fibers between days 3 and 7, ie the high cell concentration relative to the other samples at day 3 followed by a dramatic decrease, may have been due to an abnormally high initial seeding density. At 3 days, the higher number of cells present in this sample would be magnified, due to the small amount of time available for the increase in cell numbers relative to the seeding density.

Additionally, brief exposure of the samples to UV radiation in a biological hood during the changing of medium may have resulted in damage. The lack of fibers in this sample likely resulted in a greater exposure to the UV source due to the absence of fibers which provided a shielding layer by scattering or absorbing the light. Greater exposure likely resulted in the apoptosis of cells in the absence of fibers, whereas those samples with fibers were protected and probably received less direct exposure to the radiation.

The determination of an initial seeding density in the above study was unfortunately not obtained. This would have provided additional information on the immediate proliferation of cells post seeding as well as an overall percent increase in the amount of cells. An understanding of the initial numbers would further validate these results by providing the total increase. Also, the shear variability between cells obtained from different animals is likely to affect the numbers obtained from such a study. These factors must be considered in the analysis of this data, especially when expressed as actual values.

The patterns and growth curves, however, are likely to be more representative of the actual results regardless of the above factors. The patterns seen indicate the increase in the proliferation of rat MSCs with a decrease in sample porosity. This has been explained as the ability of cells to grow between adjacent fibers, thereby increasing the available space in which to proliferate. Cells seen bridging between fibers are shown in Figure 4-12.

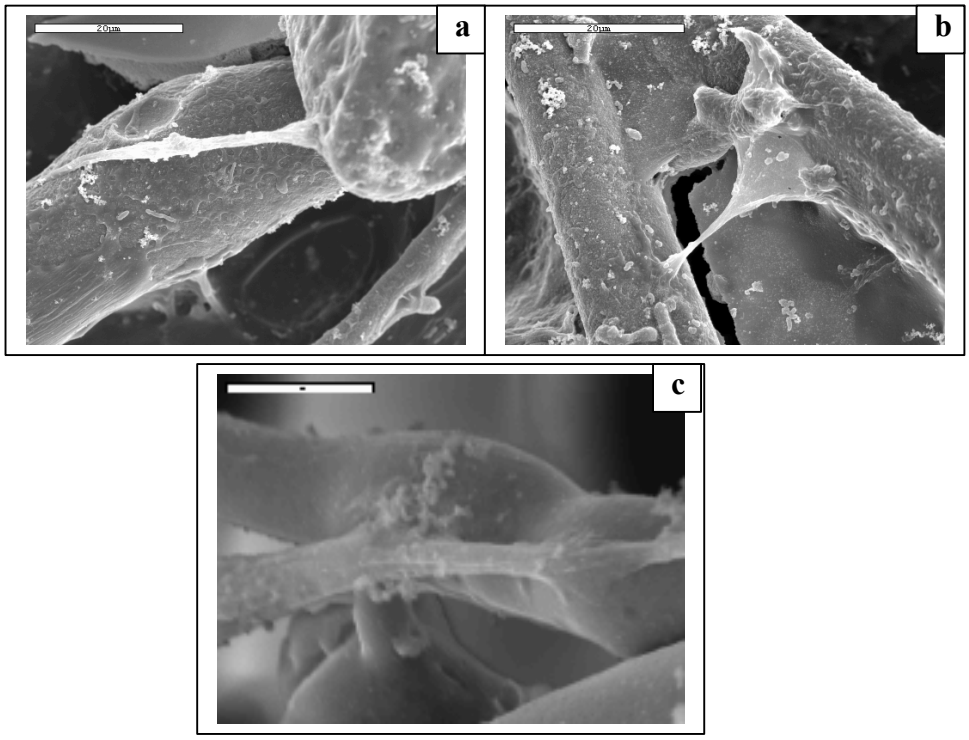

Figure 4-12. SEM images of rat MSCs shown bridging between adjacent Bioglass fibers after 14 days in culture. SB = 20μm (a and b) and SB = 5μm (c).

The ability of cells to span or bridge between adjacent surfaces has been shown by a number of authors and has been in the literature in excess of 100 years [87-90]. The presence of an interface is a necessary stimulus in the movement and morphogenesis of cells. These interfaces can be between two liquids or solids or a combination of the both. The boundaries between the culture medium, the construct and the fibers all serve as suitable areas for the expansion of cells. As cells begin to grow to confluence on the solid surfaces within the culture well they begin to experience additional tensions and stresses due to compaction. These forces prompt changes in the dimensions of the cells, leading to their differentiation. The ability of the cells to span between such things as adjacent fibers results in a greater space for their continued proliferation, allowing for an increase in the amount of cells prior to differentiation. The highest concentration of cells prior to differentiation was seen in the sample of the lowest porosity.

It is also likely that in addition to the close proximity of adjacent fibers that allowed for bridging, the variability in surface area played a role in the growth profiles of the cells in the performed study. Further investigation into its role should be examined to distinguish the effects of these two factors.

Additional SEM images of rat MSCs cultured on 77S Bioglass fibers are shown in Figure 4-13. The role of fiber diameter is known to have an effect on the elongation of cells relative to the long axis of the fiber, with diameters of less than 100μm having the most dramatic results. As the radius of curvature decreases, so does the influence of fiber diameter on the directed growth of cells along the long axis [88, 90, 109]. Cells are then seen to grow in a spiraling manner, circumferentially around the fibers. These results have been explained as the excretion of exudates from the cells. Capillary forces serve to draw the exudate along the axis of the fibers, and cells merely pattern their growth following it. The strains of elongation force the meshes of the forming ground mat to trace the exudates in a lengthwise orientation [88]. As the diameter of the fiber continues to increase, these capillary forces begin to have a decreasing affect and the exudates and ground mat loose their lengthwise orientation, resulting in a circumferential, spiraling affect of the cells.

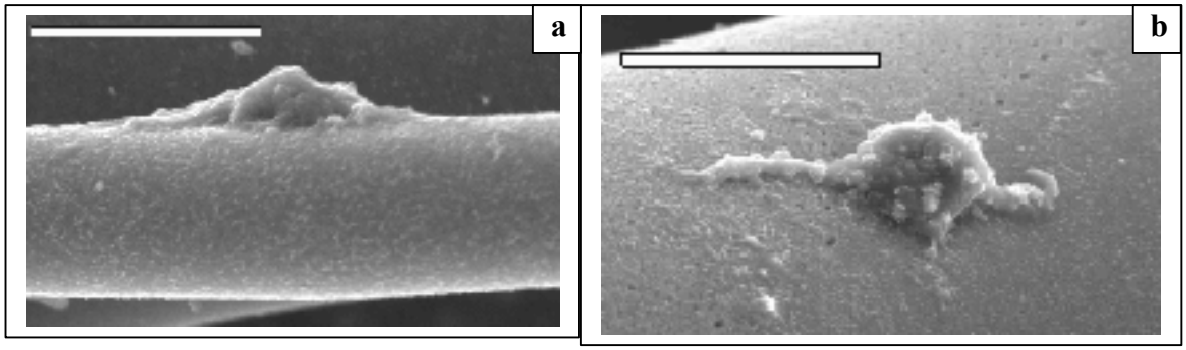

Figure 4-13. The elongation of rat MSCs cultured on 77S Bioglass fibers for 14 days. Note the effect of diameter of cell orientation, as the cell in (a) is much more elongated with respect to the fiber's long axis. SB=20μm.

Conclusions

The 77S bioactive glass fibers synthesized with polyvinylpyrrolidone were shown to exhibit *in vitro* bioactivity and influence the growth and proliferation of rat mesenchymal stem cells. Bioglass fibers were arranged in various packing densities, thereby altering the spacing between the fibers. Those fiber constructs with low porosities resulted in the greatest overall proliferation of cells and led to earlier differentiation.

The ability of these discontinuous BG fibers to influence and control rat MSC behavior through semi controlled arrangements is noteworthy. Despite their random orientation within the constructs, these fibers were able to be positioned with controllable porosities. This led to manageable rates of proliferation and differentiation. Further control over fiber orientation through the development and use of continuous and woven structures is likely to further enhance these effects. Not only can the porosities of these materials be tailored, but the organization of the fibers can be adjusted to give directionalized orientations. These properties would in turn lead to an improved ability to control the growth of tissues and the deposition of ECM.

This chapter has described the *in vitro* properties of PVP modified BG fibers. These fibers were seen to elicit the precipitation of HA and control cellular responses when arranged into varying porosities. The determination of the chemical, physical and biological properties *in vitro* represents an achievement of the second step in designing and engineering materials for implantation. Further examination into the degradation rates or mechanical properties would further contribute to this knowledge base. Application of these results can now be used in the design of *in vivo* studies based upon standardized or acceptable animal models. Based upon the observations seen within this work and that of others, these BG fibers should be able to influence cellular proliferation and tissue formation either in a bony environment or ectopic sites. Their safety and efficacy can be confirmed through implantation and serve as a basis for predicting results in human studies

CHAPTER 5
CONCLUSIONS AND FUTURE WORK

This work illustrated the synthesis of polyvinylpyrrolidone modified bioactive glass fibers and their *in vitro* ability to influence rat mesenchymal stem cell proliferation. A sol gel derived bioactive glass was modified through the incorporation of PVP, and discontinuous fibers were fabricated through an air spraying technique. Rat mesenchymal stem cells were cultured in the presence of sintered fibers, which were shown to have an affect on proliferation rates.

The incorporation of a polymeric modifier into a sol gel reaction described in Chapter 2 was done in an effort to mediate the rheological properties and stabilize the sol. The initial spraying of BG fibers without the incorporation of a polymer was laden with difficulties due to the necessity of isolating a highly viscous sol within extreme proximity to the gel point. Achieved within this work was the addition of PVP into the BG sol, which served as a rheological modifier, thereby facilitating the spraying process. Reproducibility was highly enhanced through this modification, as the need for isolation of a sol just prior to gelation was negated. Using a high molecular weight polymer (M_n = 1×10^6) served to shift the foundation of the rheological properties from the sol towards the polymer within the viscosity range needed to spray fibers.

The addition of PVP to the BG sol was also found to have a stabilizing affect. Gelation in samples containing PVP was impeded for times far exceeding sols without PVP. Even small amounts of polymer, only about 3×10^{-4} weight fraction of the sol, were shown to extend gelation times 4 fold. Therefore the period over which synthesized

materials could be stored prior to fiber spraying was greatly enhanced. The stabilizing affects of PVP were also seen during the evaporation of solvent prior to fiber spraying. The evaporation of ethanol through the introduction of heat further stimulates gelation of the sol through the provision of energy and the increase in entanglements between the growing silica chains. Sols containing PVP could be further reduced than sols without polymer, without driving the sol into gelation. The ability of PVP to coat the silica chains and further stabilize them through interchain bonding slowed the rate of gelation and mediated sol viscosity during the evaporation of ethanol.

Additionally, PVP was seen to have an affect on the behavior of the sol's rheological nature. Those sols synthesized without the presence of PVP were often shear thinning in nature, while those with PVP behaved in a more Newtonian fashion. The high shearing forces experienced by the sol as they were extruded through the gun had an affect on their ability to yield fibers when sprayed. This was directly related to the viscous behavior of the material. Those sols that were Newtonian in nature were able to withstand these forces with greater resilience, resisting the breakage of siloxane bonds during passage through the orifice. The maintenance of the molecule within a linear form led to a drawing of the material into fibers when forced through the gun.

All of the factors had profound benefits on the production of sprayed BG fibers from a viscous sol. The modification of sol viscosity combined with the stabilizing affects observed facilitated and broadened the range over which the BG sol could be sprayed into fibers.

Following the synthesis of BG fibers, their *in* vitro bioactivity and ability to influence the growth patterns of rat MSCs were examined and illustrated. Fibers were found to

elicit the precipitation of a hydroxyapatite layer on their surface, as is characteristic of all bioactive glasses. HA crystals were seen 24 hours following submersion in an SBF, and the number and size of crystals was seen to increase with time. Crystal formation was also evidenced on fibers stored under ambient conditions as well as those placed into culture containing MSCs, fibronectin, serum and a common culture medium.

Fibers were seeded into constructs in which varying porosities were achieved. Varying the packing densities of the fibers served as a means for controlling the spacing between adjacent fibers, thereby influencing the geometry within the vicinity of the cells. Increasing masses of fibers packed within a given volume served as a means for decreasing the spacing between the fibers, and was shown to increase the proliferation of rat MSCs. This was justified by the ability of cells to span between adjacent fibers, leading to an increase in the available area for their expansion. Providing the cells with an increased space for their growth led to the ability of cells to further proliferate prior to differentiation. The growth of these cells to confluence is accompanied by a reduction in their ability to spread out, which is known to stimulate differentiation. Providing the cells with the opportunity to bridge between adjacent fibers reduced the degree of compaction and led to a higher concentration of cells prior to differentiation.

An equilibration in proliferation was also seen in the highest density sample between day 14 and 21. The concentration of cells remained the same within this time period, indicating the transformation of these cells into a differentiated state. The concentration of cells within this sample was higher at day 14 than the remaining samples; however by day 21 the lower density samples had begun to approach this value. The ability of the higher density sample to prompt greater cellular concentrations at an increased rate

indicates the benefits of fiber spacing as a means of controlling the proliferation and differentiation of MSCs. These results can thus serve as a basis for designing tissue engineering, cell seeded constructs for implantation.

The directions and possibilities for the continuation of this project are quite extensive. The ability to incorporate PVP within the BG sol opens the door for the addition of numerous other polymers, with special attention to those that are soluble in aqueous solutions. Such polymers include polyvinyl alcohol, polylactic acid, polyglycolic acid, and collagen, just to name a few. Some of these such PLA/PGA are currently used in biomedical applications, and others, such as collagen occur naturally within the body. Combining these organic polymers with the BG to yield composite fibers may have numerous biological applications. Mediating heat treatments within the realms of stability for PVP or these additional polymers can be used to produce bioactive composite fibers. By varying the concentration and type of polymer, one can control degradation rates and byproducts. Mechanical properties can also be tailored to specific applications.

The natural occurrence of collagen (Type I) within the bone makes this an especially attractive addition to create hierarchical bioactive fibers. The deposition of HA on the composite BG/collagen fibers may help to further complement the HA deposition naturally found within the collagen fibrils that occurs during bone formation. This may further expediate the healing process. The addition of collagen may also serve to improve the poor mechanical properties of bioactive glasses, enhancing workability and performance *in vivo*. Adjustments of concentrations can further enhance the viability of such a composite through controllable rates of degradation.

Further development of BG fibers into continuous structures is worth attention. The discontinuous nature of the fibers synthesized within this work limit organization. While fibers could be packed into various densities, no control over their directionalized orientation was achieved. Fibers were merely spaced randomly amongst the construct. The spinning of continuous fibers can be used as a manner of more precisely controlling the growth patterns of cells, thereby influencing the deposition of extracellular matrix. This is of critical importance in the growth of functionalized tissues. Past work of the author has confirmed the ability of continuous BG fibers to be spun through a wet spinning technique; however these fibers were highly brittle in nature. Inclusion of polymer additives is likely to serve as a means of decreasing the modulus for these fibers and improving their strengths.

Key areas of focus in the processing of these continuous fibers include the type and concentration of organic polymer; the influence of sol viscosity, spinneret size, and uptake rate on fiber diameter; the modulus, mechanical properties, and heat treatments of the spun sol; and the ability of the fibers to precipitate HA *in vitro*. Following processing, the fibers should be examined for their abilities to influence cell growth based upon their diameter and composition. A large database of supporting literature currently exists on fiber scaffolds which can be used to generated hypotheses.

While single fibers have the ability to perform as tissue scaffolds and influence cellular behavior, their affects are greatly enhanced when woven together into continuous structures. This serves as a means of enhancing the construct strength and mechanical properties. Various concentrations and compositions of composite fibers can also be preferentially located within specific areas of the weave. Controlling the hierarchical

structure in this manner can be used to tailor the degradation, allowing certain areas of the structure such as those on the periphery to resorb faster. Spacings between adjacent fibers can be determined that have the highest influence over the proliferation and differentiation of cells. This can also be controlled to allow for the maximum infiltration of cells, vessels, and nutrients into the center of the construct *in vivo*.

Similar *in vitro* experiments to determine the proliferation rates of cells can be used with the continuous and woven structures. Supporting evidence on the differentiation of cells can also be obtained using biochemical assays. Genetic markers such as alkaline phosphatase and osteocalcin can be used to monitor the maturation of MSCs into osteoblasts and confirm the time scales for this transformation. These results can then serve as a means of determining which compositions and spacings appear best suited for further development and *in vivo* analysis.

Based upon the data presented within this work and that gathered from the continuous, woven structures, the design and implementation of an animal study is in order. Numerous *in vivo* studies presented in the literature on bioactive glasses make use of rat or rabbit models. Rats are often used to describe the possible effectiveness of bioactive glasses in orthopaedic applications. Both ectopic and femoral defect sites are used to determine the regenerative capabilities of bioactive materials. Femoral defects in rabbits are more commonplace in dental literature, in an effort to link the bone forming potential to the oral and maxillofacial structures.

Additionally, current collaborations with Dr. Thomas Mareci at the UF Brain Institute are under way to examine the bone healing capabilities of discontinuous BG fibers in a rat model. The development of *in situ* MR imaging through the placement of MRI coils

directly onto the spinal columns of rats by Dr. Mareci [110] represents a novel way of gaining an enhanced perspective on the events that occur during healing. Placement of BG fibers into defects created within the bone coupled with this technology may improve our understanding of bone regeneration in the presence of bioactive glasses.

The progress described herein represented the completion of steps one and two of designing and engineering a material or device for human use, as described in Chapter 1. A synthesized material has been examined for its *in vitro* properties and its effectiveness in a cell culture model representative of its intended use. The development of an animal study as just described represents the third step in the progression of a material or implant for use in a clinical environment. Additionally, the development of continuous fibers and woven structures illustrates a modification to the previously designed fibers in an effort to improve their efficacy. Thus, the achievement of this work merely represents the beginning of numerous possibilities through further research and development.

APPENDIX A
LIST OF ABBREVIATIONS

BG: Bioglass
BGF: Bioglass Fibers
BMP: Bone Morphogenetic Proteins
BSP: Bone Sialoprotein
BSS: Balanced Salt solution
EDX: Energy Dispersive X-Ray Spectroscopy
Fn: Fibronectin
GFs: Growth Factors
HA: Hydroxyapatite
HCA: Hydroxy Carbonate Apatite
MA: Metal Alkoxide
MEM: Minimum Essential Medium
MNGC: Multinucleated Giant Cells
MSC: Mesenchymal Stem Cell
PBS: Phosphate Buffered Saline
PP: Polypropylene
PS: Polystyrene
PU: Polyurethane
PVP: Polyvinylpyrrolidone
RBC: Red Blood Cell
RMSC: Rat Mesenchymal Stem Cell
SBF: Simulated Body Fluid
SEM: Scanning Electron Microscopy
TEOS: Tetraethoxysilane
TEP: Triethylphosphate
TGF-β: Transforming Growth Factor β
XRD: X-Ray Diffraction

APPENDIX B
LITERATURE REVIEW OF BIOACTIVE GLASSES HIGHLIGHTING VARIATIONS IN EXPERIMENTAL DATA

Both melt and sol gel glasses have been extensively discussed in the literature. There are, however, numerous occasions in which the results vary between authors. The contradictions in the properties often leave one unclear about the true nature of these materials. Here, the author summarizes some of these results relative to *in vitro* bioactivity and dissolution, as well as in cell culture or *in vivo* models.

The dissolution and precipitation of HA by bioactive glasses has an extensive database containing well supported general conclusions. This data has been reported on in the literature for a number of years. Sol gel glasses have high surface areas and low densities, while melt derived glasses are characterized by higher densities, low surface areas, and low intrinsic roughness [101]. The mesoporous nature of sol gel glasses that leads to its higher surface area also is responsible for the higher rate of bioactivity. This leads to more sights for the nucleation of HA crystals on the glass surface. This surface area coupled with the low density serves as the mechanism for higher degradation rates as well.

In spite of the commonly accepted generalities previously stated, a few discrepancies are present in regards to dissolution and HA deposition. In his book, An Introduction to Bioceramics, Hench claims a "great decrease in the dissolution rate for compositions > 60% SiO_2 because of the larger number of bridging oxygen bonds in the glass structure" [12]. Also the completion of step 5 resulting in the crystallization of the amorphous HA

is given as 10 minutes for 58S, 120 minutes for 45S5, and 1440 minutes for 77S. Other results within the table seem to contradict this. These are likely affected by the composition and structure of the glass, especially the surface area relative to the volume of the solution (concentration of BG). The bioactivity and degradation behavior of bioactive glasses *in vitro* is summarized in the table below.

Table B-1: Dissolution and HA deposition on bioactive glasses *in vitro*.

BG Comp	**BG Form**	**Results**	**Reference**
45S5 58S 77S 100S	Particles (300-700μm) 1mg/mL in solution	Rate of HCA precipitation: 58S>77S>45S5>100S(none) Dissolution rate, t < 6days 58S>77S>100S>45S5 Overall SiO_2 release 100S>77S>58S>45S5 Almost all SiO_2 released by day 12	[111]
45S5 58S	Particles (5-20, 90-300, 90-710 μm) 10mg/mL in solution	Rate of HCA precipitation 58S>45S5 Rate of SiO_2 release 58S>45S5 Lower dissolution rates and delayed HA deposition were also seen in culture medium compared to SBF (serum proteins) Smaller particles dissolved at a faster rate than larger particles	[100]
45S5 58S	P (d=3.4 μm) P (d=6.7 μm) 1 mg/mL to 15 mg/mL in solution	Rate and amount of HCA 1 mg/mL >15 mg/mL	[112]
45S5 58S 77S	N/A	Rate of HCA precipitation 58S>45S5>77S Dissolution rate Melt > Sol Gel	[12]
58S 77S	Cylinders 4 x 6mm	Dissolution (*in vivo*) 58S ~ 77S	[24]

In addition to the results seen relative to dissolution and HA precipitation, numerous studies have examined the affects of bioactive glasses on cellular influence *in vitro* and their ability to generate bone growth *in vivo*. The discrepancies seen within these studies far exceed those mentioned above. This is likely due to the large biological variations that occur between species and experimental groups. Factors such as age, implant type, size, and placement, surgical precision, and post op care all affect the observations and results obtained within these studies.

Table B-2: In vitro studies on bioactive glasses describing HA deposition, protein interactions, and cellular responses.

BG Comp	**BG Form**	**Results**	**Reference**
45S5	Rods d=8mm; w=1mm	Uniform protein adsorption (MEM, 10% serum) Decreased HA deposition, preferential to high surface energy regions (defects)	[84]
(S) (M) 58S 45S 68S 52S 77S 55S 86S 60S	Discs Sols: d=11mm Melt: d=10mm	Protein adsorption kinetics (sol glasses) 58S>68S>77S>86S Protein adsorption kinetics (melt glasses) 45S5>52S~55S>60S Inhibition of HA when EDTA adsorbed onto glass Proteins shown to remain active several hours on gel layer and indefinitely in HA layer	[20, 21]
45S5	Particles d<10 μm	Adsorption of fibronectin slowed HA deposition and crystallization	[83]
45S5 58S 77S	Particles d=90-700 μm	High response of macrophages to 45S5 and 77S; reduced response to 58S Chemiluminescence Response mononuclear cell activation, radical and peroxide production 45S5>>58S~77S	[80]

Table B-2. Continued

BG Comp	BG Form	Results	Reference
56%P_2O_5 20%CaO 17%Na_2O 2.4%K_2O 4%MgO 1.1%SiO_2	Blocks 0.7x0.7x1cm Pore size of 200-600 μm	Human Osteosarcoma (SaOS-2) Failed to form monolayer Cell clusters DNA Content PS Control>Neutral Glass Ceramic> α-TCP>BG	[86]
53 or 58%SiO_2 20 or 15%CaO 6%Na_2O 12%K_2O 4%MgO 4%P_2O_5	Melt Derived Plates 40x15x2mm BAG=53% BCG=58%	Human Osteosarcoma (SaOS-2) Decreasing cells counts on BAG, BCG (t=7 and 14 days) Type I Collagen BAG>BCG>Control Glass Collagen inc. t<7 days; dec. 7<t<14 ALP BAG~BCG>Control Glass ALP inc. t<7 days; dec. 7<t<14 BMP2 BAG~BCG>Control Glass BMP levels ~constant, t=1-14	[82]
46-72%SiO_2 8-42%CaO 7-24%Na_2O 0.5-6%K_2O 1-3%MgO 0-7%P_2O_5 (P) 0.1-2%Al_2O_3	Particulate coating (Ti) BVA:6% P, CaO:Na_2O 1:1 BVF:7%P, CaO:Na_2O 9:1	Human Osteoblasts Confluent monolayer, individual cells indistinquishable Proliferative results delayed relative to control; high inc t>8 days Alkalization (pH=8.7) Cellular attachment BVF (98%), BVA (92%) MTT Ti>BVA>BVF (t<4 days) BVF>BVA>Ti(t>8 days) Osteoccalcin (t=24 days) Control Glass>BVA>BVF	[113]
45S5 58S 77S	Particles d=90-150 μm	Murine Osteoblats All Glasses No affect on viability, proliferation or ALP expression 45S5 Alkalization, enhanced glycolytic activity (ATP). 58S and 77S No affect on ion levels or metabolic activity	[85]

Table B-2 Continued.

BG Comp	BG Form	Results	Reference
55S 60S (Control)	Particles d=710-790 µm (C=1mg/mL) Discs 20mm x 1mm	Fetal rat calvaria osteoblasts Attachment, proliferation and differentiation on both glasses Multilayers and mineralized nodules on both (t=22 days) 55S nodule bound to glass surface 60S nodule within cellular layer ALP Activity (t=12 days) 55S:50%>60S	[114]
45S5	Ionic dissolution products	Human Osteoblasts Upregulation of Genes CD44 (osteocyte dif.) 7x RCL (growth promoter) 5x Cyclin D1(G1 to S phase) 4x NF1 (proliferation) 2x IGF2 3.2x VEGF 2x	[7]

Table B-3. In vivo behavior of bioactive glasses.

BG Comp	BG Form	Results	Reference
45S5	Porous blocks 4.5x1.5x1.1mm 200-300 µm pores	Cortical window defect in rats Scaffolds preloaded with MSCs(t=2h or 2wks) Few MNGC 40% resorption by 12 weeks	[81]
45S5 52S 55S	Particles d=90-710 µm avg=507±180 µm	Defect 8mm x 4mm drilled into distal femoral epiphyses of rabbits 100mg BG/defect Resoption 45S5>52S>55S No MNGCs (t<7 days) Many MNGC (t>7 days) Bone Bonding 45S5>52S>55S 45S5 and 52S peaked at t=28d 55S continued to increase through t=84d	[23]

Table B-3. Continued

BG Comp	BG Form	Results	Reference
45S5 58S 77S	Cylinders 6mm x 4 mm	Defect 6mm x 4mm in rabbit femora MNGC at gel glass surface No MNGC at 45S5 surface CHAPTER 1Absorption of gel glasses at 12 weeks, reached 40% by 52 weeks. CHAPTER 2Absorbed at equal rate No degradation of 45S5 implant Greater bone for 45S5 (t<8 weeks) Reversal of trend to sol gel glasses at t>12 weeks	[24]
45S5 58S 77S	Particles	Rabbit femora 6mm defect Higher rate of bone formation for 45S5 Greater early bone formation for gel glasses[115] Resorption of particles d<90 μm Incorporation of particles d 200-300 μm[26]	[13]
41%SiO_2 32.24%CaO 9.26%P_2O_5 17.5%Al_2O_3	Fibers d=9 μm Grouped into ball (d=6-7mm) or bundle (7mm x 3 mm)	BMP-2 added to fibers Subcutaneous implantation into rats Ball (porous):cartilage to bone, ie endochondral ossification Bundle (nonporous):Fibrous tissue No bone formation in either without BMP-2	[11]
45S5	Porous cylinders 6mm x 5mm 100-600 μm pores	Intramuscular pouches adjacent to femora of dogs Cylinders covered with connective tissue No cartilage detected Bone formation through endochondral ossification More HA crystal formation in interior of pores	[34]
49.6%SiO_2 8-42%CaO 7-24%Na_2O 0.5-6%K_2O 1-3%MgO 2.7%P_2O_5 0.1-2% Al_2O_3	Cylinders 15 x 1 mm	Intramuscular and intrabony implantation in rabbits Muscle: Fibrous tissue, no inflammation Bone: No fibrous tissue, new bone formation	[35]

Table B-3. Continued.

BG Comp	BG Form	Results	Reference
45S5	Particles d=100-710 or 300-355μm	Edentulous jaws of dogs t=1-24 months d=100-710 μm:Fibrous tissue d=300-355μm:Higher bone bonding; bone formation within pouches created by particle degradation	[116]
45S5	Particles d=90-710 or 300-360μm	Distal femora of rabbits; 60mm cylinders t=1-3 months d=90-710 μm: Higher bone formation, bone to graft ration, and osteogenic pouches	[117]

MNGC=Multinucleated Giant Cells

LIST OF REFERENCES

1. Van Buskirk, W.C. and Ashman, R.B. The elastic moduli of bone, in Mechanical Properties of Bone. in Joint ASME-ASCE Applied Mechanics, Fluids Engineering and Bioengineering Conference. 1981. Boulder, CO.

2. Sambrook, P., Bone structure and function in normal and disease states, in The Musculoskeletal System. 2001, Harcourt Int., Sydney.

3. Cordioli, G., Mazzocco, C., Schepers, E., Brugnolo, E., and Majzoub, Z., Maxillary sinus floor augmentation using bioactive glass granules and autogenous bone with simultaneous implant placement. Clinical and histological findings. Clinical Oral Implants Research, 2001. **12**(3): p. 270-278.

4. Peltola, M.J., Aitasalo, K.M., Suonpaa, J.T., Yli-Urpo, A., and Laippala, P.J., In vivo model for frontal sinus and calvarial bone defect obliteration with bioactive glass S53P4 and hydroxyapatite. Journal of Biomedical Materials Research, 2001. **58**(3): p. 261-269.

5. Ohgushi, H., Dohi, Y., Tamai, S., and Tabata, S., Osteogenic differentiation of marrow stromal stem cells in porous hydroxyapatite ceramics. Journal of Biomedical Materials Research, 1993. **27**(11): p. 1401-1407.

6. Thomson, R.C., Yaszemski, M.J., Powers, J.M., and Mikos, A.G., Hydroxyapatite fiber reinforced poly(a-hydroxy ester) foams for bone regeneration. Biomaterials, 1998. **19**: p. 1935-1943.

7. Xynos, I.D., Edgar, A.J., Buttery, L.D., Hench, L.L., and Polak, J.M., Gene-expression profiling of human osteoblasts following treatment with the ionic products of Bioglass 45S5 dissolution. Journal of Biomedical Materials Research, 2001. **55**(2): p. 151-157.

8. Xynos, I.D., Edgar, A.J., Buttery, L.D.K., Hench, L.L., and Polak, J.M., Ionic products of bioactive glass dissolution increase proliferation of human osteoblasts and induce Insulin-Like Growth Factor II mRNA expression and protein synthesis. Biochemical and Biophysical Research Communications, 2000. **276**(2): p. 461-465.

9. Lalan, S., Pomerantseva, I., and Vacanti, J.P., Tissue engineering and it impact on surgery. World Journal of Surgery, 2001. **25**(11): p. 1458-1466.

10. University of Florida. Bonding to Bone, in Explore Magazine. **2**(2). 1997. http://rgp.ufl.edu/explore/v02n2/exchange.html. December 9, 2002.

11. Mahmood, J., Takita, H., Ojima, Y., Kobayashi, M., Kohgo, T., and Kuboki, Y., Geometric effect of matrix upon cell differentiation: BMP-induced osteogenesis using a new bioglass with a feasible structure. Journal of Biochemistry, 2001. **129**(1): p. 163-171.

12. Hench, L. and Wilson, J., An introduction to bioceramics. Advanced Series in Ceramics. Vol. 1. 1993, World Scientific Publishing, Singapore.

13. Hench, L.L., Bioactive materials: the potential for tissue regeneration. Journal of Biomedical Materials Research, 1998. **41**(4): p. 511-518.

14. Gallardo, J., Galliano, P., and Duran, A., Bioactive sol-gel coatings for orthopaedic prosthesis. Journal of Sol-Gel Science and Technology, 2000. **19**(1): p. 107-111.

15. Gallardo, J., Galliano, P., and Duran, A., Bioactive and protective sol-gel coatings on metals for orthopaedic prostheses. Journal of Sol-Gel Science and Technology, 2001. **21**(1): p. 65-74.

16. Ratner, B.D., Hoffman, A.S., and F, S., Biomaterials Science. 1996, Academic Press, San Diego.

17. Yuan, X., Mak, A.F., and Li, J., Formation of bone-like apatite on poly(L-lactic acid) fibers by a biomimetic process. Journal of Biomedical Materials Research, 2001. **57**(1): p. 140-150.

18. Hench, L.L., Bioceramics: Materials characteristics versus in vivo behavior, ed. Annals of New York Academy of Sciences. 1988.

19. Hench, L.L. and Wilson, J., Clinical performance of skeletal prostheses. 1996, Chapman and Hall, London.

20. Lobel, K.D., Protein interactions with bioactive glasses, in Materials Science and Engineering, Master's Thesis. 1995, University of Florida: Gainesville. p. 116.

21. Lobel, K.D. and Hench, L.L., In vitro adsorption and activity of enzymes on reaction layers of bioactive glass substrates. Journal of Biomedical Materials Research, 1998. **39**(4): p. 575-579.

22. Brinker, C. and Scherer, G., Sol-gel science: the physics and chemistry of sol-gel processing. 1990, Academic Press, New York.

23. Vogel, M., Voigt, C., Gross, U., and Muller-Mai, C., In vivo comparison of bioactive glass particles in rabbits. Biomaterials, 2001. **22**(4): p. 357-362.

24. Hamadouche, M., Meunier, A., Greenspan, D.C., Blanchat, C., Zhong, J.P., La Torre, G.P., and Sedel, L., Long-term in vivo bioactivity and degradability of bulk sol-gel bioactive glasses. Journal of Biomedical Materials Research, 2001. **54**(4): p. 560-566.

25. Oonishi, H., Hench, L.L., Wilson, J., Sugihara, F., Tsuji, E., Kushitani, S., and Iwaki, H., Comparative bone growth behavior in granules of bioceramic materials of various sizes. Journal of Biomedical Materials Research, 1999. **44**(1): p. 31-43.

26. Oonishi, H., Kushitani, S., Yasukawa, E., Iwaki, H., Hench, L.L., Wilson, J., Tsuji, E., and Sugihara, T., Particulate bioglass compared with hydroxyapatite as a bone graft substitute. Clinical Orthopaedics and Related Research, 1997(334): p. 316-325.

27. Orefice, R., Hench, L., Clark, A., and Brennan, A., Novel sol-gel bioactive fibers. Journal of Biomedical Materials Research, 2001. **55**(4): p. 460-467.

28. Dominques, R., Clark, A.E., and Brennan, A., A sol-gel derived bioactive fibrous mesh. Journal of Biomedical Materials Research, 2001. **55**(4): p. 468-474.

29. De Diego, M.A., Coleman, N.J., and Hench, L.L., Tensile properties of bioactive fibers for tissue engineering applications. Journal of Biomedical Materials Research, 2000. **53**(3): p. 199-203.

30. Marcolongo, M.S., Ducheyne, P., Ko, F., and LaCourse, W., Composite materials using bone bioactive glass and ceramic fibers. Composites Part A: Applied Science and Manufacturing, 1996. **27**(8): p. 671.

31. Sepulveda, P., Jones, J.R., and Hench, L.L., Bioactive sol-gel foams for tissue repair. Journal of Biomedical Materials Research, 2002. **59**(2): p. 340-348.

32. Niederauer, G.G., A. Slivka, M., Leatherbury, N.C., Korvick, D.L., Hugh Harroff, J., H., Ehler, W.C., Dunn, C.J., and Kieswetter, K., Evaluation of multiphase implants for repair of focal osteochondral defects in goats. Biomaterials, 2000. **21**(24): p. 2561-2574.

33. Efflandt, W.E., Magne, P., Douglas, W.H., and Francis, L.F., Interaction between bioactive glasses and human dentin. Journal of Materials Science: Materials in Medicine, 2002. **13**: p. 557-565.

34. Yuan, H., de Bruijn, J.D., Zhang, X., van Blitterswijk, C.A., and de Groot, K., Bone induction by porous glass ceramic made from Bioglass (45S5). Journal of Biomedical Materials Research, 2001. **58**(3): p. 270-276.

35. Merollo, A., Leali, P.T., and Guidi, P.L., Comparison in *in vivo* response between a bioctive glass and a nonbioactive glass. Journal of Materials Science: Materials in Medicine, 2000. **11**: p. 219-222.

36. Jinno, T., Goldberg, V.M., Davy, D., and Stevenson, S., Osseointegration of surface-blasted implants made of titanium alloy and cobalt-chromium alloy in a rabbit intramedullary model. Journal of Biomedical Materials Research, 1998. **42**(1): p. 20-29.

37. Hatcher, B.M., Seegert, C.A., and Brennan, A.B., Polyvinylpyrrolidone modified bioactive glass fibers as tissue constructs: in vitro mesenchymal stem cell response. Journal of Biomedical Materials Research, Submitted July 2002.

38. Hench, L., Molecular control of bioactivity in sol-gel glasses. Journal of Sol-Gel Science and Technology, 1998. **13**(1): p. 245-250.

39. Hench, L.L. and West, J.K., The sol-gel process. Chemical Reviews, 1990. **90**(1): p. 33-72.

40. Wilkes, G. and Brennan, A., Use of polymeric catalyst in synthesis of sol-gel derived ceramic materials, in USPTO. 1994, Virginia Tech Intellectual Properties, Inc. Blacksburg, VA.

41. Agren, P. and Rosenholm, J.B., Phase behavior and structural changes in tetraethylorthosilicate-derived gels in the presence of polyethylene glycol, studied by rheological techniques and visual observations. Journal of Colloid and Interface Science, 1998. **204**(1): p. 45-52.

42. Sarmento, V.H.V., Dahmouche, K., Santilli, C.V., and Pulcinelli, S.H., Gelation of siloxane-poly(oxypropylene) composites. Journal of Non-Crystalline Solids, 2002. **304**(1-3): p. 134-142.

43. Vong, M., Bazin, N., and Sermon, P., Chemical modification of silica gels. Journal of Sol-Gel Science and Technology, 1997. **8**: p. 499-505.

44. Nagpal, V.J., Davis, R.M., and Riffle, J.S., In situ steric stabilization of titanium dioxide particles synthesized by a sol--gel process. Colloids and Surfaces A: Physicochemical and Engineering Aspects, 1994. **87**(1): p. 25-31.

45. Oh, I.S., Park, N.H., and Suh, K.D., Mechanical and surface hardness properties of UV cured polyurethane acrylate anionomer/silica composite film. Journal of Applied Polymer Science, 2000. **75**: p. 968-975.

46. Otsubo, Y., Rheology of colloidal suspensions flocculated by reversible bridging. Chemical Engineering Science, 2001. **56**(9): p. 2939-2946.

47. Otsubo, Y., Rheological behavior of suspensions flocculated by weak bridging of polymer coils. Journal of Colloid and Interface Science, 1999. **215**(1): p. 99-105.

48. Biggs, S., Habgood, M., Jameson, G.J., and Yan, Y.-d., Aggregate structures formed via a bridging flocculation mechanism. Chemical Engineering Journal, 2000. **80**(1-3): p. 13-22.

49. Martin, R.B., Bone as a ceramic composite material. Materials Science Forum, 1999. **293**: p. 5-16.

50. Guyton, A., Textbook of medical physiology. 1991, Saunders, Philadelphia.

51. University of Sydney, School of Biomedical Sciences. Bone. http://casino.cchs.usyd.edu.au/bio/1128bone.pdf. December 9, 2002.

52. Weiner, S. and Wagner, H.D., Letter to the editor. Bone, 2000. **27**(6): p. 875-876.

53. Giraud-Guille, M.M., Twisted plywood architecture of collagen fibrils in human compact bone osteons. Calcified Tissue International, 1988. **42**(3): p. 167-180.

54. Lennon, D.P., Haynesworth, S.E., Young, R.G., Dennis, J.E., and Caplan, A.I., A chemically defined medium supports in vitro proliferation and maintains the osteochondral potential of rat marrow-derived mesenchymal stem cells. Experimental Cell Research, 1995. **219**(1): p. 211-222.

55. Cooper, L.F., Harrris, C.T., Bruder, S.P., Kowalski, R., and Kadiyala, S., Incipient analysis of mesenchymal stem cell derived osteogenesis. Journal of Dental Research, 2001. **80**(1): p. 314-320.

56. Hanada, K., Dennis, J.E., and Caplan, A.I., Stimulatory effects of basic fibroblast growth factor and bone morphogenetic protein-2 on osteogenic differentiation of rat bone marrow-derived mesenchymal stem cells. Journal of Bone and Mineral Research: the Official Journal of the American Society for Bone and Mineral Research, 1997. **12**(10): p. 1606-1614.

57. Turgeman, G., Pittman, D.D., Muller, R., Kurkalli, B.G., Zhou, S., Pelled, G., Peyser, A., Zilberman, Y., Moutsatsos, I.K., and Gazit, Engineered human mesenchymal stem cells: a novel platform for skeletal cell mediated gene therapy. The Journal of Gene Medicine. **3**(3): p. 240-251.

58. Andrades, J.A., Santamaria, J.A., Nimni, M.E., and Becerra, J., Selection and amplification of a bone marrow cell population and its induction to the chondro-osteogenic lineage by rhOP-1: an in vitro and in vivo study. The International Journal of Developmental Biology, 2001. **45**(4): p. 689-693.

59. Pearson, R.G., Bhandari, R., Quirk, R.A., and Shakesheff, K.M., Recent advances in tissue engineering: an invited review. Journal of Long-Term Effects of Medical Implants, 2002. **12**(1): p. 1-33.

60. Seal, B.L., Otero, T.C., and Panitch, A., Polymeric biomaterials for tissue and organ regeneration. Materials Science and Engineering: R: Reports, 2001. **34**(4-5): p. 147-230.

61. Rose, F. and Oreffoe, R., Bone tissue engineering: hope vs hype. Biochemical and Biophysical Research Communications, 2002. **292**: p. 1-7.

62. Wright, K.A., Nadire, K.B., Busto, P., Tubo, R., McPherson, J.M., and Wentworth, B.M., Alternative delivery of keratinocytes using a polyurethane membrane and the implications for its use in the treatment of full-thickness burn injury. Burns, 1998. **24**(1): p. 7-17.

63. Muhart, M., McFalls, S., Kirsner, R.S., Elgart, G.W., Kerdel, F., Sabolinski, M.L., Hardin-Young, J., and Eaglstein, W.H., Behavior of tissue-engineered skin: a comparison of a living skin equivalent, autograft, and occlusive dressing in human donor sites. Archives of Dermatology, 1999. **135**(8): p. 913-918.

64. Nanchahal, J., Dover, R., and Otto, W.R., Allogeneic skin substitutes applied to burns patients. Burns, 2002. **28**(3): p. 254-257.

65. Machens, H.G., Berger, A.C., and Mailaender, P., Bioartificial skin. Cells, Tissues, Organs, 2000. **167**(2-3): p. 88-94.

66. Purdue, G.F., Hunt, J.L., Still, J.M., Jr, Law, E.J., Herndon, D.N., Goldfarb, I.W., Schiller, W.R., Hansbrough, J.F., and Hickerson et, a., A multicenter clinical trial of a biosynthetic skin replacement, Dermagraft-TC, compared with cryopreserved human cadaver skin for temporary coverage of excised burn wounds. The Journal of Burn Care & Rehabilitation, 1997. **18**(1): p. 52-57.

67. Noordenbos, J., Dore, C., and Hansbrough, J.F., Safety and efficacy of TransCyte for the treatment of partial-thickness burns. The Journal of Burn Care & Rehabilitation, 1999. **20**(4): p. 275-281.

68. Slivka, M.A., Chu, C.C., and Adisaputro, I.A., Fiber-matrix interface studies on bioabsorbable composite materials for internal fixation of bone fractures. I. Raw material evaluation and measurement of fiber-matrix interfacial adhesion. Journal of Biomedical Materials Research, 1997. **36**: p. 469-477.

69. Mikos, A.G. and Temenoff, J.S., Formation of highly porous biodegradable scaffolds for tissue engineering. Electronic Journal of Biotechnology, 2000. **3**(2).

70. Hutmacher, D.W., Scaffolds in tissue engineering bone and cartilage. Biomaterials, 2000. **21**: p. 2529-2543.

71. Tan, W., Krishnaraj, R., and Desai, T.A., Evaluation of nanostrucures composite collagen-chitosan matrices for tissue engineering. Tissue Engineering, 2001. **7**(2): p. 203-210.

72. Salgado, A.J., Gomes, M.E., Chou, A., Coutinho, O.P., Reis, R.L., and Hutmacher, D.W., Preliminary study on the adhesion and proliferation of human osteoblasts on starch based scaffolds. Materials Science and Engineering C, 2002. **758**.

73. Hartgerink, J.D., Beniash, E., and Stupp, S.I., Self assembly and mineralization of peptide-amphiphile nanofibers. Science, 2001. **294**: p. 1684-1688.

74. Okumura, M., Ohgushi, H., Dohi, Y., Katuda, T., Tamai, S., Koerten, H.K., and Tabata, S., Osteoblastic phenotype expression on the surface of hydroxyapatite ceramics. Journal of Biomedical Materials Research, 1997. **37**(1): p. 122-129.

75. Yuan, H., de Bruijn, J.D., Zhang, X., van Blitterswijk, C.A., and de Groot, K., Bone induction by porous glass ceramic made from Bioglass (45S5). Journal of Biomedical Materials Research: Applied Biomaterials, 2001. **58**: p. 270-276.

76. Marcolongo, M., Ducheyne, P., Garino, J., and Schepers, E., Bioactive glass fiber/polymeric composites bond to bone tissue. Journal of Biomedical Materials Research, 1998. **39**(1): p. 161-170.

77. Silver, I., Deas, J., and Erecinska, M., Interactions of bioactive glasses with osteoblasts in vitro: effects of 45S5 Bioglass®, and 58S and 77S bioactive glasses on metabolism, intracellular ion concentrations and cell viability. Biomaterials, 2001. **22**(2): p. 175-185.

78. Stanley, H.R., Hall, M.B., Clark, A.E., King, C.J., 3rd, Hench, L.L., and Berte, J.J., Using 45S5 bioglass cones as endosseous ridge maintenance implants to prevent alveolar ridge resorption: a 5-year evaluation. The International Journal of Oral & Maxillofacial Implants. **12**(1): p. 95-105.

79. Hench, L.L., Bioactive glasses and glass-ceramics. Materials Science Forum, 1999. **293**: p. 37-64.

80. Bosetti, M., Hench, L., and Cannas, M., Interaction of bioactive glasses with peritoneal macrophages and monocytes in vitro. Journal of Biomedical Materials Research, 2002. **60**(1): p. 79-85.

81. Livingston, T., Ducheyne, P., and Garino, J., In vivo evaluation of a bioactive scaffold for bone tissue engineering. Journal of Biomedical Materials Research, 2002. **62**: p. 1-13.

82. Gao, T., Aro, H.T., Ylanen, H., and Vuorio, E., Silica-based bioactive glasses modulate expression of bone morphogenetic protein-2 mRNA in Saos-2 osteoblasts in vitro. Biomaterials, 2001. **22**(12): p. 1475-1483.

83. Lu, H.H., Pollack, S.R., and Ducheyne, P., 45S5 bioactive glass surface charge variations and the formation of a surface calcium phosphate layer in a solution containing fibronectin. Journal of Biomedical Materials Research, 2001. **54**(3): p. 454-461.

84. Kaufmann, E.A., Ducheyne, P., Radin, S., Bonnell, D.A., and Composto, R., Initial events at the bioactive glass surface in contact with protein-containing solutions. Journal of Biomedical Materials Research, 2000. **52**(4): p. 825-830.

85. Silver, I.A., Deas, J., and Erecinska, M., Interactions of bioactive glasses with osteoblasts in vitro: effects of 45S5 Bioglass(R), and 58S and 77S bioactive glasses on metabolism, intracellular ion concentrations and cell viability. Biomaterials, 2001. **22**(2): p. 175-185.

86. Mayr-Wohlfart, U., Fiedler, J., Gunther, K.P., Puhl, W., and Kessler, S., Proliferation and differentiation rates of a human osteoblast-like cell line (SaOS-2) in contact with different bone substitute materials. Journal of Biomedical Materials Research, 2001. **57**(1): p. 132-139.

87. Harrison, R., The reaction of embryonic cells to solid structures. Journal of Experimental Zoology. **17**(4): p. 521-544.

88. Weiss, P., Experiments on cell and axon orientation in vitro: the role of colloidal exudates in tissue organization.

89. Curtis, A.S.G. and Seehar, G.M., The control of cell division by tension or diffusion. Nature, 1978. **274**: p. 52-53.

90. Curtis, A. and Varde, M., Control of cell behavior: topological factors. Journal of National Cancer Institute, 1964. **33**: p. 15-26.

91. Peltola, T., Jokinen, M., Veittola, S., Rahiala, H., and Yli-Urpo, A., Influence of sol and stage of spinnability on in vitro bioactivity and dissolution of sol-gel derived SiO 2 fibers. Biomaterials, 2001. **22**(6): p. 589-598.

92. Oonishi, H., Hench, L.L., Wilson, J., Sugihara, F., Tsuji, E., Matsuura, M., Kin, S., Yamamoto, T., and Mizokawa, S., Quantitative comparison of bone growth behavior in granules of Bioglass, A-W glass-ceramic, and hydroxyapatite. Journal of Biomedical Materials Research, 2000. **51**(1): p. 37-46.

93. Kursawe, M., Glaubitt, W., and Thierauf, A., Biodegradable silica fibers from sols. Journal of Sol-Gel Science and Technology, 1998. **13**: p. 267-271.

94. Jokinen, M., Peltola, T., Veittola, S., Rahiala, H., and Rosenholm, J., Adjustable biodegradation for ceramic fibres derived from silica sols. Journal of European Ceramic Society, 2000. **20**(11): p. 1739-1748.

95. Yu, J.C., Yu, J.C., Bei, C., Xiujian, Z., Zhi, Z., and Li, A.S.K., Atomic force microscopic studies of porous TiO2 thin films prepared by the sol-gel method. Journal of Sol-Gel Science and Technology, 2002. **24**(3): p. 229-240.

96. Nakanishi, K., Takahashi, R., and Soga, N., Effects of aging and solvent exchange on pore structure of silica gels with interconnected macropores. Journal of Non-Crystalline Solids, 1995. **189**(1-2): p. 66-76.

97. Nakanishi, K., Soga, N., and Kaji, H., Formation of porous gel morphology by phase separation in gelling alkoxy-derived silica: Phenomenological study. Journal of Non-Crystalline Solids, 1995. **185**(1-2): p. 18-30.

98. Kaji, H., Nakanishi, K., and Soga, N., Formation of porous gel morphology by phase separation in gelling alkoxy-derived silica: Affinity between silica polymers and solvent. Journal of Non-Crystalline Solids, 1995. **181**(1-2): p. 16-26.

99. Gedde, U., Polymer physics. 1995, Kluwer Academic, Dordrecht.

100. Sepulveda, P., Jones, J.R., and Hench, L.L., In vitro dissolution of melt-derived 45S5 and sol-gel derived 58S bioactive glasses. Journal of Biomedical Materials Research, 2002. **61**(2): p. 301-311.

101. Sepulveda, P., Jones, J.R., and Hench, L.L., Characterization of melt-derived 45S5 and sol-gel-derived 58S bioactive glasses. Journal of Biomedical Materials Research, 2001. **58**(6): p. 734-740.

102. Kokubo, T., Kushitani, H., Sakka, S., Kitsugi, T., and Yamamuro, T., Solutions able to reproduce in vivo surface structure changes in bioactive glass ceramic A-W. Journal of Biomedical Materials Research, 1990. **24**: p. 721-734.

103. Maniatopoulos, C., Sodek, J., and Melcher, A.H., Bone formation in vitro by stromal cells obtained from bone marrow of young adult rats. Cell and Tissue Research, 1988. **254**(2): p. 317-330.

104. Dennis, J.E., Haynesworth, S.E., Young, R.G., and Caplan, A.I., Osteogenesis in marrow-derived mesenchymal cell porous ceramic composites transplanted subcutaneously: effect of fibronectin and laminin on cell retention and rate of osteogenic expression. Cell Transplantation, 1992. **1**(1): p. 23-32.

105. Smith, Calcium phosphate hydroxide. CAS # 1306-06-5. 1996, JCPDS International Center for Diffraction Data.

106. Weiner, S., Traub, W., and Wagner, H.D., Lamellar bone: structure-function relations. Journal of Structural Biology, 1999. **126**(3): p. 241-255.

107. Weiner, S., Arad, T., Sabanay, I., and Traub, W., Rotated plywood structure of primary lamellar bone in the rat: orientations of the collagen fibril arrays. Bone, 1997. **20**(6): p. 509-514.

108. Pittenger, M.F., Mbalaviele, G., Black, M., Mosca, J.D., and Marshak, D.R., Mesenchymal stem cells, in Human cell culture: primary mesenchymal cells. 2001, Kluwer Academic, Dordrecht.

109. Seegert, C., Fiber based scaffolds in connective tissue engineering: using the architecture of woven scaffolds to influence and control the formation of organized tissues, in Department of Biomedical Engineering. 2002, University of Florida: Gainesville. p. 150.

110. Silver, X., Ni, W.X., Mercer, E.V., Beck, B.L., Bossart, E.L., Inglis, B., and Mareci, T.H., In vivo 1H magnetic resonance imaging and spectroscopy of the rat spinal cord using an inductively-coupled chronically implanted RF coil. Magnetic Resonance in Medicine: Official Journal of the Society of Magnetic Resonance in Medicine / Society of Magnetic Resonance in Medicine, 2001. **46**(6): p. 1216-1222.

111. Zhong, J. and Greenspan, D., Processing and properties of sol-gel bioactive glasses. Journal of Biomedical Materials Research, 2000. **53**(6): p. 694-701.

112. Jones, J.R., Sepulveda, P., and Hench, L.L., Dose-dependent behavior of bioactive glass dissolution. Journal of Biomedical Materials Research, 2001. **58**(6): p. 720-726.

113. Oliva, A., Salerno, A., Locardi, B., Riccio, V., Della Ragione, F., Iardino, P., and Zappia, V., Behaviour of human osteoblasts cultured on bioactive glass coatings. Biomaterials, 1998. **19**(11-12): p. 1019-1025.

114. Loty, C., Sautier, J.M., Tan, M.T., Oboeuf, M., Jallot, E., Boulekbache, H., Greenspan, D., and Forest, N., Bioactive glass stimulates in vitro osteoblast differentiation and creates a favorable template for bone tissue formation. Journal of Bone and Mineral Research: the Official Journal of the American Society for Bone and Mineral Research, 2001. **16**(2): p. 231-239.

115. Wheeler, D.L. and Stokes, K.E. In vivo evaluation of sol gel Bioglass: Part 1: Histological findings. in Society for Biomaterials. 1997. New Orleans, LA.

116. Schepers, E.J. and Ducheyne, P., Bioactive glass particles of narrow size range for the treatment of oral bone defects: a 1-24 month experiment with several materials and particle sizes and size ranges. Journal of Oral Rehabilitation, 1997. **24**(3): p. 171-181.

117. Wheeler, D.L., Stokes, K.E., Hoellrich, R.G., Chamberland, D.L., and McLoughlin, S.W., Effect of bioactive glass particle size on osseous regeneration of cancellous defects. Journal of Biomedical Materials Research, 1998. **41**(4): p. 527-533.

BIOGRAPHICAL SKETCH

Brian Hatcher was born in Augusta, Georgia, on March 13, 1978. He was the first of 3 children, and the only son, born to his parents, Tony and Linda Hatcher. He spent most of his childhood in Augusta and moved to Charlotte, North Carolina, at age 11. Following his sophomore year he again moved to Panama City, Florida, where he graduated high school in 1996.

Following graduation, Hatcher attended the University of Florida where he received his Bachelor of Science degree in chemistry in August of 2000. Immediately after he began his graduate studies in the Program of Biomedical Engineering at the University of Florida under Dr. Anthony Brennan. Upon completion of his master's degree he will continue work towards his Ph.D. in the new Department of Biomedical Engineering at the University of Florida.